

LINEAR AND NON-LINEAR MECHANISTIC MODELING AND SIMULATION OF THE
FORMATION OF CARBON ADSORBENTS

by

ALVARO ANDRES ARGOTI CAICEDO

B.S., Universidad Nacional de Colombia, Bogotá, 1998
M.S., Kansas State University, 2003

AN ABSTRACT OF A DISSERTATION

submitted in partial fulfillment of the requirements for the degree

DOCTOR OF PHILOSOPHY

Department of Chemical Engineering
College of Engineering

KANSAS STATE UNIVERSITY
Manhattan, Kansas

2007

Abstract

Carbon adsorbents, namely, activated carbons and carbon molecular sieves, can be variously applied in the purification and separation of gaseous and liquid mixtures, e.g., in the separation of nitrogen or oxygen from air; often, carbon adsorbents also serve as catalysts or catalyst supports. The formation of carbon adsorbents entails the modification of the original internal surfaces of carbonaceous substrates by resorting to a variety of chemical or physical methods, thereby augmenting the carbonaceous substrates' adsorbing capacity. The formation of carbon adsorbents proceeds randomly, which is mainly attributable to the discrete nature, mesoscopic sizes, and irregular shapes of the substrates utilized as well as to their intricate internal surface configuration. Moreover, any process of carbon-adsorbent formation may fluctuate increasingly severely with time. It is desirable that such a process involving discrete and mesoscopic entities undergoing complex motion and behavior be explored by means of the statistical framework or a probabilistic paradigm.

This work aims at probabilistic analysis, modeling, and simulation of the formation of carbon adsorbents on the basis of mechanistic rate expressions. Specifically, the current work has formulated a set of linear and non-linear models of varied complexity; derived the governing equations of the models formulated; obtained the analytical solutions of the governing equations whenever possible; simulated one of the models by the Monte Carlo method; and validated the results of solution and simulation in light of the available experimental data for carbon-adsorbent formation from carbonaceous substrates, e.g., biomass or coal, or simulated data obtained by sampling them from a probability distribution. It is expected that the results from this work will be useful in establishing manufacturing processes for carbon adsorbents. For instance, they can be adopted in planning bench-scale or pilot-scale experiments; preliminary design and economic analysis of production facilities; and devising the strategies for operating and controlling such facilities.

LINEAR AND NON-LINEAR MECHANISTIC MODELING AND SIMULATION OF THE
FORMATION OF CARBON ADSORBENTS

by

ALVARO ANDRES ARGOTI CAICEDO

B.S., Universidad Nacional de Colombia, Bogotá, 1998

M.S., Kansas State University, 2003

A DISSERTATION

submitted in partial fulfillment of the requirements for the degree

DOCTOR OF PHILOSOPHY

Department of Chemical Engineering
College of Engineering

KANSAS STATE UNIVERSITY
Manhattan, Kansas

2007

Approved by:

Co-Major Professor
L. T. Fan

Co-Major Professor
Dr. Walter P. Walawender

Abstract

Carbon adsorbents, namely, activated carbons and carbon molecular sieves, can be variously applied in the purification and separation of gaseous and liquid mixtures, e.g., in the separation of nitrogen or oxygen from air; often, carbon adsorbents also serve as catalysts or catalyst supports. The formation of carbon adsorbents entails the modification of the original internal surfaces of carbonaceous substrates by resorting to a variety of chemical or physical methods, thereby augmenting the carbonaceous substrates' adsorbing capacity. The formation of carbon adsorbents proceeds randomly, which is mainly attributable to the discrete nature, mesoscopic sizes, and irregular shapes of the substrates utilized as well as to their intricate internal surface configuration. Moreover, any process of carbon-adsorbent formation may fluctuate increasingly severely with time. It is desirable that such a process involving discrete and mesoscopic entities undergoing complex motion and behavior be explored by means of the statistical framework or a probabilistic paradigm.

This work aims at probabilistic analysis, modeling, and simulation of the formation of carbon adsorbents on the basis of mechanistic rate expressions. Specifically, the current work has formulated a set of linear and non-linear models of varied complexity; derived the governing equations of the models formulated; obtained the analytical solutions of the governing equations whenever possible; simulated one of the models by the Monte Carlo method; and validated the results of solution and simulation in light of the available experimental data for carbon-adsorbent formation from carbonaceous substrates, e.g., biomass or coal, or simulated data obtained by sampling them from a probability distribution. It is expected that the results from this work will be useful in establishing manufacturing processes for carbon adsorbents. For instance, they can be adopted in planning bench-scale or pilot-scale experiments; preliminary design and economic analysis of production facilities; and devising the strategies for operating and controlling such facilities.

Table of Contents

| | |
|--|------|
| List of Figures | viii |
| List of Tables | ix |
| Acknowledgements..... | x |
| Dedication | xi |
| CHAPTER 1 - Introduction | 1 |
| Objectives | 2 |
| Rationale | 3 |
| Description of the Systems | 7 |
| Formation of activated carbons (ACs)..... | 7 |
| Formation of carbon molecular sieves (CMSs) | 7 |
| CHAPTER 2 - Formation of Activated Carbons: Pure-Birth Process with a Linear Intensity of Transition Based on a Single Random Variable..... | 9 |
| Identification of Random Variable and State Space | 9 |
| Transition Diagram | 10 |
| Definition of Intensity of Transition | 10 |
| Master Equation..... | 10 |
| Mean and Variance | 12 |
| Mean | 12 |
| Variance | 12 |
| Analysis of Experimental Data | 13 |
| Results and Discussion | 17 |
| Summary | 21 |
| Notation | 23 |
| CHAPTER 3 - Formation of Carbon Molecular Sieves by Carbon Deposition: Pure-Birth Process with a Non-Linear Intensity of Transition Based on a Single Random Variable..... | 24 |
| Identification of Random Variable and State Space | 24 |
| Transition Diagram | 25 |
| Master Equation..... | 25 |

| | |
|--|----|
| Mean and Variance | 27 |
| Analysis of Experimental Data | 28 |
| Monte Carlo Simulation..... | 34 |
| Event-driven approach | 34 |
| Time-driven approach..... | 36 |
| Results and Discussion | 38 |
| Summary..... | 43 |
| Notation | 44 |
| CHAPTER 4 - Formation of Carbon Molecular Sieves by Carbon Deposition: Pure-Death | |
| Process with a Non-Linear Intensity of Transition Based on a Single Random Variable..... | 45 |
| Identification of Random Variable and State Space | 45 |
| Transition Diagram | 45 |
| Master Equation..... | 47 |
| Mean and Variance | 47 |
| Analysis of Experimental Data | 49 |
| Results and Discussion | 51 |
| Summary..... | 55 |
| Notation | 55 |
| CHAPTER 5 - Conclusions and Recommendations for Future Work | |
| Conclusions..... | 57 |
| Recommendations..... | 58 |
| References..... | 59 |
| Appendix A - Derivation of the Master Equation of a Pure-Birth Process | 72 |
| Appendix B - Formation of Activated Carbons: Derivation of Mean and Variance of the Pure-Birth Process with Linear Intensity of Transition Based on a Single Random Variable..... | 75 |
| Mean | 76 |
| Variance | 77 |
| Appendix C - Formation of Carbon Molecular Sieves: System-Size Expansion of the Master Equation of the Pure-Birth Process with a Non-Linear Intensity of Transition Based on a Single Random Variable..... | 80 |

| | |
|---|-----|
| Appendix D - Formation of Carbon Molecular Sieves: Derivation of the Mean and Variance for the Pure-Birth Process with a Non-Linear Intensity of Transition Based on a Single Random Variable | 85 |
| Appendix E - Formation of Carbon Molecular Sieves: Derivation of the Probability Density Function and the Cumulative Distribution Function of Waiting Time for the Pure-Birth Process with a Non-Linear Intensity of Transition Based on a Single Random Variable | 93 |
| Appendix F - Formation of Carbon Molecular Sieves: Estimation of Waiting Time for the Pure-Birth Process with a Non-Linear Intensity of Transition Based on a Single Random Variable | 96 |
| Appendix G - Formation of Carbon Molecular Sieves: Computer Codes for Performing Monte Carlo Simulation of the Pure-Birth Process with a Non-Linear Intensity of Transition Based on a Single Random Variable via the Event-Driven and Time-Driven Approaches | 100 |
| Appendix H - Formation of Carbon Molecular Sieves: Scheme for Simulating Experimental Data for the Pure-Birth Process with a Non-Linear Intensity of Transition Based on a Single Random Variable | 109 |
| Appendix I - Derivation of the Master Equation of a Pure-Death Process | 113 |
| Appendix J - Formation of Carbon Molecular Sieves: System-Size Expansion of the Master Equation for the Pure-Death Process with a Non-Linear Intensity of Transition Based on a Single Random Variable | 116 |
| Appendix K - Formation of Carbon Molecular Sieves: Derivation of the Mean and Variance of the Pure-Death Process with a Non-Linear Intensity of Transition Based on a Single Random Variable | 120 |

List of Figures

| | |
|--|-----|
| Figure 1.1. Schematic of the progression of formation of activated carbons (ACs)..... | 4 |
| Figure 1.2. Schematic of the progression of formation of carbon molecular sieves (CMSs) | 5 |
| Figure 2.1. Transition diagram of the pure-birth process representing the formation of pores on a carbonaceous substrate..... | 11 |
| Figure 2.2. Experimentally measured conversion of a carbonaceous substrate into ACs at different temperatures | 14 |
| Figure 2.3. Mean fractional conversion and standard deviation envelope for the formation of ACs. | 19 |
| Figure 2.4. Arrhenius plot for the kinetic constant, κ | 22 |
| Figure 3.1. Transition diagram of the pure-birth process representing pore-narrowing on ACs | 26 |
| Figure 3.2. Experimentally measured weights of carbon deposited on activated carbon at different temperatures | 29 |
| Figure 3.3. Normalized mean and normalized standard deviation envelope for the pore- narrowing | 40 |
| Figure 3.4. Normalized mean and normalized standard deviation envelope at the early stage of the pore-narrowing at 973 K | 42 |
| Figure 4.1. Transition diagram of the pure-death process representing pore-narrowing on ACs | 46 |
| Figure 4.2. Normalized mean and normalized standard deviation envelope for the pore- narrowing | 54 |
| Figure A.1. Probability balance for the pure-birth process in the time interval, $(t, t + \Delta t)$ | 73 |
| Figure C.1. Temporal evolution of the probability distribution, $p_n(t)$ or $p(n;t)$ | 81 |
| Figure F.1. Schematic for estimating realization v of the random variable, T_n , representing the waiting time..... | 99 |
| Figure I.1. Probability balance for the pure-death process in the time interval, $(t, t + \Delta t)$ | 114 |

List of Tables

| | | |
|------------|--|-----|
| Table 2.1. | Experimentally Measured Fractional Conversion of a Carbonaceous Substrate into ACs at Different Temperatures..... | 15 |
| Table 2.2. | Values of κ for the Formation of ACs at Different Temperatures..... | 18 |
| Table 3.1. | Experimentally Measured Weights of Carbon Deposited (C) on Activated Carbon (AC) at Different Temperatures..... | 30 |
| Table 3.2. | Values of α' and W_M for the Pore-narrowing at Different Temperatures. | 39 |
| Table 4.1. | Values of α , β , and W_0 for the Pore-narrowing at Different Temperatures. | 53 |
| Table G.1. | Computer Code in Microsoft Visual Basic for Performing Monte Carlo Simulation of the Pure-Birth Process via the Event-Driven Approach..... | 101 |
| Table G.2. | Computer Code in Microsoft Visual Basic for Performing Monte Carlo Simulation of the Pure-Birth Process via the Time-Driven Approach..... | 105 |
| Table H.1. | Computer Code in R for Generating Simulated Experimental Data as Poisson Deviates for the Pure-Birth Process..... | 112 |

Acknowledgements

The author wishes to express his most profound appreciation to Dr. L. T. Fan for his excellent guidance, constant encouragement, and invaluable advice in directing this work. Appreciation is extended to the author's co-major advisor, Dr. W. P. Walawender, for his advice and guidance; to Dr. K. Hohn of Department of Chemical Engineering and Dr. S.-S. Yang of Department of Statistics, for critically reviewing this dissertation and serving as members of the author's doctoral committee; and to Dr. Z. J. Pei of Department of Industrial and Manufacturing Systems Engineering, who served as the committee's chair. Special gratitude is also extended to Dr. S. T. Chou of Department of Finance and Banking, Kun Shan University of Technology, Taiwan, for his advice and assistance. The financial support provided by Kansas Agricultural Experiment Station, Department of Chemical Engineering, and Institute for Systems Design and Optimization of Kansas State University is gratefully acknowledged.

Dedication

To my parents, Alvaro and Betty, and my sisters, Marcela and Ximena.

CHAPTER 1 - Introduction

Carbon adsorbents, specifically, activated carbons (ACs) and carbon molecular sieves (CMSs), are highly porous materials that can be applied in the purification and separation of gaseous and liquid mixtures,¹⁻⁷ e.g., in the separation of nitrogen or oxygen from air. Various carbon adsorbents can also be effective as catalysts or catalyst supports.⁸⁻¹⁹ The formation of carbon adsorbents entails the modification of the original internal surfaces of carbonaceous substrates by resorting to a variety of chemical or physical methods, thereby augmenting the carbonaceous substrates' adsorbing capacity.²⁰

Activated carbons (ACs) can be manufactured from many varieties of carbonaceous substrates such as agricultural residues,²¹⁻²³ asphalt,²⁴ coal,²⁵⁻³⁵ coffee bean husks,³⁶ corn and corn cobs,^{37, 38} oil-palm and walnut shells,^{39, 40} sorghum and wheat,^{41, 42} and waste tire.⁴³ The activation of these carbonaceous substrates is carried out by physical or chemical methods, thereby leading to the formation of porosities on their internal surfaces. Physical activation of a carbonaceous substrate is usually performed by carbonizing it in an inert atmosphere at a temperature below 700 C, and subsequently activating it in the presence of steam, carbon dioxide, and/or air at a temperature between 800 C and 1000 C.^{23, 44-49} Similarly, chemical activation of a carbonaceous substrate is generally carried out by impregnating it with a strong dehydrating agent, e.g., phosphoric acid, and subsequently heating this mixture to a temperature between 400 C and 800 C.^{42, 50-54} The porosities on ACs can roughly be classified as micropores (< 2 nm), mesopores (2 – 50 nm), and macropores (> 50 nm)^{20, 55} depending on the lengths of their diameters. Carbon molecular sieves (CMSs) are a special form of ACs whose pores have diameters of the order of molecular dimensions (0.4 – 0.9 nm),⁵⁶ they can be produced in two stages. In the first stage, ACs are manufactured from carbonaceous substrates as described earlier. In the second stage, very fine carbon particles are deposited on the pores' mouths of ACs to narrow them; some of the narrowed pores will eventually become blocked.⁵⁷⁻⁶⁰ The carbon

particles are generated by decomposing gaseous organics of low-molecular weights, for instance, methane,⁶¹ propylene and isobutylene,^{62, 63} or benzene.⁶⁴⁻⁶⁶

Because of the discrete nature, mesoscopic sizes, irregular shapes, and intricate internal surface configuration of the carbonaceous substrates as well as the highly convoluted motion of the participating materials including reacting chemical species and carbon particles, the formation of carbon adsorbents tend to occur irregularly and randomly.

Objectives

It is natural or even desirable that the analysis and modeling of a process involving discrete and mesoscopic entities with convoluted motion and behavior, such as the formation of carbon adsorbents, be explored via the statistical framework or a probabilistic, i.e., stochastic paradigm. In fact, stochastic analysis and modeling are capable of revealing inherent fluctuations, or internal noises, of the phenomenon or system of interest.⁶⁷⁻⁶⁹ Among various classes of stochastic processes, the birth-death process and its subclasses, the pure-birth and pure-death processes, have been most widely adopted.⁶⁹⁻⁷²

The work presented in this dissertation aims at stochastic analysis and modeling of the formation of carbon adsorbents on the basis of mechanistic rate expressions. Specific objectives of this work are as follows:

a. To formulate a series of linear and non-linear stochastic models of increasing sophistication based on the pure-birth and pure-death processes. In the pure-birth process, the population of interest only increases temporally; in other words, this population does not decrease, thereby indicating the absence of the death process. Naturally, the opposite is the case for the pure-death process, i.e., the population of concern only decreases as time progresses.^{69, 71,}

⁷²

b. To derive the governing equation for each of the models formulated, which is termed the master equation in the parlance of stochastic processes.^{71, 73, 74}

c. To solve analytically or semi-analytically the master equations of the models derived.

d. To simulate one of the models by the Monte Carlo method.^{74, 75}

e. To validate the results of solution and simulation in light of the available experimental data for carbon-adsorbent formation from carbonaceous substrates, such as biomass or coal, or simulated data obtained by sampling them from a probability distribution.

Rationale

As indicated earlier, the process of formation of carbon adsorbents tends to proceed randomly or stochastically. The randomness or stochasticity of the process is attributable to a variety of causes. For the formation of ACs, the causes of stochasticity include the following. First, the discreteness and mesoscopic nature of the carbonaceous substrates whose shapes are highly irregular and their internal surface configurations extremely intricate.^{20, 76} Second, the random encounters between the activation agent, e.g., carbon dioxide or phosphoric acid, and the carbon atoms on the surfaces of the carbonaceous substrate: This is a chemical reaction, which is known to occur randomly.⁷⁷⁻⁸⁵ Third, the random distribution of the pores formed on the carbonaceous substrate's internal surfaces whose sizes and shapes are also highly irregular.²⁰ A schematic of these phenomena is presented in Figure 1.1.

For the formation of CMSs, the causes of stochasticity include the following. First, the decomposition of a gaseous carbon source, e.g., methane or benzene, which is a randomly-occurring chemical reaction as mentioned above. Second, the generation of fine carbon particles from the decomposed carbon source; these carbon particles are discrete and mesoscopic in size and their motion in the gas phase is extremely convoluted. Third, the formation of large carbon clusters, or packets, through random collisions between these fine carbon particles. Fourth, the deposition of these carbon packets onto the pores' mouths of ACs, which progresses temporally and occurs as a consequence of random encounters between the depositing carbon packets and pores. A schematic of these phenomena is presented in Figure 1.2.

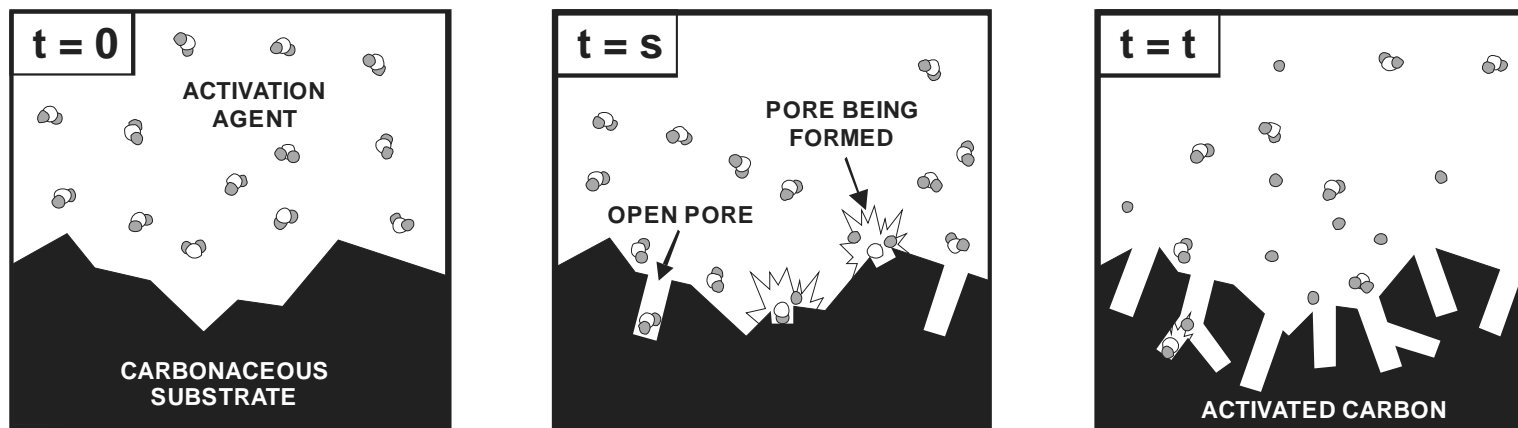


Figure 1.1. Schematic of the progression of activated-carbon (AC) formation: side view.

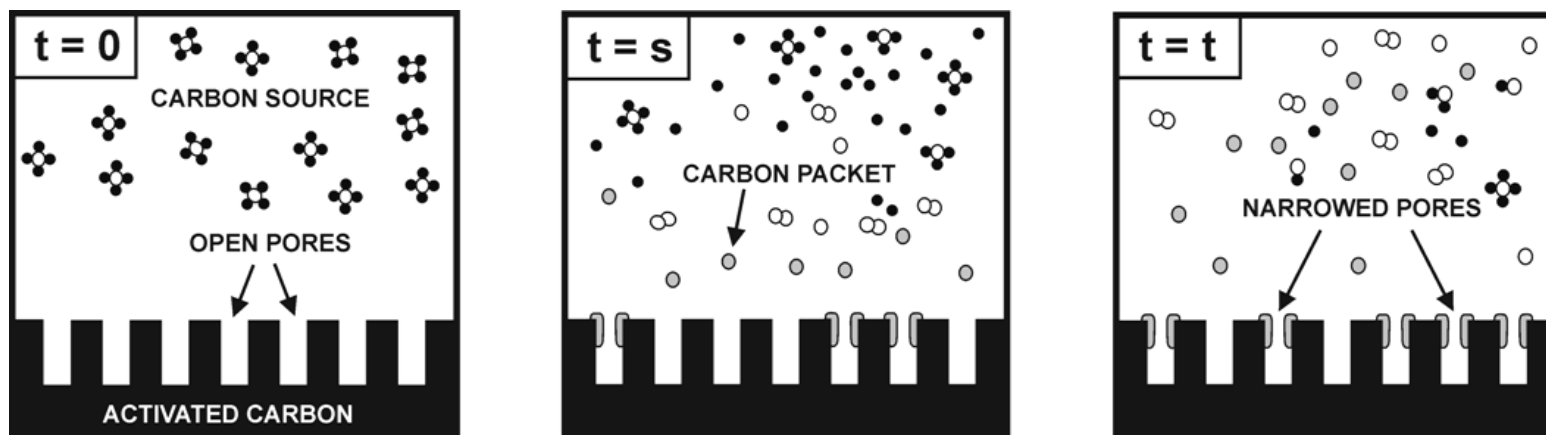


Figure 1.2. Schematic of the progression of carbon-molecular-sieve (CMS) formation: side view.

The randomness or stochasticity of any discrete or particulate system or process manifests itself in the form of incessant fluctuations in the macroscopic variables describing the system or process, which are inherent to it. These inherent fluctuations impede the prediction with certainty of any temporal or spatial variation in the evolution of the process. Such uncertainty can be accommodated by taking into account the probability distribution of the variables describing the process, thereby giving rise to the definition of random variables.^{69, 71} Hence, the analysis and modeling of a process described by random variables must be performed in light of a stochastic paradigm. Unlike a deterministic model, a stochastic model renders it possible to predict the inherent fluctuations of a system or process; moreover, the mean component of the stochastic model is equivalent to the deterministic model.^{67-69, 71}

The formation of ACs is essentially a fluid-solid reaction for which various mathematical models have been formulated;⁸⁶⁻⁹³ their complexity ranges from linear⁸⁸ to highly non-linear.⁹⁰ In such models, the experimentally measurable variable is usually the conversion of the solid material as it reacts with the chemical species present in the fluid phase. Naturally, the kinetics of formation of ACs has been formulated in light of these models;^{40, 94-101} nevertheless, they are deterministic in nature. So far, the stochastic formulation of the rate of formation of ACs has not been attempted; this work aims at providing it in the form of a linear stochastic model. Similarly, the formation of CMSs closely parallels the coke deposition process onto the pores of catalysts, thereby giving rise to their deactivation. A substantial number of works have been published on the deterministic analysis and modeling of coke deposition on catalysts.¹⁰²⁻¹⁰⁸ These models have served as the starting point for the stochastic formulation of the rate of formation of CMSs on the basis of linear kinetic expressions.^{109, 110} Hitherto, no effort has been made on the stochastic formulation of the formation of CMSs based on non-linear rate expressions, which is attempted in this work.

Stochastic analysis and modeling constitute viable tools that can greatly facilitate the development of an effective control strategy for randomly behaving systems and processes, e.g., the formation of carbon adsorbents. The mean component of the resultant stochastic model can be the basis for scaling up or designing the process; in addition, the inherent fluctuations predicted by the model are the limit of accuracy achievable by any control strategy.

Description of the Systems

To formulate the stochastic models for the formation of carbon adsorbents, including ACs and CMSs, the systems of concern must be properly identified; this is elaborated below.

Formation of activated carbons (ACs)

Figure 1.1 depicts the system of concern comprising the pores on the internal surfaces of a carbonaceous substrate being activated. The formation of pores is considered to be attributable exclusively to the chemical reaction between the carbon atoms constituting the carbonaceous substrate and the activation agent. Naturally, the number of pores being formed through the activation process increases temporally. In addition, these pores are randomly distributed over the internal surfaces of the carbonaceous substrate, thereby giving rise to a convoluted pore network. It is assumed that the reaction terminates prior to the collapse of the internal structure of the activated substrate.

Formation of carbon molecular sieves (CMSs)

Figure 1.2 exhibits the system of interest comprising carbon packets, or simply packets, and pores on ACs. These carbon packets are aggregates or clusters of fine carbon particles, which are generated by the decomposition of a gaseous carbon source. At the outset, the pores' mouths are completely open; subsequently, they are narrowed as time progresses by the deposition of packets onto them to a size suitable for effecting molecular sieving. Naturally, the number of narrowed pores increases and that of open pores decreases temporally. It is considered that a pore is narrowed by a single packet; moreover, the fraction of narrowed pores that become blocked by one packet is assumed to be negligible. The process of formation of CMSs as described herein is termed pore-narrowing for brevity.

Besides the current chapter, this dissertation contains four additional chapters, i.e., Chapters 2 through 5. Chapter 2 presents the analysis and modeling of the kinetics of formation of ACs as a pure-birth process with a linear intensity of transition, or intensity function, based on a single random variable. Chapter 3 focuses on the kinetics of formation of CMSs by carbon deposition, which is analyzed and modeled as a pure-birth process with a non-linear intensity function, based on a single random variable; in contrast, Chapter 4 views the formation of CMSs by carbon deposition as a pure-death process. Finally, the major conclusions are drawn and recommendations for possible extensions are proposed in Chapter 5.

CHAPTER 2 - Formation of Activated Carbons: Pure-Birth Process with a Linear Intensity of Transition Based on a Single Random Variable

As indicated in the introductory chapter, the formation of activated carbons (ACs) is analyzed and modeled in the current chapter as a pure-birth process with a linear intensity function based on a single random variable. In general, it is reasonable to consider that the driving force, or potential, of the formation of ACs is a function of the number of pores that have formed on the internal surfaces of a carbonaceous substrate being activated, which temporally increases. Naturally, one of the simplest forms of such a function is of the first-order. Thus, the corresponding intensity function is linear in the number of pores that have formed on the carbonaceous substrate's internal surfaces.

It is expected that the resultant model constitutes an insightful preliminary exploration of the stochastic nature of the formation of ACs. This exploration would improve the conceptual design of a reactor for manufacturing ACs of superior quality.

Identification of Random Variable and State Space

The available experimental data for the formation of ACs are given in terms of the conversion of a carbonaceous substrate into ACs at different temperatures.⁴⁰ It would be reasonable to equate the weight loss due to the reaction between the carbonaceous substrate and the activation agent to the number of pores that have formed on the carbonaceous substrate's internal surfaces. Thus, the number of pores that have already formed on the carbonaceous substrate's internal surfaces per unit weight of the activated substrate at time t is taken as the random variable of the process, $N(t)$, whose realization is n . All possible values of $N(t)$ are the states of the process and their collection, $\{ 0, 1, 2, \dots, n_L - 1, n_L \}$, is its state space where n_L is the maximum number of pores that could form on the carbonaceous substrate's internal surfaces per unit weight of the activated substrate. Note that the random variable, $N(t)$, in the current

model exclusively accounts for the number of pores that have already formed on the carbonaceous substrate's internal surfaces at any time t ; hence, the analysis of the change in the pores' sizes or lengths would require the formulation of models with different variables designated as the random variables.

Transition Diagram

The transition diagram of the process is presented in Figure 2.1. The circles indicate the system's possible states, which have already been identified in the preceding section, and the arrows describe transitions of the system at any moment.

Definition of Intensity of Transition

The intensity of transition, or simply intensity function, is defined as the instantaneous rate of change of the transition probability.⁷¹ The intensity function for the pure-birth process of interest, which is termed intensity of birth, is given by

$$\lambda_n(t) = \frac{dn}{dt} = \kappa(n_L - n) \quad (2.1)$$

where κ is a proportionality constant whose dimension is inverse time (t^{-1}).

Master Equation

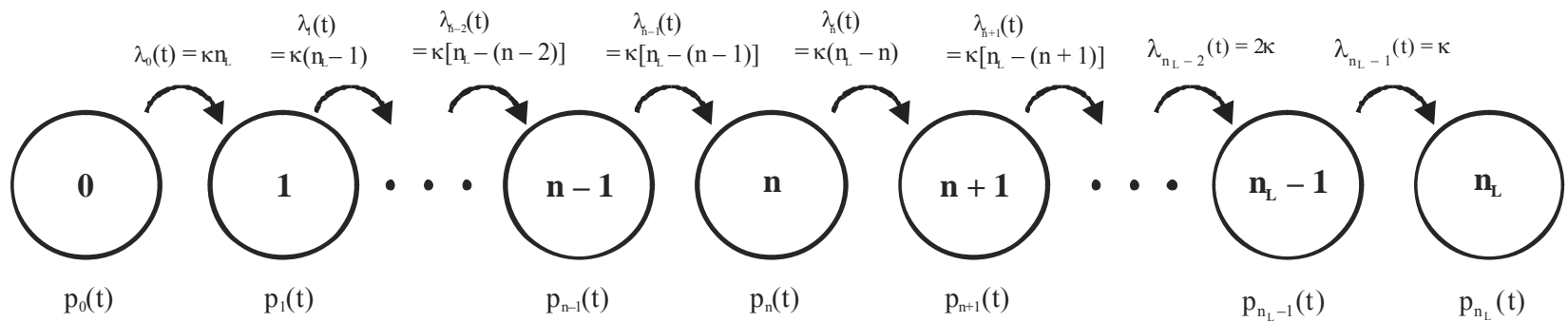
For the pure-birth process, the probability balance around state n leads to

$$\frac{d}{dt} p_n(t) = \lambda_{n-1}(t)p_{n-1}(t) - \lambda_n(t)p_n(t), \quad n = 0, 1, 2, \dots, n_L - 1, n_L \quad (2.2)$$

which is the master, i.e., governing, equation of the process;^{71, 73} its derivation is detailed in Appendix A. The term, $p_n(t)$, in the above expression denotes the probability that n pores have formed at time t . Inserting the expression for the intensity of birth, $\lambda_n(t)$, into the above expression yields

$$\frac{d}{dt} p_n(t) = \{\kappa[n_L - (n-1)]\}p_{n-1}(t) - [\kappa(n_L - n)]p_n(t) \quad (2.3)$$

Clearly, this equation is dependent on realization n but independent of time t .



11

Figure 2.1. Transition diagram of the pure-birth process representing the formation of pores on a carbonaceous substrate: The symbols, $0, 1, 2, \dots, (n - 1), n, (n + 1), \dots, (n_L - 1), n_L$, are the states of the process; $p_0(t), p_1(t), \dots, p_{n-1}(t), p_n(t), p_{n+1}(t), \dots, p_{n_L-1}(t), p_{n_L}(t)$, are the corresponding state probabilities; and $\lambda_n(t) = \kappa(n_L - n)$ is the intensity of birth, which is a linear function of n for each transition.

Mean and Variance

The mean, i.e., and higher moments about the mean can be computed from the master equation of the pure-birth process, Eq. (2.3). Among these higher moments, the second moment about the mean, i.e., the variance, is of special importance: It signifies the fluctuations or scatterings of the random variable about its mean,^{69, 111} which should be the focus of any stochastic analysis and modeling.

Mean

As detailed in Appendix B, the mean, or expected value, of $N(t)$ is obtained as

$$m(t) = n_L [1 - \exp(-\kappa t)] \quad (2.4)$$

where κ is a proportionality constant. From this expression, the normalized form of the mean, denoted by $\eta(\tau)$, is given by

$$\eta(\tau) = \frac{m(\tau)}{n_L} = [1 - \exp(-\tau)] \quad (2.5)$$

where $\tau = (\kappa t)$ is the dimensionless time. Note that this expression is solely a function of τ .

Variance

The variance, $\text{Var}[N(t)]$ or $\sigma^2(t)$, of $N(t)$, which is also derived in Appendix B, is given by

$$\sigma^2(t) = n_L [1 - \exp(-\kappa t)] \exp(-\kappa t) \quad (2.6)$$

In terms of dimensionless time τ , this expression becomes

$$\sigma^2(\tau) = n_L [1 - \exp(-\tau)] \exp(-\tau) \quad (2.7)$$

The standard deviation, $\sigma(t)$, is the square root of the variance, $\sigma^2(t)$; thus,

$$\sigma(t) = n_L^{1/2} \{ [1 - \exp(-\kappa t)] \exp(-\kappa t) \}^{1/2} \quad (2.8)$$

From this equation, the normalized form of the standard deviation, $\zeta(\tau)$, is obtained as

$$\zeta(\tau) = \frac{\sigma(\tau)}{n_L} = \frac{1}{n_L^{1/2}} \{ [1 - \exp(-\tau)] \exp(-\tau) \}^{1/2} \quad (2.9)$$

Note that this expression is a function of τ and n_L . The standard deviation relative to the mean, termed the coefficient of variation, is defined as¹¹²

$$CV(t) = \frac{\sigma(t)}{m(t)} \quad (2.10)$$

Inserting Eqs. (2.4) and (2.8) for $m(t)$ and $\sigma(t)$, respectively, into the above equation yields the coefficient of variation, $CV(t)$, of the pure-birth process as

$$CV(t) = \left\{ \frac{\exp(-\kappa t)}{n_L [1 - \exp(-\kappa t)]} \right\}^{1/2} \quad (2.11)$$

or in terms of τ ,

$$CV(\tau) = \left\{ \frac{\exp(-\tau)}{n_L [1 - \exp(-\tau)]} \right\}^{1/2} \quad (2.12)$$

Note that this expression is also a function of τ and n_L .

Analysis of Experimental Data

The available experimental data are presented in terms of the temporal evolution of the conversion of oil-palm shell char, a carbonaceous substrate, into ACs via physical activation with carbon dioxide at five temperatures.⁴⁰ The data are illustrated in

Figure 2.2, and also listed in Table 2.1. Naturally, the model derived in this work is validated with these data. To fit the model to the data, the random variable, $N(t)$, i.e., the number of pores that have already formed on the carbonaceous substrate's internal surfaces per unit weight of the activated substrate, needs to be related to the experimentally measurable variable, $Y(t)$, signifying the conversion of the carbonaceous substrate into ACs, which is defined as

$$Y(t) = \frac{W(t)}{W_L} \quad (2.13)$$

where $W(t)$ is the amount of carbon that has reacted with the activation agent at any time t , and W_L , the maximum amount of carbon that reacts before the internal structure of the carbonaceous substrate collapses. By assuming that the formation of pores on the carbonaceous substrate's internal surfaces is only attributable to the reaction between the carbon in the substrate and the activation agent, we have

$$W(t) = \delta N(t) \quad (2.14)$$

where δ is the amount of carbon that reacts, thereby giving rise to the formation of a single pore. In light of this equation, W_L can be related to n_L as

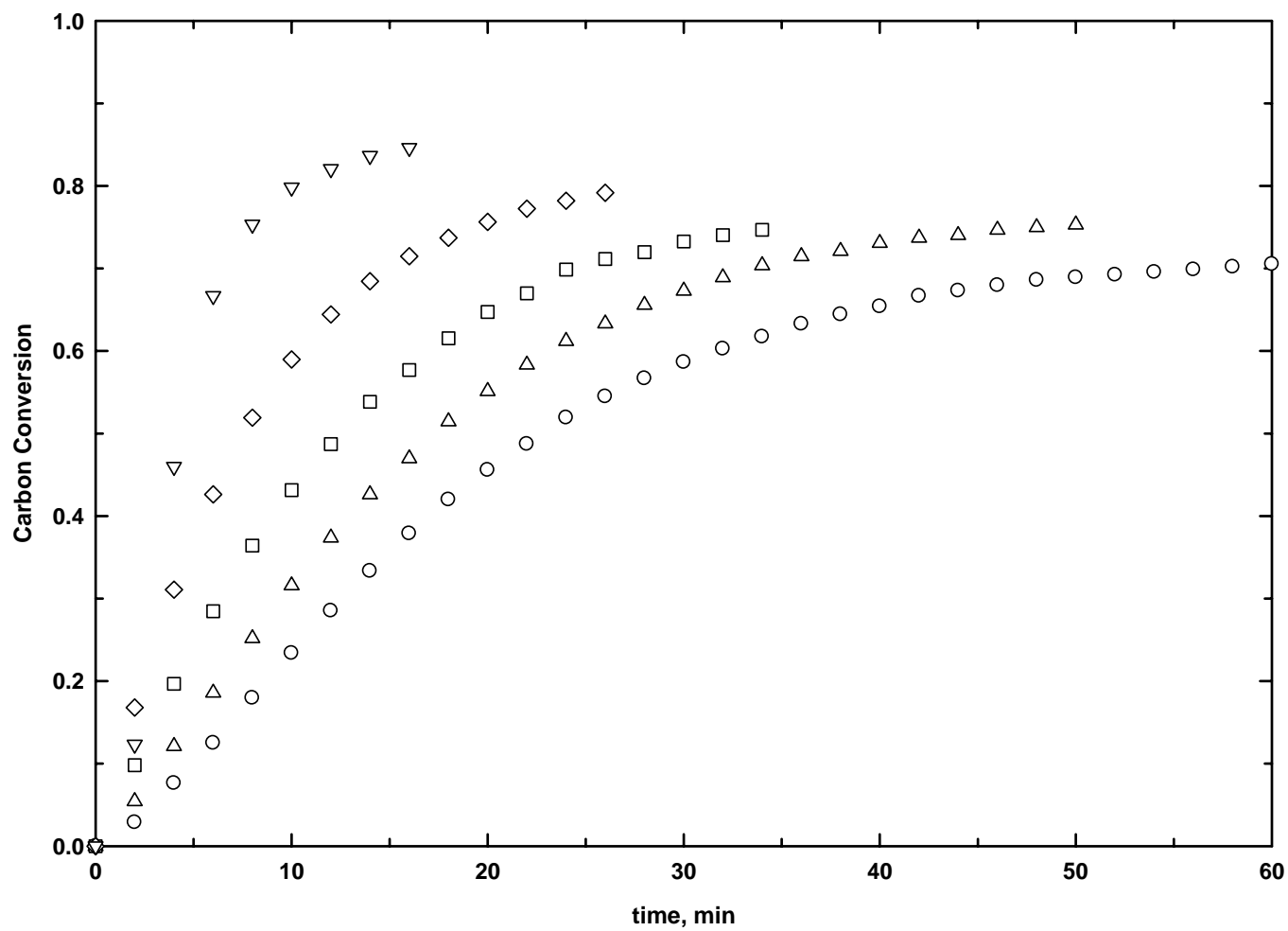


Figure 2.2. Experimentally measured conversion of a carbonaceous substrate into ACs at different temperatures.*

* Data were obtained with oil-palm-shell char.⁴⁰

Table 2.1. Experimentally Measured Fractional Conversion of a Carbonaceous Substrate into ACs at Different Temperatures*

| time, min | Carbon Conversion | | | | |
|-----------|-------------------|------------|------------|------------|------------|
| | T = 973 K | T = 1023 K | T = 1073 K | T = 1123 K | T = 1173 K |
| 0.0 | 0.000 | 0.000 | 0.000 | 0.000 | 0.000 |
| 2.0 | 0.029 | 0.054 | 0.098 | 0.168 | 0.123 |
| 4.0 | 0.076 | 0.121 | 0.197 | 0.311 | 0.460 |
| 6.0 | 0.125 | 0.186 | 0.285 | 0.426 | 0.667 |
| 8.0 | 0.179 | 0.252 | 0.364 | 0.519 | 0.753 |
| 10.0 | 0.234 | 0.316 | 0.431 | 0.590 | 0.798 |
| 12.0 | 0.285 | 0.374 | 0.487 | 0.644 | 0.821 |
| 14.0 | 0.333 | 0.426 | 0.538 | 0.685 | 0.837 |
| 16.0 | 0.379 | 0.470 | 0.577 | 0.715 | 0.846 |
| 18.0 | 0.420 | 0.515 | 0.615 | 0.737 | |
| 20.0 | 0.456 | 0.551 | 0.647 | 0.756 | |
| 22.0 | 0.487 | 0.583 | 0.670 | 0.772 | |
| 24.0 | 0.519 | 0.612 | 0.699 | 0.782 | |
| 26.0 | 0.545 | 0.633 | 0.712 | 0.792 | |
| 28.0 | 0.567 | 0.656 | 0.720 | | |
| 30.0 | 0.587 | 0.673 | 0.733 | | |
| 32.0 | 0.603 | 0.689 | 0.740 | | |
| 34.0 | 0.617 | 0.704 | 0.747 | | |
| 36.0 | 0.633 | 0.715 | | | |
| 38.0 | 0.644 | 0.721 | | | |
| 40.0 | 0.654 | 0.731 | | | |
| 42.0 | 0.667 | 0.737 | | | |
| 44.0 | 0.673 | 0.740 | | | |
| 46.0 | 0.679 | 0.747 | | | |
| 48.0 | 0.686 | 0.750 | | | |
| 50.0 | 0.689 | 0.753 | | | |
| 52.0 | 0.692 | | | | |
| 54.0 | 0.696 | | | | |
| 56.0 | 0.699 | | | | |
| 58.0 | 0.702 | | | | |
| 60.0 | 0.705 | | | | |

* Data were obtained with oil-palm shell char.⁴⁰

$$W_L = (\delta n_L) \quad (2.15)$$

The mean value of $Y(t)$, denoted by $m_Y(t)$, is obtained from this equation in conjunction with Eqs. (2.13) and (2.14) as follows:

$$\begin{aligned} m_Y(t) &= E[Y(t)] \\ &= E\left[\frac{W(t)}{W_L}\right] \\ &= \frac{1}{W_L} E[\delta N(t)] \end{aligned}$$

or

$$m_Y(t) = \frac{\delta}{W_L} E[N(t)]$$

or

$$m_Y(t) = \frac{\delta}{W_L} m(t)$$

Substituting Eq. (2.4) for $m(t)$ into this equation yields

$$m_Y(t) = \left(\frac{\delta}{W_L}\right) n_L [1 - \exp(-\kappa t)]$$

Because $W_L = (\delta n_L)$, this expression reduces to

$$m_Y(t) = [1 - \exp(-\kappa t)] \quad (2.16)$$

In terms of dimensionless time τ , the above equation can be rewritten as

$$m_Y(\tau) = [1 - \exp(-\tau)] \quad (2.17)$$

Note that this expression is identical to Eq. (2.5) for $\eta(\tau)$. Similarly, the variance of $Y(t)$, denoted by $\sigma_Y^2(t)$, is obtained from Eqs. (2.13), (2.14), and (2.15) as

$$\begin{aligned} \sigma_Y^2(t) &= \text{Var}\left[\frac{W(t)}{W_L}\right] \\ &= \text{Var}\left[\frac{\delta N(t)}{W_L}\right] \\ &= \left(\frac{\delta}{\delta n_L}\right)^2 \text{Var}[N(t)] \end{aligned}$$

or

$$\sigma_Y^2(t) = \frac{1}{n_L^2} [\sigma^2(t)]$$

Substituting Eq. (2.6) for $\sigma^2(t)$ into the above expression yields

$$\sigma_Y^2(t) = \frac{1}{n_L^2} \{n_L [1 - \exp(-\kappa t)] \exp(-\kappa t)\}$$

or

$$\sigma_Y^2(t) = \frac{1}{n_L} [1 - \exp(-\kappa t)] \exp(-\kappa t)$$

Naturally, the standard deviation of $Y(t)$, i.e., $\sigma_Y(t)$, is given by

$$\sigma_Y(t) = \frac{1}{n_L^{1/2}} \{[1 - \exp(-\kappa t)] \exp(-\kappa t)\}^{1/2} \quad (2.18)$$

In terms of τ , this equation can be transformed into

$$\sigma_Y(\tau) = \frac{1}{n_L^{1/2}} \{[1 - \exp(-\tau)] \exp(-\tau)\}^{1/2} \quad (2.19)$$

Note that this expression is identical to Eq. (2.9) for $\zeta(\tau)$. From Eqs. (2.16) and (2.18), the coefficient of variation, $CV_Y(\tau)$, is obtained as

$$CV_Y(t) = \frac{\sigma_Y(t)}{m_Y(t)} = \left\{ \frac{\exp(-\kappa t)}{n_L [1 - \exp(-\kappa t)]} \right\}^{1/2} \quad (2.20)$$

or in terms of τ

$$CV_Y(\tau) = \left\{ \frac{\exp(-\tau)}{n_L [1 - \exp(-\tau)]} \right\}^{1/2} \quad (2.21)$$

Note that this equation is identical to Eq. (2.12) for $CV(\tau)$.

Results and Discussion

The model formulated, in terms of $m_Y(\tau)$ as given in Eq. (2.16), has been regressed on the available experimental data⁴⁰ by resorting to the adaptive random search procedure.^{113, 114} The regression has resulted in the values of κ , which are listed in Table 2.2. These values have rendered it possible to evaluate the dimensionless time, $\tau = (\kappa t)$, as well as the mean, $m_Y(\tau)$, from Eq. (2.17), whose values are plotted in Figure 2.3 as a function of τ . The corresponding experimentally measured values of the fractional conversion of the carbonaceous substrate into

Table 2.2. Values of κ for the Formation of ACs at Different Temperatures.

| temperature, K (C) | $\kappa, \text{s}^{-1} \cdot 10^4 \text{ (min}^{-1}\text{)}$ |
|--------------------|--|
| 973 (699.85) | 4.38 (0.026) |
| 1023 (749.85) | 5.94 (0.036) |
| 1073 (799.85) | 8.36 (0.050) |
| 1123 (849.85) | 13.16 (0.079) |
| 1173 (899.85) | 24.93 (0.150) |

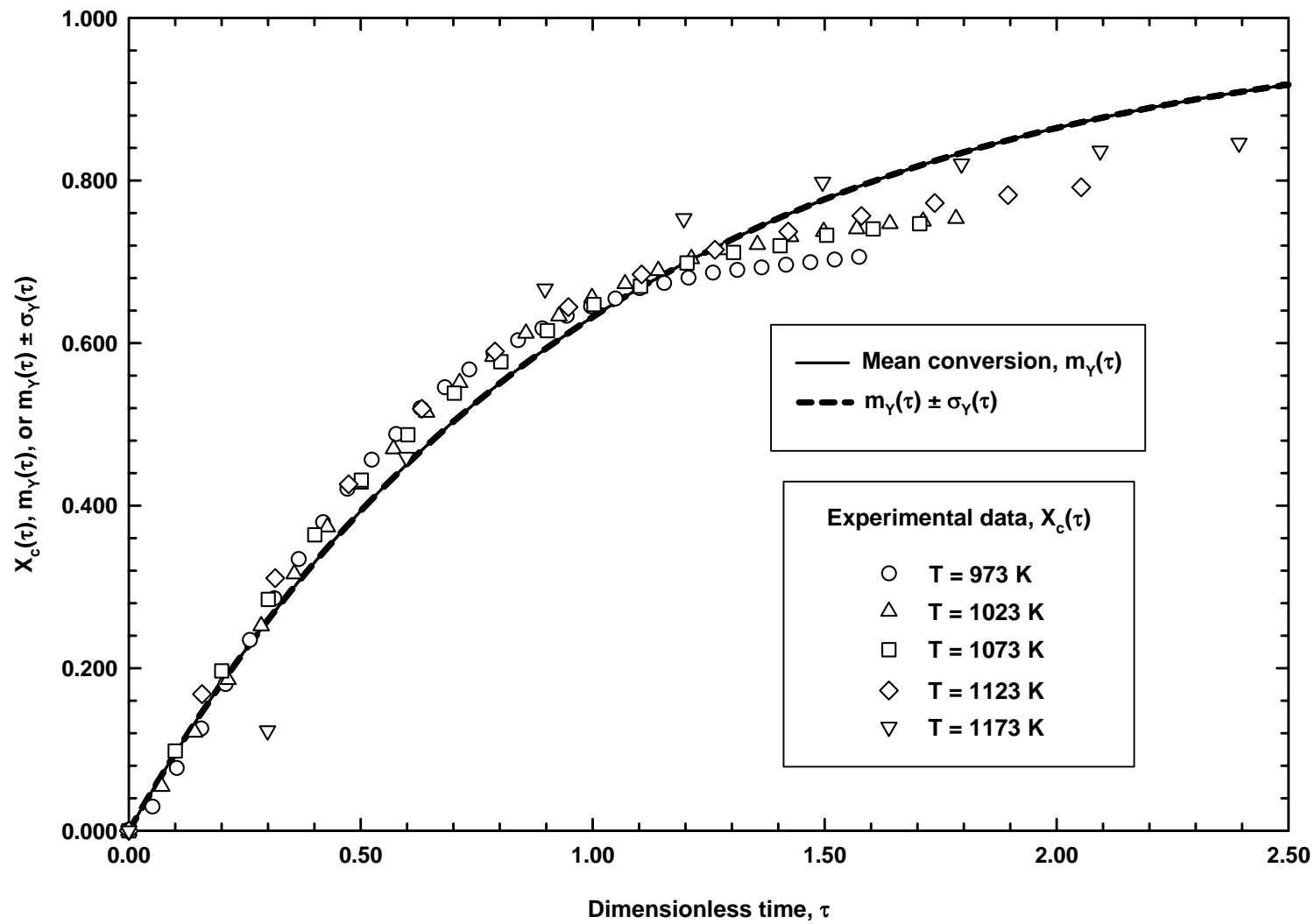


Figure 2.3. Mean fractional conversion $m_Y(\tau)$ and standard deviation envelope $[m_Y(\tau) \pm \sigma_Y(\tau)]$ as functions of dimensionless time τ for the formation of ACs.

ACs, denoted as $X_c(\tau)$, are superimposed in the same figure for comparison. Clearly, $m_Y(\tau)$ increases and asymptotically approaches to 1 as τ progresses; this asymptotic value for $m_Y(\tau)$ can be discerned from Eq. (2.17). The normalized standard deviation, $\sigma_Y(\tau)$, as computed by Eq. (2.19), signifies the deviations attributable to the internal or characteristic noises of the process as predicted by the stochastic model.¹⁰⁹ The standard deviation envelope, i.e., $m_Y(\tau) \pm \sigma_Y(\tau)$, is plotted in Figure 2.3. Note that the majority of the experimental data⁴⁰ lie appreciably beyond the expected variation, or scattering; this is almost always the case: The overall deviations of the experimental data include not only those attributable to the internal noises of the process as predicted by the model, but also to the external noises due to unavoidable measurement errors and instrumental deficiencies that can never be totally eliminated. The coefficient of variation, $CV(t)$, as defined by Eq. (2.11), provides a more meaningful relative measurement of the variability or dispersion of the values of a random variable about their mean than the standard deviation, $\sigma(t)$. In general, the smaller the values of random variable $N(t)$, i.e., the population size, the greater the extent of the expected fluctuations about their mean.

Clearly, Eq. (2.19) for $\sigma_Y(\tau)$ depends on n_L , i.e., the maximum number of pores that could form on the carbonaceous substrate's internal surfaces per unit weight of activated substrate. The number of pores on ACs is profoundly large,^{115, 116} thus, it is reasonable to expect that the value of n_L be enormous. The order of magnitude estimate of n_L is obtained by dividing the total volume of pores per unit weight of ACs by the volume of a single pore. The former can be obtained from the experimental characterization of ACs produced from a carbonaceous substrate under specific activation conditions, and the latter can be computed under the assumption that the shape of the pore is perfectly cylindrical. For illustration, the total volume of pores for ACs prepared at 873 K is 0.96 cm³ per gram of ACs.⁴⁰ Moreover, the volume of a single pore is given by

$$v_p = \pi(\bar{r})^2 \ell \quad (2.22)$$

where \bar{r} and ℓ are the pore's average radius and the pore's length, respectively. For a perfectly cylindrical pore, \bar{r} can be expressed as¹¹⁷

$$\bar{r} = \frac{2 \varepsilon_s}{\rho_s S_g} \quad (2.23)$$

where ε_s , ρ_s , and S_g are structural properties of ACs, specifically, their porosity, apparent density, and surface area per unit weight of ACs, respectively. For ACs prepared at 873 K, the corresponding values of these properties are 0.66, 0.69 g · cm⁻³, and 1,366 m² · g⁻¹,⁴⁰ thereby yielding \bar{r} as 1.40 nm. By changing ℓ from 1 nm to 50 nm, the volume of a single pore, v_p , varies from 6.16 · 10⁻²¹ cm³ to 3.08 · 10⁻¹⁹ cm³ as computed from Eq. (2.22). Thus, the value of n_L falls within the range between 3.12 · 10¹⁸ and 1.56 · 10²⁰ pores per gram of ACs.

The parameter, κ , in Eq. (2.16) has the connotation of kinetic constant. Thus, it is temperature dependent and varies according to the Arrhenius law; hence,

$$\kappa = \kappa_0 \exp\left(-\frac{E_a}{RT}\right) \quad (2.24)$$

where κ_0 is the frequency factor and E_a the activation energy.

Figure 2.4 exhibits the Arrhenius plot of the values of κ against their corresponding values of inverse temperature for the available experimental data.⁴⁰ From this plot, κ_0 and E_a are computed as 7.88 s⁻¹ and 80.2 kJ · mol⁻¹, respectively. These values differ from those obtained by Guo and Lua⁴⁰ of 1.26 · 10⁻³ s⁻¹ and 38.7 kJ · mol⁻¹, respectively, on the basis of a non-linear kinetic model.

Summary

A stochastic model has been derived for the formation of ACs from carbonaceous substrates. Specifically, the model is based on a pure-birth process with a linear intensity of transition. The mean and variance of the conversion of a carbonaceous substrate into ACs, have been computed from the master equation of the pure-birth process. The model has been validated by fitting it to the available experimental data. The mean values of the model at various times follow the general trend of these data. As expected, the data's fluctuations around the mean values are more noticeable than those predicted by the model: In addition to the process' internal noises, the deviations of the experimental data also account for the external noises due to unavoidable measurement errors.

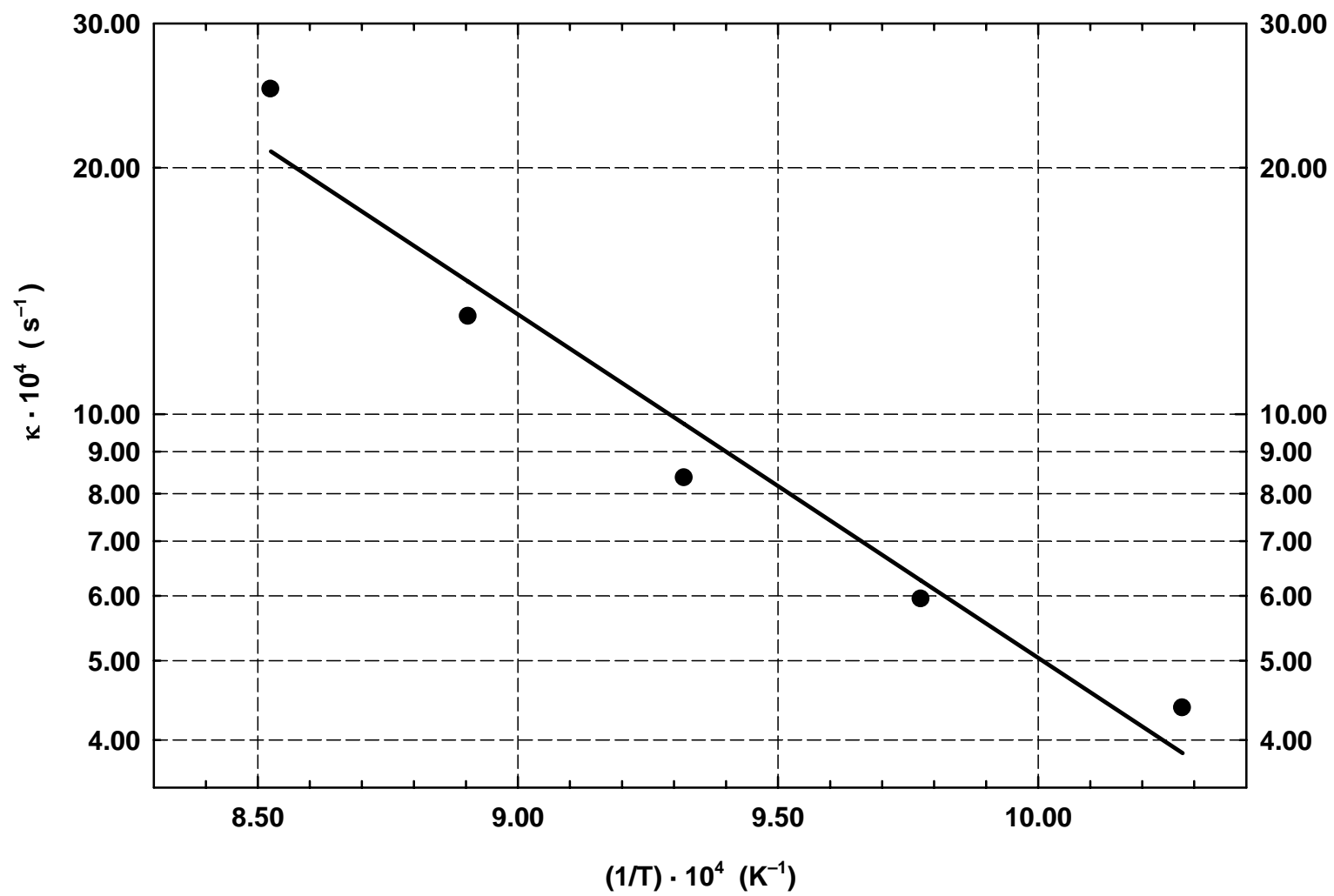


Figure 2.4. Arrhenius plot for the kinetic constant, κ .

Notation

$m(t)$ = mean of the random variable, $N(t)$

$m_Y(t)$ = mean of the experimental measurable variable, $Y(t)$, mg C

$N(t)$ = random variable representing the number of pores that have already formed on the internal surfaces of ACs at time t

n = realization of the random variable, $N(t)$

$p_n(t)$ = probability that n pores have formed at time t

t = time

$Y(t)$ = experimentally measurable variable representing the conversion of a carbonaceous substrate into ACs

Greek letters

κ = kinetic constant in the intensity of birth, $(t)^{-1}$

$\lambda_n(t)$ = intensity of birth for the pure-birth process in state n at time t

$\sigma^2(t)$ = variance of the random variable, $N(t)$

$\sigma_Y^2(t)$ = variance of the experimentally measurable variable, $Y(t)$

τ = dimensionless time

CHAPTER 3 - Formation of Carbon Molecular Sieves by Carbon Deposition: Pure-Birth Process with a Non-Linear Intensity of Transition Based on a Single Random Variable

As indicated in the introductory chapter, the formation of CMSs due to the narrowing of pores by carbon deposition is analyzed and modeled herein as a pure-birth process with a non-linear intensity of transition based on a single random variable. In general, it is reasonable to consider that the driving force, or potential, of the pore-narrowing process by carbon deposition is a function of the number of carbon packets, or packets, that deposit onto the pores' mouths, which increases with time.¹⁰⁹ In this chapter, the form of such a function is of the second-order, thereby incorporating into the model the effect of collisions or interactions between pairs of carbon packets as they deposit onto the pores' mouths of ACs. Hence, the corresponding intensity function is non-linear in the number of packets to be deposited. For brevity, the pore-narrowing process under consideration is referred to as pore-narrowing hereafter.

Identification of Random Variable and State Space

The available experimental data for formation of CMSs are usually given in terms of the weight of carbon aggregates, or packets, deposited on ACs.^{8, 65, 118, 119} It would be plausible to equate the weight gain due to the deposition of carbon packets to the number of such packets.^{109, 110} In this connection, the number of packets that have already deposited onto the pores' mouths, thereby causing them to narrow, at time t is taken as the random variable of the process, $N(t)$, whose realization is n . All possible values of $N(t)$ are the states of the process and their collection, $\{ 0, 1, 2, \dots, n_M - 1, n_M \}$, is its state space where n_M is the number of packets that would deposit onto the maximum number of pores susceptible to narrowing. Note that the random variable, $N(t)$, in the current model exclusively accounts for the number of packets that have already deposited onto the pores' mouths at any time t ; hence, the analysis of the change in

the pores' sizes or lengths would require the formulation of models with different variables designated as the random variables.

Transition Diagram

The transition diagram of the process is presented in Figure 3.1. The circles indicate the system's possible states as identified in the preceding section, and the arrows describe transitions of the system at any moment.

Master Equation

For the pure-birth process, the probability balance around state n leads to

$$\frac{d}{dt}p_n(t) = \lambda_{n-1}(t)p_{n-1}(t) - \lambda_n(t)p_n(t), \quad n = 0, 1, 2, \dots, n_M - 1, n_M \quad (3.1)$$

which is the master, i.e., governing, equation of the process;^{71, 73} see Appendix A. The term, $p_n(t)$, in the above expression denotes the probability that n carbon packets, or packets, have deposited at time t . Moreover, the intensity of birth, $\lambda_n(t)$, in Eq. (3.1) is given by

$$\lambda_n(t) = \frac{dn}{dt} = \alpha(n_M - n)^2 \quad (3.2)$$

where α is a proportionality constant. In this equation, the term, $(n_M - n)$, is the number of packets yet to deposit onto the pores' mouths at time t . Inserting Eq. (3.2) into Eq. (3.1) yields

$$\begin{aligned} & \frac{d}{dt}p_n(t) \\ & = \{\alpha[n_M - (n-1)]^2\}p_{n-1}(t) - [\alpha(n_M - n)^2]p_n(t), \quad n = 0, 1, 2, \dots, n_M - 1, n_M \end{aligned} \quad (3.3)$$

Clearly, the above equation depends on realization n but is independent of time t .

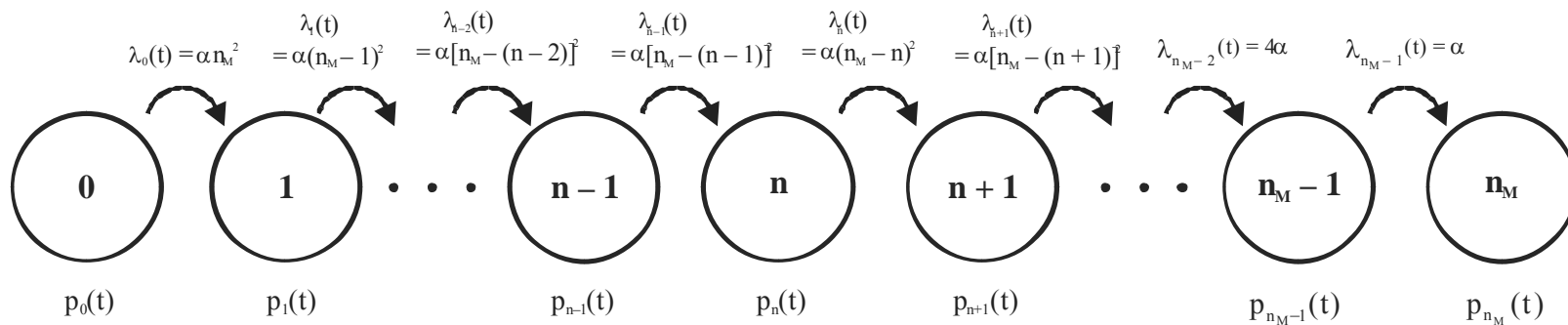


Figure 3.1. Transition diagram of the pure-birth process representing pore-narrowing on ACs: The symbols, $0, 1, 2, \dots, (n-1), n, (n+1), \dots, (n_M-1), n_M$, are the states of the process; $p_0(t), p_1(t), \dots, p_{n-1}(t), p_n(t), p_{n+1}(t), \dots, p_{n_M-1}(t), p_{n_M}(t)$, are the corresponding state probabilities; and $\lambda_n(t) = \alpha(n_M - n)^2$ is the intensity of birth, which is a non-linear function of n for each transition.

Mean and Variance

The mean and variance of the process are evaluated by solving the process' master equation, Eq. (3.3). Clearly, the intensity of birth, $\lambda_n(t)$, is embedded in the master equation; for the process of concern, $\lambda_n(t)$ is non-linear as given by Eq. (3.2). The non-linearity arising from the intensity of birth renders the solution of the master equation exceedingly complex to obtain. Nevertheless, this complexity can be circumvented by resorting to a rational approximation method, the system-size expansion of the master equation; see Appendix C. The system-size expansion entails that the random variable, $N(t)$, be expressed as the sum of the macroscopic term, $\Omega\varphi(t)$, and the fluctuation term, $\Omega^{1/2}\Xi(t)$. The symbol, Ω , is the system's size, which is n_M in this work. Hence, the system-size expansion of the master equation yields the macroscopic equation in terms of $\varphi(t)$ governing the overall, i.e., mean, behavior of the process, and the equation in terms of $\Xi(t)$ governing the fluctuations of the process around the macroscopic values. Integration of the macroscopic equation results in an explicit expression for $\varphi(t)$. This expression, in turn, yields the mean of $N(t)$, $E[N(t)]$ or $m(t)$, of the pore-narrowing as

$$m(t) = n_M \left(\frac{\alpha't}{\alpha't+1} \right) \quad (3.4)$$

where $\alpha' = (\alpha n_M)$. From this expression, the normalized form of the mean, $\eta(\tau)$, is

$$\eta(\tau) = \frac{m(\tau)}{n_M} = \left(\frac{\tau}{\tau+1} \right) \quad (3.5)$$

where $\tau = (\alpha't)$ is the dimensionless time. Similarly, from the equation governing the fluctuations, the variance of $N(t)$, $\text{Var}[N(t)]$ or $\sigma^2(t)$, of the pore-narrowing is

$$\sigma^2(t) = \frac{n_M}{3(\alpha't+1)} \left[1 - \frac{1}{(\alpha't+1)^3} \right] \quad (3.6)$$

or in terms of dimensionless time τ ,

$$\sigma^2(\tau) = \frac{n_M}{3(\tau+1)} \left[1 - \frac{1}{(\tau+1)^3} \right] \quad (3.7)$$

The standard deviation, $\sigma(t)$, is the square root of the variance, $\sigma^2(t)$; thus,

$$\sigma(t) = \left\{ \frac{n_M}{3(\alpha't+1)} \left[1 - \frac{1}{(\alpha't+1)^3} \right] \right\}^{1/2} \quad (3.8)$$

From this equation, the normalized form of the standard deviation, $\zeta(\tau)$, is obtained as

$$\zeta(\tau) = \frac{\sigma(\tau)}{n_M} = \left\{ \frac{1}{3n_M(\tau+1)} \left[1 - \frac{1}{(\tau+1)^3} \right] \right\}^{1/2} \quad (3.9)$$

Note that this expression is a function of τ and n_M . The standard deviation relative to the mean, termed the coefficient of variation, is defined as¹¹²

$$CV(t) = \frac{\sigma(t)}{m(t)} \quad (3.10)$$

Inserting Eqs. (3.4) and (3.8) for $m(t)$ and $\sigma(t)$, respectively, into the above equation yields the coefficient of variation, $CV(t)$, of the pore-narrowing as

$$CV(t) = \frac{1}{(\alpha't)} \left\{ \frac{(\alpha't+1)}{3n_M} \left[1 - \frac{1}{(\alpha't+1)^3} \right] \right\}^{1/2} \quad (3.11)$$

or in terms of dimensionless time τ ,

$$CV(\tau) = \frac{1}{\tau} \left\{ \frac{(\tau+1)}{3n_M} \left[1 - \frac{1}{(\tau+1)^3} \right] \right\}^{1/2} \quad (3.12)$$

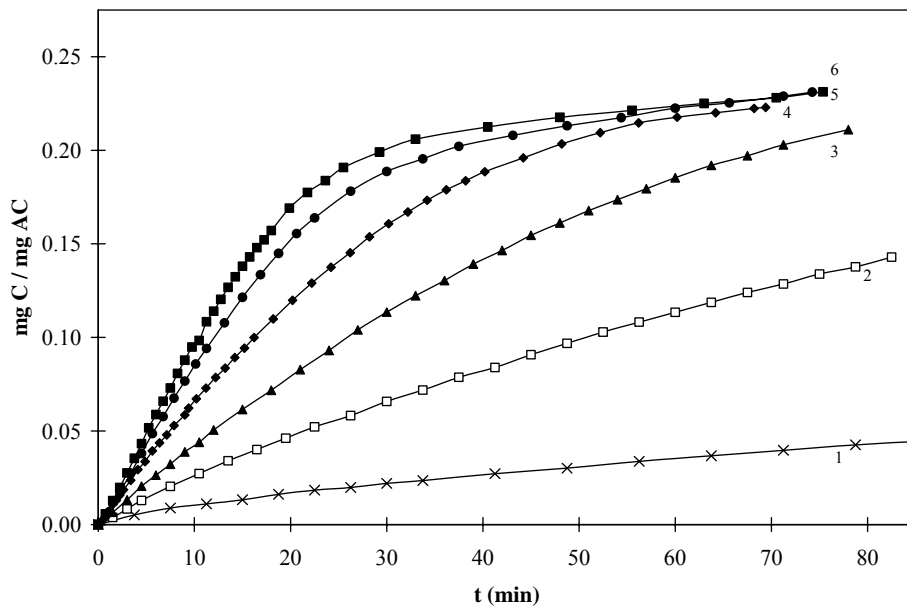
Note that this expression is also a function of τ and n_M .

Analysis of Experimental Data

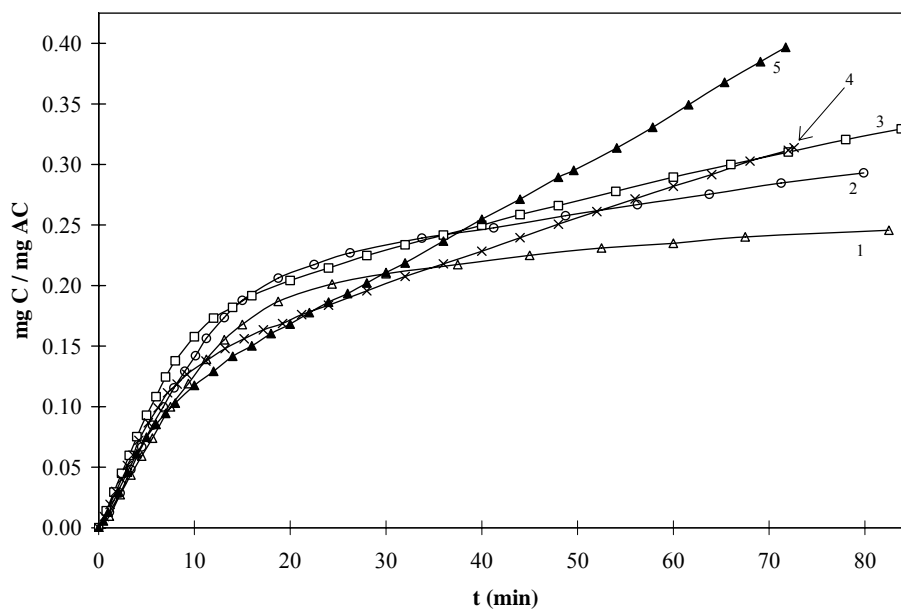
As illustrated in Figure 3.2, the available experimental data are presented in terms of the temporal increase in the amount of carbon deposited per unit weight of ACs at eleven temperatures. Specifically, they are given in the unit of milligrams of carbon per milligram of ACs, i.e., mg C/mg AC,⁶⁵ as listed in Table 3.1. The model derived in this work is validated with these data. To fit the model to the data, the number of carbon packets that have narrowed the pores, which is the random variable, $N(t)$, needs to be related to the experimentally measurable variable, $W(t)$, representing the weight of carbon already deposited on ACs. At any time t , $W(t)$ should be proportional to $N(t)$; thus,

$$W(t) = \omega N(t) \quad (3.13)$$

where ω is the weight of a single packet of carbon. The mean value of $W(t)$, denoted by $m_W(t)$, is obtained from the above expression as follows:



(a)



(b)

Figure 3.2. Experimentally measured weights of carbon deposited (C) on activated carbon (AC) at different temperatures: (a) 1 – 873 K, 2 – 923 K, 3 – 948 K, 4 – 973 K, 5 – 1023 K, and 6 – 1048 K; (b) 1 – 1073 K, 2 – 1098 K, 3 – 1123 K, 4 – 1173 K, and 5 – 1223 K.*

* Data were obtained with activated carbon ACW.⁶⁵

Table 3.1. Experimentally Measured Weights of Carbon Deposited (C) on Activated Carbon (AC) at Different Temperatures*

| T = 873 K | | T = 923 K | | T = 948 K | | T = 973 K | |
|-----------|------------|-----------|------------|-----------|------------|-----------|------------|
| t, min | mg C/mg AC | t, min | mg C/mg AC | t, min | mg C/mg AC | t, min | mg C/mg AC |
| 0.00 | 0.000 | 0.00 | 0.000 | 0.00 | 0.000 | 0.00 | 0.000 |
| 3.75 | 0.005 | 1.50 | 0.004 | 1.50 | 0.007 | 0.38 | 0.002 |
| 7.50 | 0.009 | 3.00 | 0.008 | 3.00 | 0.013 | 0.75 | 0.004 |
| 11.25 | 0.011 | 4.50 | 0.013 | 4.50 | 0.021 | 1.13 | 0.007 |
| 15.00 | 0.013 | 7.50 | 0.020 | 6.00 | 0.026 | 1.50 | 0.011 |
| 18.75 | 0.016 | 10.50 | 0.027 | 7.50 | 0.032 | 1.88 | 0.013 |
| 22.50 | 0.018 | 13.50 | 0.034 | 9.00 | 0.039 | 2.25 | 0.016 |
| 26.25 | 0.020 | 16.50 | 0.040 | 10.50 | 0.044 | 2.63 | 0.019 |
| 30.00 | 0.022 | 19.50 | 0.046 | 12.00 | 0.051 | 3.38 | 0.024 |
| 33.75 | 0.024 | 22.50 | 0.052 | 15.00 | 0.062 | 4.13 | 0.029 |
| 41.25 | 0.027 | 26.25 | 0.058 | 18.00 | 0.072 | 4.88 | 0.034 |
| 48.75 | 0.030 | 30.00 | 0.066 | 21.00 | 0.083 | 5.63 | 0.039 |
| 56.25 | 0.034 | 33.75 | 0.072 | 24.00 | 0.093 | 6.38 | 0.044 |
| 63.75 | 0.037 | 37.50 | 0.079 | 27.00 | 0.104 | 7.13 | 0.048 |
| 71.25 | 0.040 | 41.25 | 0.084 | 30.00 | 0.114 | 7.88 | 0.053 |
| 78.75 | 0.043 | 45.00 | 0.091 | 33.00 | 0.122 | 9.00 | 0.059 |
| 86.25 | 0.045 | 48.75 | 0.097 | 36.00 | 0.130 | 9.40 | 0.062 |
| 93.75 | 0.048 | 52.50 | 0.103 | 39.00 | 0.139 | 10.20 | 0.067 |
| 101.25 | 0.051 | 56.25 | 0.108 | 42.00 | 0.147 | 11.20 | 0.073 |
| 104.25 | 0.051 | 60.00 | 0.113 | 45.00 | 0.155 | 12.20 | 0.079 |
| | | 63.75 | 0.119 | 48.00 | 0.161 | 13.20 | 0.084 |
| | | 67.50 | 0.124 | 51.00 | 0.168 | 14.20 | 0.089 |
| | | 71.25 | 0.129 | 54.00 | 0.174 | 15.20 | 0.094 |
| | | 75.00 | 0.134 | 57.00 | 0.179 | 16.20 | 0.100 |
| | | 78.75 | 0.138 | 60.00 | 0.185 | 18.20 | 0.110 |
| | | 82.50 | 0.143 | 63.75 | 0.192 | 20.20 | 0.120 |
| | | | | 67.50 | 0.197 | 22.20 | 0.129 |
| | | | | 71.25 | 0.203 | 24.20 | 0.138 |
| | | | | 78.00 | 0.211 | 26.20 | 0.145 |
| | | | | | | 28.20 | 0.154 |
| | | | | | | 30.20 | 0.161 |
| | | | | | | 32.20 | 0.167 |
| | | | | | | 34.20 | 0.173 |
| | | | | | | 36.20 | 0.179 |
| | | | | | | 38.20 | 0.184 |
| | | | | | | 40.20 | 0.189 |
| | | | | | | 44.20 | 0.196 |
| | | | | | | 48.20 | 0.203 |
| | | | | | | 52.20 | 0.209 |
| | | | | | | 56.20 | 0.215 |
| | | | | | | 60.20 | 0.218 |
| | | | | | | 64.20 | 0.220 |
| | | | | | | 68.20 | 0.222 |
| | | | | | | 69.40 | 0.223 |

* Data were obtained with activated carbon ACW.⁶⁵

Table 3.1. (Cont'd.)

| T = 1023 K | | T = 1048 K | | T = 1073 K | | T = 1098 K | |
|-------------------|------------|-------------------|------------|-------------------|------------|-------------------|------------|
| t, min | mg C/mg AC | t, min | mg C/mg AC | t, min | mg C/mg AC | t, min | mg C/mg AC |
| 0.00 | 0.000 | 0.00 | 0.000 | 0.00 | 0.000 | 0.00 | 0.000 |
| 1.13 | 0.007 | 0.75 | 0.006 | 1.13 | 0.010 | 1.13 | 0.013 |
| 2.25 | 0.017 | 1.50 | 0.013 | 2.25 | 0.027 | 2.25 | 0.029 |
| 3.38 | 0.027 | 2.25 | 0.020 | 3.38 | 0.044 | 3.38 | 0.048 |
| 4.50 | 0.038 | 3.00 | 0.028 | 4.50 | 0.059 | 4.50 | 0.067 |
| 5.63 | 0.049 | 3.75 | 0.035 | 5.63 | 0.074 | 5.63 | 0.085 |
| 6.75 | 0.058 | 4.50 | 0.043 | 7.50 | 0.100 | 6.75 | 0.100 |
| 7.88 | 0.068 | 5.25 | 0.052 | 9.38 | 0.119 | 7.88 | 0.116 |
| 9.00 | 0.077 | 6.00 | 0.059 | 11.25 | 0.139 | 9.00 | 0.129 |
| 10.13 | 0.086 | 6.75 | 0.066 | 13.13 | 0.155 | 10.13 | 0.142 |
| 11.25 | 0.094 | 7.50 | 0.073 | 15.00 | 0.168 | 11.25 | 0.156 |
| 13.13 | 0.108 | 8.25 | 0.081 | 18.75 | 0.187 | 13.13 | 0.174 |
| 15.00 | 0.121 | 9.00 | 0.088 | 24.38 | 0.201 | 15.00 | 0.188 |
| 16.88 | 0.134 | 9.75 | 0.095 | 30.00 | 0.210 | 18.75 | 0.206 |
| 18.75 | 0.145 | 10.50 | 0.098 | 37.50 | 0.217 | 22.50 | 0.217 |
| 20.63 | 0.156 | 11.25 | 0.108 | 45.00 | 0.225 | 26.25 | 0.227 |
| 22.50 | 0.164 | 12.00 | 0.114 | 52.50 | 0.231 | 33.75 | 0.239 |
| 26.25 | 0.178 | 12.75 | 0.120 | 60.00 | 0.235 | 41.25 | 0.248 |
| 30.00 | 0.189 | 13.50 | 0.127 | 67.50 | 0.240 | 48.75 | 0.258 |
| 33.75 | 0.195 | 14.25 | 0.132 | 82.50 | 0.246 | 56.25 | 0.267 |
| 37.50 | 0.202 | 15.00 | 0.138 | | | 63.75 | 0.275 |
| 43.13 | 0.208 | 15.75 | 0.143 | | | 71.25 | 0.285 |
| 48.75 | 0.213 | 16.50 | 0.148 | | | 79.88 | 0.293 |
| 54.38 | 0.217 | 17.25 | 0.152 | | | | |
| 60.00 | 0.223 | 18.00 | 0.157 | | | | |
| 65.63 | 0.225 | 19.88 | 0.169 | | | | |
| 71.25 | 0.229 | 21.75 | 0.178 | | | | |
| 74.25 | 0.231 | 23.63 | 0.184 | | | | |
| | | 25.50 | 0.191 | | | | |
| | | 29.25 | 0.199 | | | | |
| | | 33.00 | 0.206 | | | | |
| | | 40.50 | 0.212 | | | | |
| | | 48.00 | 0.218 | | | | |
| | | 55.50 | 0.221 | | | | |
| | | 63.00 | 0.225 | | | | |
| | | 70.50 | 0.228 | | | | |
| | | 75.38 | 0.231 | | | | |

Table 3.1. (Cont'd.)

| T = 1123 K | | T = 1173 K | | T = 1223 K | |
|------------|------------|------------|------------|------------|------------|
| t, min | mg C/mg AC | t, min | mg C/mg AC | t, min | mg C/mg AC |
| 0.00 | 0.000 | 0.00 | 0.000 | 0.00 | 0.000 |
| 0.80 | 0.014 | 0.60 | 0.009 | 0.50 | 0.006 |
| 1.60 | 0.029 | 1.20 | 0.019 | 1.00 | 0.013 |
| 2.40 | 0.045 | 1.80 | 0.030 | 2.00 | 0.029 |
| 3.20 | 0.060 | 2.40 | 0.040 | 3.00 | 0.046 |
| 4.00 | 0.075 | 3.00 | 0.051 | 4.00 | 0.061 |
| 5.00 | 0.093 | 3.60 | 0.060 | 5.00 | 0.075 |
| 6.00 | 0.108 | 4.20 | 0.072 | 6.00 | 0.085 |
| 7.00 | 0.125 | 5.20 | 0.087 | 7.00 | 0.095 |
| 8.00 | 0.138 | 6.20 | 0.099 | 8.00 | 0.103 |
| 10.00 | 0.158 | 7.20 | 0.111 | 10.00 | 0.118 |
| 12.00 | 0.173 | 8.20 | 0.119 | 12.00 | 0.129 |
| 14.00 | 0.182 | 9.20 | 0.127 | 14.00 | 0.142 |
| 16.00 | 0.192 | 11.20 | 0.138 | 16.00 | 0.150 |
| 20.00 | 0.204 | 13.20 | 0.148 | 18.00 | 0.160 |
| 24.00 | 0.214 | 15.20 | 0.156 | 20.00 | 0.168 |
| 28.00 | 0.225 | 17.20 | 0.163 | 22.00 | 0.178 |
| 32.00 | 0.234 | 19.20 | 0.169 | 24.00 | 0.186 |
| 36.00 | 0.242 | 21.20 | 0.176 | 26.00 | 0.193 |
| 40.00 | 0.250 | 24.00 | 0.184 | 28.00 | 0.202 |
| 44.00 | 0.259 | 28.00 | 0.196 | 30.00 | 0.211 |
| 48.00 | 0.266 | 32.00 | 0.208 | 32.00 | 0.219 |
| 54.00 | 0.278 | 36.00 | 0.218 | 36.00 | 0.237 |
| 60.00 | 0.290 | 40.00 | 0.228 | 40.00 | 0.255 |
| 66.00 | 0.300 | 44.00 | 0.240 | 44.00 | 0.271 |
| 72.00 | 0.310 | 48.00 | 0.251 | 48.00 | 0.289 |
| 78.00 | 0.321 | 52.00 | 0.261 | 49.60 | 0.295 |
| 83.80 | 0.329 | 56.00 | 0.272 | 54.10 | 0.314 |
| | | 60.00 | 0.282 | 57.85 | 0.331 |
| | | 64.00 | 0.292 | 61.60 | 0.349 |
| | | 68.00 | 0.303 | 65.35 | 0.368 |
| | | 72.00 | 0.312 | 69.10 | 0.385 |
| | | 72.60 | 0.314 | 71.73 | 0.397 |

$$\begin{aligned}
m_w(t) &= E[W(t)] \\
&= E[\omega N(t)] \\
&= \omega E[N(t)]
\end{aligned}$$

or

$$m_w(t) = \omega m(t)$$

Substituting Eq. (3.4) for $m(t)$ into this equation yields

$$m_w(t) = \omega n_M \left(\frac{\alpha' t}{\alpha' t + 1} \right)$$

or

$$m_w(t) = W_M \left(\frac{\alpha' t}{\alpha' t + 1} \right) \quad (3.14)$$

where W_M , or (ωn_M) , is the weight of carbon that would deposit onto the maximum number of pores susceptible to narrowing. In terms of dimensionless time τ , the above equation can be rewritten as

$$m_w(\tau) = W_M \left(\frac{\tau}{\tau + 1} \right) \quad (3.15)$$

From this expression, the normalized form of the mean, $\eta_w(\tau)$, is,

$$\eta_w(\tau) = \frac{m_w(\tau)}{W_M} = \left(\frac{\tau}{\tau + 1} \right) \quad (3.16)$$

Note that this expression is identical to Eq. (3.5) for $\eta(\tau)$. Similarly, the variance of $W(t)$, $\sigma_w^2(t)$, is obtained from Eq. (3.13) as

$$\begin{aligned}
\sigma_w^2(t) &= \text{Var}[W(t)] \\
&= \text{Var}[\omega N(t)] \\
&= \omega^2 \text{Var}[N(t)]
\end{aligned}$$

or

$$\sigma_w^2(t) = \omega^2 [\sigma^2(t)]$$

Substituting Eq. (3.6) for $\sigma^2(t)$ into the above expression yields

$$\sigma_w^2(t) = \frac{\omega^2 n_M}{3(\alpha' t + 1)} \left[1 - \frac{1}{(\alpha' t + 1)^3} \right]$$

From this equation, the standard deviation of $W(t)$, $\sigma_w(t)$, is,

$$\sigma_w(t) = \omega \left\{ \frac{n_M}{3(\alpha't+1)} \left[1 - \frac{1}{(\alpha't+1)^3} \right] \right\}^{1/2}$$

or

$$\sigma_w(t) = W_M \left\{ \frac{1}{3n_M(\alpha't+1)} \left[1 - \frac{1}{(\alpha't+1)^3} \right] \right\}^{1/2}$$

In terms of dimensionless time τ , this equation can be transformed into

$$\sigma_w(\tau) = W_M \left\{ \frac{1}{3n_M(\tau+1)} \left[1 - \frac{1}{(\tau+1)^3} \right] \right\}^{1/2} \quad (3.17)$$

From this expression, the normalized form of the standard deviation, $\zeta_w(\tau)$, is,

$$\zeta_w(\tau) = \frac{\sigma_w(\tau)}{W_M} = \left\{ \frac{1}{3n_M(\tau+1)} \left[1 - \frac{1}{(\tau+1)^3} \right] \right\}^{1/2} \quad (3.18)$$

Note that this equation is identical to Eq. (3.9) for $\zeta(\tau)$. From Eqs. (3.15) and (3.17), the coefficient of variation, $CV_w(\tau)$, is obtained as

$$CV_w(\tau) = \frac{\sigma_w(\tau)}{m_w(\tau)} = \frac{1}{\tau} \left\{ \frac{(\tau+1)}{3n_M} \left[1 - \frac{1}{(\tau+1)^3} \right] \right\}^{1/2} \quad (3.19)$$

Note that this equation is identical to Eq. (3.12) for $CV(\tau)$.

Monte Carlo Simulation

The master equation of the pure-birth process, Eq. (3.1), is stochastically simulated by means of the Monte Carlo method. The two basic procedures to implement the method, one resorting to the event-driven approach^{74, 79, 120-127} and the other resorting to the time-driven approach,^{124, 128} are described in detail; these two approaches differ in the manner of updating the simulation clock of the process' temporal evolution.

Event-driven approach

The event-driven approach advances the simulation clock by a random waiting time, v , which has an exponential distribution.^{74, 122} No event takes place during the time interval, $(t, t+v)$, and only one event occurs at the end of this time interval at which the state of the

system is specified by the probability of transition corresponding to each event. For the pure-birth process of interest, the series of steps to perform the Monte Carlo simulation via the event-driven approach is given below.

Step 1. Define the initial number of carbon packets, n_0 , the total number of simulations, Z_f , and the length of each simulation, t_f . Initialize the simulation counter as $Z \leftarrow 1$.

Step 2. Initialize clock time t , data-recording time θ ,¹²⁹ the realization of $N(t)$ at time t for simulation Z , $n_Z(t)$, and the realization of $N(\theta)$ at time θ for simulation Z , $n_Z(\theta)$, as follows:

$$t \leftarrow t_0$$

$$\theta_0 \leftarrow t_0$$

$$n_Z(t_0) \leftarrow n_0$$

$$n_Z(\theta_0) \leftarrow n_Z(t_0)$$

Step 3. Sample a realization u from the uniform random variable, U , on interval $(0, 1)$. Estimate v according to the following expression,^[74]

$$v = \frac{-1}{[\alpha(n_M - n)^2]} \ell n(1 - u) \quad (3.20)$$

with $n = n_Z(t)$. Note that the denominator on the right-hand side of this expression is the intensity of birth, $\lambda_n(t)$, as given by Eq. (3.2); see Appendices E and F.

Step 4. Advance clock time as $t \leftarrow (t + v)$.

Step 5. If $(\theta < t)$, then continue to the next step; otherwise, continue to Step 8.

Step 6. Compute the sample mean, variance, and standard deviation at time θ as follows:

a. Record the value of realization at θ :

$$n_Z(\theta) \leftarrow n_Z(t - v)$$

b. Store the sum of realizations at θ :

$$\Xi_Z(\theta) \leftarrow \sum_{Z=1}^Z n_Z(\theta)$$

c. Store the sum of squares of realizations at θ :

$$\Phi_Z(\theta) \leftarrow \sum_{Z=1}^Z n_Z^2(\theta)$$

d. Store the square of sum of realizations at θ :

$$\Psi_Z(\theta) \leftarrow \left[\sum_{z=1}^Z n_z(\theta) \right]^2 = [\Xi_Z(\theta)]^2$$

e. Compute the sample mean at θ :^{75, 122, 123}

$$m_Z(\theta) \leftarrow \frac{1}{Z} \sum_{z=1}^Z n_z(\theta) = \frac{1}{Z} \Xi_Z(\theta) \quad (3.21)$$

f. If $1 < Z \leq Z_f$, then compute the sample variance and standard deviation at θ :^{75, 122, 123}

$$s_Z^2(\theta) \leftarrow \frac{1}{(Z-1)} \left\{ \sum_{z=1}^Z n_z^2(\theta) - \frac{1}{Z} \left[\sum_{z=1}^Z n_z(\theta) \right]^2 \right\} = \frac{1}{(Z-1)} \left\{ \Phi_Z(\theta) - \frac{1}{Z} \Psi_Z(\theta) \right\} \quad (3.22)$$

$$s_Z(\theta) \leftarrow [s_Z^2(\theta)]^{1/2} \quad (3.23)$$

Step 7. Advance θ by a conveniently small $\Delta\theta$ as $\theta \leftarrow (\theta + \Delta\theta)$. If $(\theta \leq t_f)$, then return to Step 5; otherwise, continue to Step 10.

Step 8. Determine the state of the system at the end of time interval $(t, t + \nu)$. At this juncture, a birth event occurs, i.e., the population of carbon packets increases by one; thus,

$$n_z(t) \leftarrow [n_z(t - \nu) + 1]$$

$$n_z(\theta) \leftarrow n_z(t)$$

Step 9. Repeat Steps 3 through 8 until t_f is reached.

Step 10. Update simulation counter as $Z \leftarrow (Z + 1)$.

Step 11. Repeat Steps 2 through 10 until Z_f is reached.

Given in Appendix G is the computer code for performing Monte Carlo simulation of the pure-birth process via the event-driven approach as presented above.

Time-driven approach

As briefly indicated at the outset of this section, the time-driven approach^{124, 128} differs from the event-driven approach: It advances the simulation clock by a fixed time increment of Δt , which is sufficiently small so that at most one or no event occurs during time interval $(t, t + \Delta t)$. At the end of this interval, the state of the process is determined by the probability of

transition corresponding to each event. For the pure-birth process of interest, the series of steps to perform the Monte Carlo simulation via the time-driven approach is given below.

Step 1. Define the initial number of carbon packets, n_0 , the total number of simulations, Z_f , and the length of each simulation, t_f . Initialize the simulation counter as $Z \leftarrow 1$. Compute time increment Δt as follows:

$$\Delta t = \frac{1}{[c \lambda_n^M(t)]} \quad (3.24)$$

where c is a constant greater than 1,¹²⁴ and $\lambda_n^M(t)$, the maximum possible value of the intensity of birth; for the pure-birth process, $\lambda_n^M(t) = \alpha n_M^2$.

Step 2. Initialize clock time t , and the realization of $N(t)$ at time t for simulation Z , $n_Z(t)$, as follows:

$$t \leftarrow t_0$$

$$n_Z(t_0) \leftarrow n_0$$

Step 3. Compute the sample mean, variance, and standard deviation at time t as follows:

a. Record the value of realization at t :

$$n_Z(t) \leftarrow n_Z$$

b. Store the sum of realizations at t :

$$\Xi_Z(t) \leftarrow \sum_{Z=1}^Z n_Z(t)$$

c. Store the sum of squares of realizations at t :

$$\Phi_Z(t) \leftarrow \sum_{Z=1}^Z n_Z^2(t)$$

d. Store the square of sum of realizations at t :

$$\Psi_Z(t) \leftarrow \left[\sum_{Z=1}^Z n_Z(t) \right]^2 = [\Xi_Z(t)]^2$$

e. Compute the sample mean at t :

$$m_Z(t) \leftarrow \frac{1}{Z} \sum_{Z=1}^Z n_Z(t) = \frac{1}{Z} \Xi_Z(t) \quad (3.25)$$

f. If $1 < Z \leq Z_f$, then compute the sample variance and standard deviation at t :

$$s_z^2(t) \leftarrow \frac{1}{(Z-1)} \left\{ \sum_{z=1}^Z n_z^2(t) - \frac{1}{Z} \left[\sum_{z=1}^Z n_z(t) \right]^2 \right\} = \frac{1}{(Z-1)} \left\{ \Phi_z(t) - \frac{1}{Z} \Psi_z(t) \right\} \quad (3.26)$$

$$s_z(t) \leftarrow [s_z^2(t)]^{1/2} \quad (3.27)$$

Step 4. Advance time as $t \leftarrow (t + \Delta t)$.

Step 5. Estimate the probability of transition for the birth event as $\{[\lambda_n(t)]\Delta t\}$ with $n = n_z(t)$.

Step 6. Determine the state of the system at the end of time interval $(t, t + \Delta t)$. In this connection, sample a realization u from the uniform random variable U on interval $(0, 1)$ and compare it with $\{[\lambda_n(t)]\Delta t\}$. If $u < \{[\lambda_n(t)]\Delta t\}$, then a birth event occurs; thus,

$$n_z(t) \leftarrow [n_z(t - \Delta t) + 1]$$

Otherwise, no event occurs; hence,

$$n_z(t) \leftarrow n_z(t - \Delta t)$$

Step 7. Repeat Steps 3 through 6 until t_f is reached.

Step 8. Update the simulation counter as $Z \leftarrow (Z + 1)$.

Step 9. Repeat Steps 2 through 8 until Z_f is reached.

Given in Appendix G is the computer code for performing Monte Carlo simulation of the pure-birth process via the time-driven approach as presented above.

Results and Discussion

The model formulated, in terms of $m_w(t)$ as given in Eq. (3.14), has been regressed on the available experimental data⁶⁵ by resorting to the adaptive random search procedure;^{113, 114} it has resulted in the values of W_M and those of α' listed in Table 3.2. These values have rendered it possible to evaluate the dimensionless time, $(\alpha't)$, i.e., τ , and the normalized mean, $\eta_w(\tau)$, from Eq. (3.16), the values of which are plotted in Figure 3.3 as a function of τ . The corresponding experimentally measured weights in milligrams of carbon deposited per milligram of ACs are normalized by dividing them by W_M ; the values of the resultant quantity, denoted as $w(\tau)$, are superimposed in the same figure for comparison. Clearly, $\eta_w(\tau)$ increases and asymptotically

Table 3.2. Values of α' and W_M for the Pore-narrowing at Different Temperatures.

| temperature, K (C) | α' , $s^{-1} \cdot 10^4$ (min^{-1}) | W_M (mg C) |
|----------------------|---|--------------|
| 873 (599.85) | 1.48 (0.009) | 0.105 |
| 923 (649.85) | 1.04 (0.006) | 0.419 |
| 948 (674.85) | 1.62 (0.010) | 0.501 |
| 973 (699.85) | 3.70 (0.022) | 0.385 |
| 1023 (749.85) | 6.68 (0.040) | 0.322 |
| 1048 (774.85) | 8.25 (0.050) | 0.312 |
| 1073 (799.85) | 12.21 (0.073) | 0.296 |
| 1098 (824.85) | 11.13 (0.067) | 0.346 |
| 1123 (849.85) | 11.17 (0.067) | 0.362 |
| 1173 (899.85) | 7.73 (0.046) | 0.378 |
| 1223 (949.85) | 2.77 (0.017) | 0.680 |

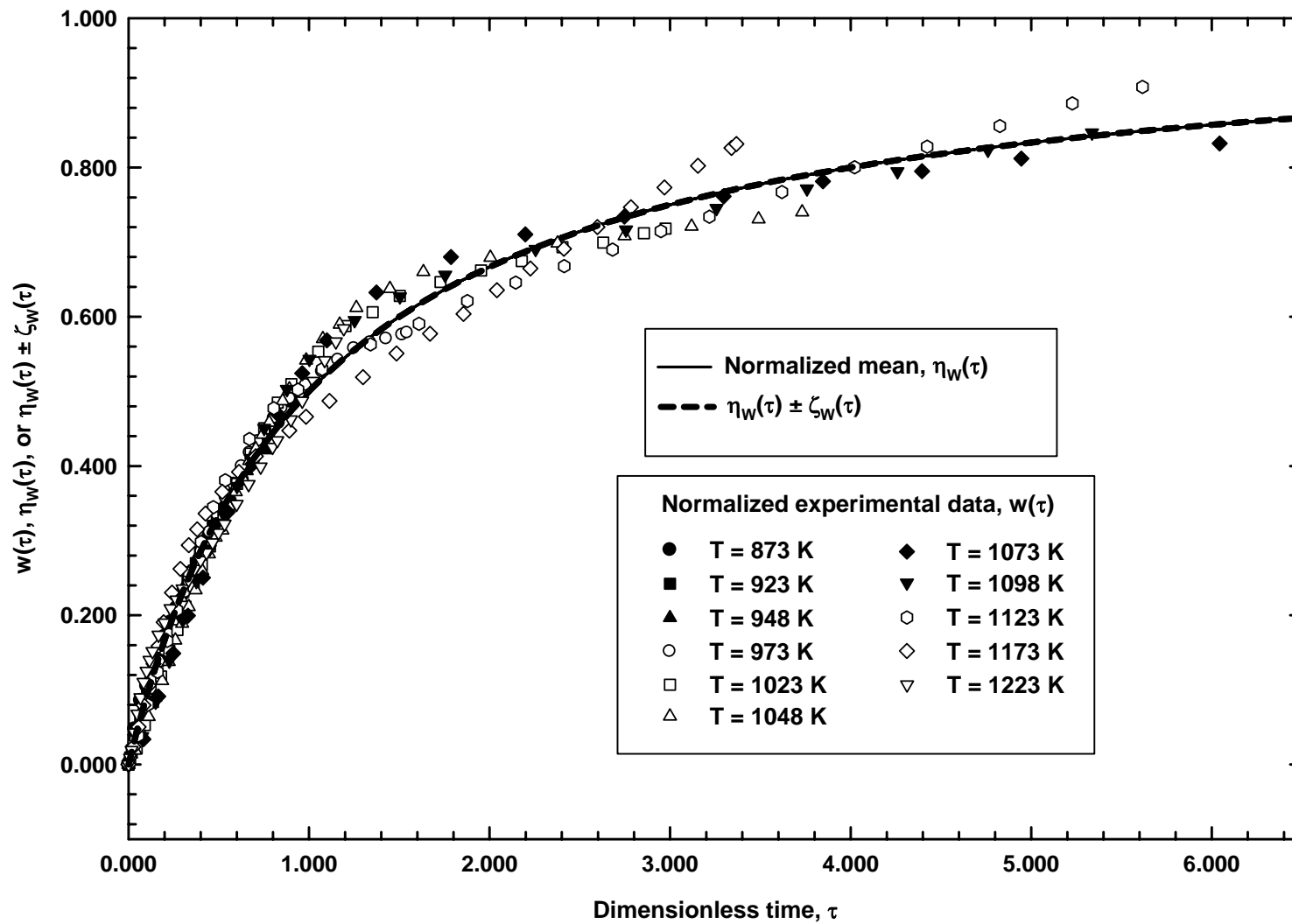


Figure 3.3. Normalized mean $\eta_w(\tau)$ and normalized standard deviation envelope $[\eta_w(\tau) \pm \zeta_w(\tau)]$ as functions of dimensionless time τ for the pore-narrowing.

approaches to 1 as τ progresses; this asymptotic value for $\eta_w(\tau)$ can be discerned from Eq. (3.16). The normalized standard deviation, $\zeta_w(\tau)$, as computed by Eq. (3.18), signifies the deviations attributable to the internal or characteristic noises of the process as predicted by the stochastic model.¹⁰⁹ The normalized standard deviation envelope, i.e., $\eta_w(\tau) \pm \zeta_w(\tau)$, is plotted in Figure 3.3. Note that many of the experimental data⁶⁵ lie appreciably beyond the expected variation, or scattering; this is almost always the case: The overall deviations of the experimental data include not only those attributable to the internal noises of the process as predicted by the model, but also to the external noises due to unavoidable measurement errors and instrumental deficiencies that can never be totally suppressed. The coefficient of variation, $CV(t)$, as defined by Eq. (3.11), provides a more meaningful relative measurement of the variability or dispersion of the values of a random variable about their mean than the standard deviation, $\sigma(t)$. In general, the smaller the values of random variable $N(t)$, i.e., the population size, the greater the extent of the expected fluctuations about their mean.

As evident from Eqs. (3.18) and (3.19), the value of n_M must be estimated in view of the uncertainty involved in its actual value. The order of magnitude estimate of n_M is obtained by dividing the weight of carbon that would deposit onto the maximum number of pores susceptible to narrowing, W_M , at a temperature of reference by the weight of a single packet of carbon, ω . For illustration, the temperature of reference is selected as 973 K, and thus, the value of W_M is 0.385 mg C as listed in Table 3.2. The order of magnitude estimate for ω is obtained by multiplying the volume of a single ideal carbon packet by the density of carbon. The former is assumed to be equivalent to that of a single ideal mesopore, which has been estimated approximately as $3 \cdot 10^{-17} \text{ cm}^3$,¹⁰⁹ and the latter is $2.1 \text{ g} \cdot \text{cm}^{-3}$,¹³⁰ thus, the value of ω is estimated as $0.63 \cdot 10^{-13} \text{ mg C}$. These values of W_M and ω yield the estimate of n_M as $6.12 \cdot 10^{12}$ packets per milligram of ACs.

Figure 3.4 shows the normalized mean, $\eta_w(\tau)$, and the normalized standard deviation envelope, $\eta_w(\tau) \pm \zeta_w(\tau)$, resulting from Monte Carlo simulation via the event-driven and time-driven approaches; these values have been computed by averaging 200 iterations, i.e., $Z = 200$.

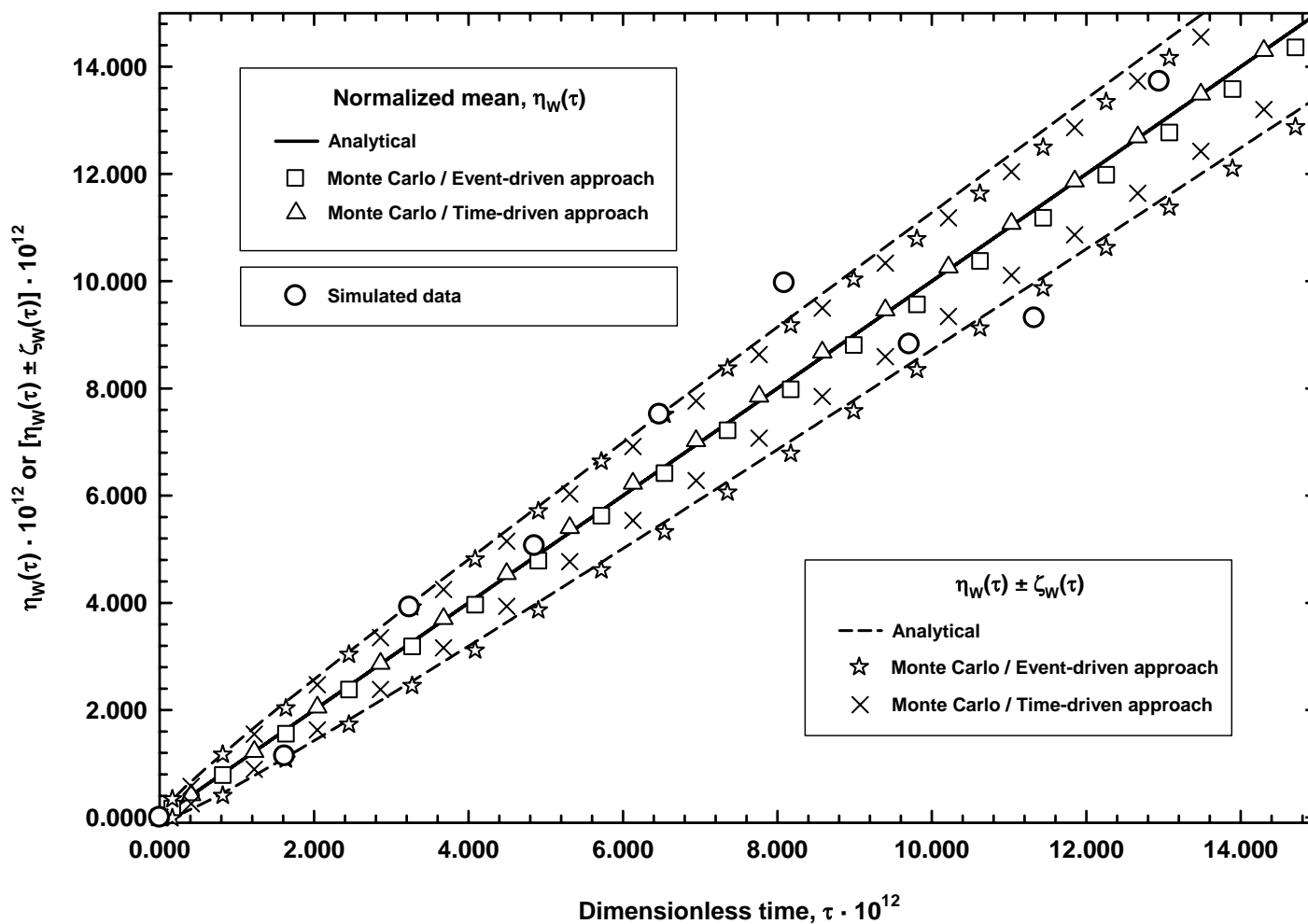


Figure 3.4. Normalized mean $\eta_w(\tau)$ and normalized standard deviation envelope $[\eta_w(\tau) \pm \zeta_w(\tau)]$ as functions of dimensionless time τ at the early stage of the pore-narrowing at 973 K: The average of 200 Monte Carlo simulations via the event-driven and time-driven approaches are compared with the analytical solutions resulting from the system-size expansion of the master equation.

As an example, the simulation has been carried out until the time when approximately 100 carbon packets have deposited onto the mouths of an equal number of open pores on activated carbons at 973 K; this time has been estimated as $7.44 \cdot 10^{-10}$ min; see Appendix H. Thus, the time span of the simulation corresponds to the very outset of the pore-narrowing where the number of carbon packets is small, thereby magnifying the fluctuations of the process about its mean value. Figure 3.4 also presents simulated experimental data to illustrate the process' inherent fluctuations; they have been generated according to the procedure outlined in Appendix H. Moreover, the values of $\eta_w(\tau)$ and $[\eta_w(\tau) \pm \zeta_w(\tau)]$ computed analytically from the system-size expansion of the master equation are superimposed in the same figure for comparison. Note that the results from Monte Carlo simulation are in accord with the corresponding analytical results.

Summary

A stochastic model has been derived for the formation of CMSs by carbon deposition on ACs. Specifically, the model is based on a pure-birth process with a non-linear intensity of transition. The complexity in solving the resultant master equation has been circumvented by resorting to a rational approximation method, system-size expansion. The mean and variance of the amount of carbon deposited onto the open pores of ACs have been computed on the basis of expressions derived from the system-size expansion of the master equation. The model has been validated by fitting it to the available experimental data. The mean values of the model at various times are in good accord with these data. As expected, the data's fluctuations around the mean values are more noticeable than those predicted by the model: In addition to the process' internal noises, the deviations of the experimental data also account for the external noises due to unavoidable measurement errors. Moreover, the non-linear master equation of the model based on the pure-birth process has been simulated by the Monte Carlo method via the event-driven and time-driven approaches at the very outset of the pore-narrowing. The model's mean and variance resultant from Monte Carlo simulation are in line with those obtained analytically based on the system-size expansion of the master equation.

Notation

$m(t)$ = mean of the random variable, $N(t)$

$m_w(t)$ = mean of the experimental measurable variable, $W(t)$, mg C

$N(t)$ = random variable representing the number of carbon packets that have already deposited onto the pores' mouths of ACs at time t

n = realization of the random variable, $N(t)$

$p_n(t)$ = probability that n carbon packets have deposited at time t

t = time

$W(t)$ = experimentally measurable variable representing the weight of carbon already deposited on ACs, mg C

Greek letters

α = proportionality constant in the intensity of birth, $(\text{number})^{-1} \cdot (\text{t})^{-1}$

$\lambda_n(t)$ = intensity of birth for the pure-birth process in state n at time t

$\sigma^2(t)$ = variance of the random variable, $N(t)$

$\sigma_w^2(t)$ = variance of the experimentally measurable variable, $W(t)$

τ = dimensionless time

CHAPTER 4 - Formation of Carbon Molecular Sieves by Carbon Deposition: Pure-Death Process with a Non-Linear Intensity of Transition Based on a Single Random Variable

In this chapter, the formation of CMSs due to the narrowing of pores by carbon deposition is analyzed and modeled as a pure-death process with a non-linear intensity of transition based on a single random variable. This is in contrast to Chapter 3, where the formation of CMSs has been analyzed and modeled as a pure-birth process. In this chapter, it is considered that the driving force of the pore-narrowing process by carbon deposition is a function of not only the number of pores susceptible to narrowing, or open pores, but also of the number of pores that have already been narrowed at any time. Herein, the form of such a function is of the second-order; as a result, the corresponding intensity function is non-linear.

Identification of Random Variable and State Space

As discerned from the prologue, the random variable of the process, $N(t)$, with realization n is identified as the number of pores susceptible to narrowing, i.e., the open pores, at time t . All possible values of $N(t)$ are the states of the process and their collection, $\{ n_0, n_0 - 1, \dots, 2, 1, 0 \}$, is its state space where n_0 is the initial number of open pores, i.e., n at $t = 0$. Note that the random variable, $N(t)$, in the current model exclusively accounts for the number of open pores at any time t ; thus, the analysis of the change in the pores' sizes or lengths would require the formulation of models with different variables designated as the random variables.

Transition Diagram

Figure 4.1 illustrates the transition diagram of the pure-death process under consideration. Note that the transitions of the system in the pure-death process occur in the opposite direction of those in the pure-birth process as presented in Figure 3.1.

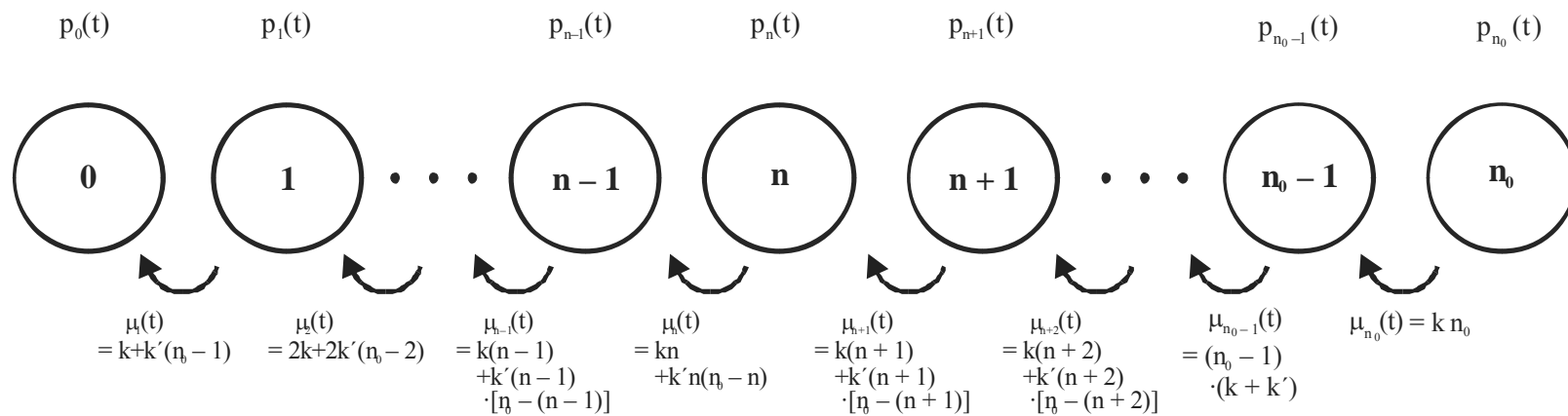


Figure 4.1. Transition diagram of the pure-death process representing pore-narrowing on ACs: The symbols, n_0 , $(n_0 - 1)$, ..., $(n + 1)$, n , $(n - 1)$, ..., 2 , 1 , 0 , are the states of the process; $p_{n_0}(t)$, $p_{n_0-1}(t)$, ..., $p_{n+1}(t)$, $p_n(t)$, $p_{n-1}(t)$, ..., $p_1(t)$, $p_0(t)$, are the corresponding state probabilities; and $\mu_n(t) = kn + k'n(n_0 - n)$ is the intensity of death, which is a non-linear function of n for each transition.

Master Equation

For the pure-death process, the probability balance around state n leads to

$$\frac{d}{dt} p_n(t) = \mu_{n+1} p_{n+1}(t) - \mu_n p_n(t), \quad n = n_0, n_0 - 1, \dots, 2, 1, 0 \quad (4.1)$$

which is the master, i.e., governing, equation of the process;^{71, 73} see Appendix I. The term, $p_n(t)$, in the above expression denotes the probability that n pores are open at time t . Moreover, the term, $\mu_n(t)$, is the intensity function or intensity of death, which is given by

$$\mu_n(t) = -\frac{dn}{dt} = kn + k'n(n_0 - n) \quad (4.2)$$

where k and k' are proportionality constants. In this equation, the term, $(n_0 - n)$, i.e., the difference between the maximum number of open pores and the number of open pores at any time t , is the number of pores that have already been narrowed at time t . Thus, the intensity of death, Eq. (4.2), is a function of not only the number of open pores but also the number of pores that have already been narrowed at time t . Inserting Eq. (4.2) into Eq. (4.1) gives rise to

$$\begin{aligned} & \frac{d}{dt} p_n(t) \\ &= \{k(n+1) + k'(n+1)[n_0 - (n+1)]\} p_{n+1}(t) \\ & \quad - [kn + k'n(n_0 - n)] p_n(t), \quad n = n_0, n_0 - 1, \dots, 2, 1, 0 \end{aligned} \quad (4.3)$$

Clearly, this equation depends on realization n but is independent of time t .

Mean and Variance

The intensity of death, $\mu_n(t)$, as given by Eq. (4.2) is non-linear, thereby rendering the solution of the master equation, Eq. (4.3), exceedingly complex. Thus, the mean and variance of the process need be evaluated via the system-size expansion of the master equation; see Appendix J. Upon expansion, the mean of $N(t)$, $E[N(t)]$ or $m(t)$, for the pore-narrowing is obtained from Eq. (4.3) as

$$m(t) = n_0 \left\{ \frac{1}{1 + \beta[\exp(\alpha t) - 1]} \right\} \quad (4.4)$$

where $\alpha = (k + k'n_0)$ and $\beta = k(k + k'n_0)^{-1}$. From this expression, the normalized, or dimensionless, form of the mean, $\eta(\tau)$, is

$$\eta(\tau) = \frac{m(\tau)}{n_0} = \frac{1}{1 + \beta[\exp(\tau) - 1]} \quad (4.5)$$

where $\tau = (\alpha t)$ is the dimensionless time. Similarly, the variance of $N(t)$, $\text{Var}[N(t)]$ or $\sigma^2(t)$, of the pore-narrowing is

$$\begin{aligned} \sigma^2(t) = n_0 & \frac{\beta \exp(\alpha t)}{\{1 + \beta[\exp(\alpha t) - 1]\}^4} \\ & \cdot \left(2\beta - 1 + \exp(\alpha t) \{1 - 2\beta[1 + (\beta - 1)(\alpha t)] + 2\beta^2 \sinh(\alpha t)\} \right) \end{aligned} \quad (4.6)$$

or in terms of dimensionless time τ ,

$$\begin{aligned} \sigma^2(\tau) = n_0 & \frac{\beta \exp(\tau)}{\{1 + \beta[\exp(\tau) - 1]\}^4} \\ & \cdot \left(2\beta - 1 + \exp(\tau) \{1 - 2\beta[1 + (\beta - 1)\tau] + 2\beta^2 \sinh(\tau)\} \right) \end{aligned} \quad (4.7)$$

From Eq. (4.6), the standard deviation, $\sigma(t)$, is obtained as

$$\begin{aligned} \sigma(t) = n_0^{1/2} & \frac{[\beta \exp(\alpha t)]^{1/2}}{\{1 + \beta[\exp(\alpha t) - 1]\}^2} \\ & \cdot \left(2\beta - 1 + \exp(\alpha t) \{1 - 2\beta[1 + (\beta - 1)(\alpha t)] + 2\beta^2 \sinh(\alpha t)\} \right)^{1/2} \end{aligned} \quad (4.8)$$

The normalized form of the standard deviation, $\zeta(\tau)$, is obtained from Eq. (4.7) as

$$\begin{aligned} \zeta(\tau) &= \frac{\sigma(\tau)}{n_0} \\ &= \frac{1}{n_0^{1/2}} \cdot \frac{[\beta \exp(\tau)]^{1/2}}{\{1 + \beta[\exp(\tau) - 1]\}^2} \\ & \cdot \left(2\beta - 1 + \exp(\tau) \{1 - 2\beta[1 + (\beta - 1)\tau] + 2\beta^2 \sinh(\tau)\} \right)^{1/2} \end{aligned} \quad (4.9)$$

From Eqs. (4.4) and (4.8), the coefficient of variation, $CV(t)$, is

$$\begin{aligned} CV(t) &= \frac{\sigma(t)}{m(t)} \\ &= \frac{1}{n_0^{1/2}} \cdot \frac{[\beta \exp(\alpha t)]^{1/2}}{\{1 + \beta[\exp(\alpha t) - 1]\}} \\ &\quad \cdot \left(2\beta - 1 + \exp(\alpha t) \{1 - 2\beta[1 + (\beta - 1)(\alpha t)] + 2\beta^2 \sinh(\alpha t)\} \right)^{1/2} \end{aligned} \quad (4.10)$$

or in terms of τ ,

$$\begin{aligned} CV(\tau) &= \frac{1}{n_0^{1/2}} \cdot \frac{[\beta \exp(\tau)]^{1/2}}{\{1 + \beta[\exp(\tau) - 1]\}} \\ &\quad \cdot \left(2\beta - 1 + \exp(\tau) \{1 - 2\beta[1 + (\beta - 1)\tau] + 2\beta^2 \sinh(\tau)\} \right)^{1/2} \end{aligned} \quad (4.11)$$

Note that this expression is a function of n_0 .

Analysis of Experimental Data

The available experimental data⁶⁵ are listed in Table 3.1 and also exhibited in Figure 3.2 in the preceding chapter; they are given in the unit of milligrams of carbon per milligram of ACs, i.e., mg C/mg AC. The model derived in this chapter is also validated with the same set of data; this validation is carried out by relating the number of open pores at time t , which is the random variable, $N(t)$, to the experimentally measurable variable, $W(t)$. This variable represents the weight of carbon already deposited on ACs at time t . Accordingly, it is assumed that a fixed amount of carbon, δ , deposits onto an open pore and its surroundings, thus causing the pore to narrow. Hence, at any time t ,

$$W(t) = \delta[n_0 - N(t)] \quad (4.12)$$

where the term, $[n_0 - N(t)]$, is the number of narrowed pores at any time t . The mean value of $W(t)$, denoted by $m_w(t)$, is obtained from the above expression as follows:

$$\begin{aligned} m_w(t) &= E[W(t)] \\ &= E\{\delta [n_0 - N(t)]\} \\ &= \delta \{n_0 - E[N(t)]\} \end{aligned}$$

or

$$m_w(t) = \delta[n_0 - m(t)] \quad (4.13)$$

Substituting (4.4) for $m(t)$ into this equation gives

$$m_w(t) = \delta n_0 \left\{ 1 - \frac{1}{1 + \beta [\exp(\alpha t) - 1]} \right\}$$

or

$$m_w(t) = W_0 \left\{ \frac{\beta [\exp(\alpha t) - 1]}{1 + \beta [\exp(\alpha t) - 1]} \right\} \quad (4.14)$$

where W_0 , or (δn_0) , is the weight of carbon that would deposit onto the initial number of open pores. From the above expression, the dimensionless form of the mean, $\eta_w(\tau)$, is

$$\eta_w(\tau) = \frac{m_w(\tau)}{W_0} = \frac{\beta [\exp(\tau) - 1]}{1 + \beta [\exp(\tau) - 1]} \quad (4.15)$$

Note that $\eta_w(\tau) \rightarrow 1$ as $\tau \rightarrow \infty$. Multiplying both sides of this equation by $\beta^{-1} \{1 + \beta [\exp(\tau) - 1]\}$ gives rise to

$$\eta_w^*(\tau) = \exp(\tau) - 1 \quad (4.16)$$

where $\eta_w^*(\tau) = \beta^{-1} \{1 + \beta [\exp(\tau) - 1]\} \eta_w(\tau)$. Note that $\eta_w^*(\tau) \rightarrow \infty$ as $\tau \rightarrow \infty$.

Similarly, the variance of $W(t)$, $\sigma_w^2(t)$, is obtained from (4.12) as

$$\begin{aligned} \sigma_w^2(t) &= \text{Var}[W(t)] \\ &= \text{Var}\{\delta[n_0 - N(t)]\} \\ &= \delta^2 \text{Var}[N(t)] \end{aligned}$$

or

$$\sigma_w^2(t) = \delta^2 [\sigma^2(t)] \quad (4.17)$$

Substituting (4.6) for $\sigma^2(t)$ into the above expression leads to

$$\begin{aligned} \sigma_w^2(t) &= \delta^2 n_0 \frac{\beta \exp(\alpha t)}{\{1 + \beta [\exp(\alpha t) - 1]\}^4} \\ &\quad \cdot \left(2\beta - 1 + \exp(\alpha t) \{1 - 2\beta [1 + (\beta - 1)(\alpha t)] + 2\beta^2 \sinh(\alpha t)\} \right) \end{aligned} \quad (4.18)$$

From this equation, the standard deviation, $\sigma^2(t)$, is

$$\begin{aligned} \sigma_w(t) &= \delta n_0^{1/2} \frac{[\beta \exp(\alpha t)]^{1/2}}{\{1 + \beta[\exp(\alpha t) - 1]\}^2} \\ &\quad \cdot \left(2\beta - 1 + \exp(\alpha t) \{1 - 2\beta[1 + (\beta - 1)(\alpha t)] + 2\beta^2 \sinh(\alpha t)\}\right)^{1/2} \end{aligned} \quad (4.19)$$

The dimensionless form of σ_w^2 , i.e., $\zeta_w(\tau)$, is given by

$$\begin{aligned} \zeta_w(\tau) &= \frac{\sigma_w(\tau)}{W_0} \\ &= \frac{1}{n_0^{1/2}} \cdot \frac{[\beta \exp(\tau)]^{1/2}}{\{1 + \beta[\exp(\tau) - 1]\}^2} \\ &\quad \cdot \left(2\beta - 1 + \exp(\tau) \{1 - 2\beta[1 + (\beta - 1)\tau] + 2\beta^2 \sinh(\tau)\}\right)^{1/2} \end{aligned} \quad (4.20)$$

Note that this equation is identical to (4.9) for $\zeta(\tau)$; moreover, $\zeta_w(\tau) \rightarrow 0$ as $\tau \rightarrow \infty$. By multiplying both sides of this equation by $\beta^{-1} \{1 + \beta[\exp(\tau) - 1]\}$, we have

$$\begin{aligned} \zeta_w^*(\tau) &= \frac{1}{n_0^{1/2}} \cdot \frac{1}{\beta^{1/2}} \cdot \frac{[\exp(\tau)]^{1/2}}{\{1 + \beta[\exp(\tau) - 1]\}} \\ &\quad \cdot \left(2\beta - 1 + \exp(\tau) \{1 - 2\beta[1 + (\beta - 1)\tau] + 2\beta^2 \sinh(\tau)\}\right)^{1/2} \end{aligned} \quad (4.21)$$

where $\zeta_w^*(\tau) = \beta^{-1} \{1 + \beta[\exp(\tau) - 1]\} \zeta_w(\tau)$. Note that $\zeta_w^*(\tau) \rightarrow \infty$ as $\tau \rightarrow \infty$. The coefficient of variation, $CV_w(\tau)$, is obtained as

$$\begin{aligned} CV_w(\tau) &= \frac{\sigma_w(\tau)}{m_w(\tau)} \\ &= \frac{1}{n_0^{1/2}} \cdot \frac{[\beta \exp(\tau)]^{1/2}}{\beta[\exp(\tau) - 1] \{1 + \beta[\exp(\tau) - 1]\}} \\ &\quad \cdot \left(2\beta - 1 + \exp(\tau) \{1 - 2\beta[1 + (\beta - 1)\tau] + 2\beta^2 \sinh(\tau)\}\right)^{1/2} \end{aligned} \quad (4.22)$$

Note that this equation is also a function of n_0 .

Results and Discussion

The model formulated, in terms of the temporal mean given in Eq. (4.14), has been fitted to the available experimental data⁶⁵ through regression without linearization via the adaptive

random search procedure.^{113, 114} The regression has resulted in the values of W_0 and those of α and β , which are listed in Table 4.1. These values have rendered it possible to evaluate the dimensionless time, (αt) , i.e., τ , as well as the dimensionless mean, $\eta_w(\tau)$, from Eq. (4.15). The values of $\eta_w^*(\tau)$ computed from Eq. (4.16) as a function of τ are presented in Figure 4.2 at the eleven temperature levels. The corresponding experimentally measured weights in milligrams of carbon deposited per milligram of ACs are rendered dimensionless by dividing them by W_0 and multiplying them by $\beta^{-1}\{1 + \beta[\exp(\tau) - 1]\}$; the values of the resultant quantity, denoted as $w^*(\tau)$, are superimposed in the same figure for comparison. As indicated earlier, note that $\eta_w^*(\tau)$ increases boundlessly as τ progresses.

The standard deviation signifies the deviations attributable to the internal or characteristic noises of the process as predicted by the stochastic model.¹¹⁰ The values of $\zeta_w^*(\tau)$ around $\eta_w^*(\tau)$, i.e., $\eta_w^*(\tau) \pm \zeta_w^*(\tau)$, are also plotted in Figure 4.2. As expected, many of the experimental data⁶⁵ lie appreciably beyond the expected variation, or scattering, which is almost always the case: The overall deviations of the experimental data include not only those attributable to the internal noises of the process as predicted by the model, but also to the external noises due to inevitable measurement errors and instrumental deficiencies that can never be totally eliminated. As evident from Eq. (4.21), the expression for $\zeta_w^*(\tau)$ depends on the initial number of open pores per milligram of ACs, i.e., n_0 , whose order of magnitude estimate is $1.67 \cdot 10^{13}$ pores.¹¹⁰

Table 4.1. Values of α , β , and W_0 for the Pore-narrowing at Different Temperatures.

| temperature, K (C) | $\alpha, s^{-1} \cdot 10^4$ (min ⁻¹) | $\beta, (-)$ | W_0 (mg C) |
|----------------------|--|--------------|--------------|
| 873 (599.85) | 2.73 (0.016) | 0.817 | 0.064 |
| 923 (649.85) | 2.90 (0.017) | 0.683 | 0.206 |
| 948 (674.85) | 4.00 (0.024) | 0.698 | 0.267 |
| 973 (699.85) | 8.65 (0.052) | 0.569 | 0.235 |
| 1023 (749.85) | 13.45 (0.081) | 0.485 | 0.226 |
| 1048 (774.85) | 17.75 (0.107) | 0.397 | 0.225 |
| 1073 (799.85) | 16.83 (0.101) | 0.637 | 0.235 |
| 1098 (824.85) | 12.13 (0.073) | 0.916 | 0.277 |
| 1123 (849.85) | 6.85 (0.038) | 1.862 | 0.308 |
| 1173 (899.85) | 1.78 (0.011) | 4.712 | 0.344 |
| 1223 (949.85) | 1.10 (0.007) | 2.950 | 0.577 |

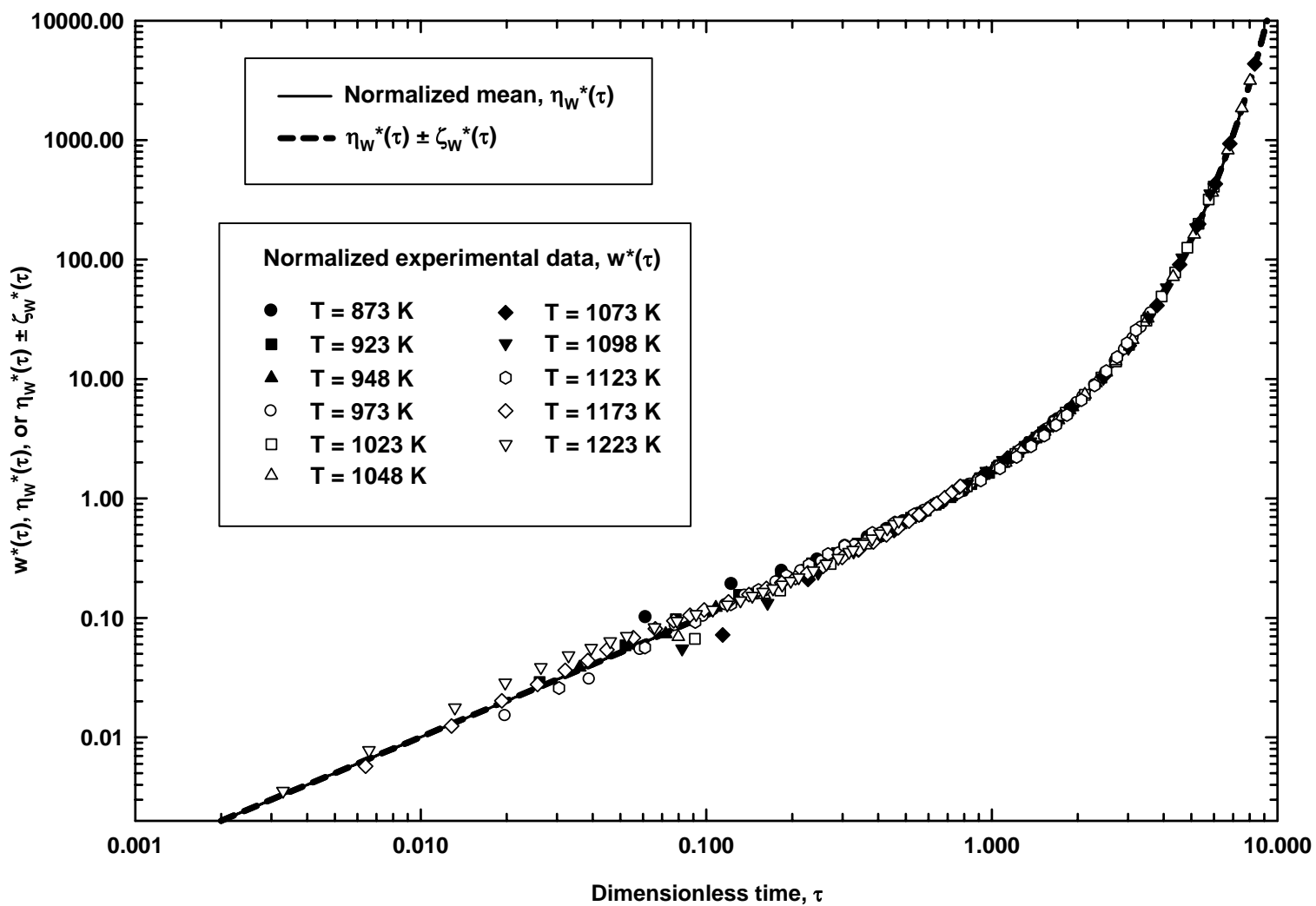


Figure 4.2. Normalized mean $\eta_w^*(\tau)$ and normalized standard deviation envelope $[\eta_w^*(\tau) \pm \zeta_w^*(\tau)]$ as functions of dimensionless time τ for the pore-narrowing: The values on both axes are presented in logarithmic scale to facilitate their visualization.

Summary

A stochastic model has been derived for the formation of CMSs by the deposition of carbon particles on ACs as a pure-death process based on a non-linear intensity function. The complexity in solving the resultant master equation of the process has been circumvented by resorting to a rational approximation method, system-size expansion. The mean and variance of the amount of carbon deposited onto the pores susceptible to narrowing, i.e., the open pores, have been computed from the master equation. The model derived has been validated by fitting it to the available experimental data. The mean value of the model is in excellent accord with these data. As expected, the data's fluctuations around their mean are more noticeable than those predicted by the model: In addition to the process' internal noises, the deviations of the experimental data also account for the external noises due to unavoidable measurement errors.

Notation

- $k =$ proportionality constant in the intensity of death, $(t)^{-1}$
- $(k'n_0) =$ proportionality constant in the intensity of death, $(t)^{-1}$
- $m(t) =$ mean of the random variable, $N(t)$
- $m_w(t) =$ mean of the experimental measurable variable, $W(t)$, mg C
- $N(t) =$ random variable representing the number of pores susceptible to narrowing, i.e., the number of open pores, at time t
- $n =$ realization of the random variable, $N(t)$
- $p_n(t) =$ probability that n pores are open at time t
- $t =$ time
- $W(t) =$ experimentally measurable variable representing the weight of carbon already deposited on ACs, mg C

Greek letters

- $\alpha =$ constant $(k + k'n_0)$, $(t)^{-1}$
- $\beta =$ dimensionless constant, $k(k + k'n_0)^{-1}$
- $\mu_n(t) =$ intensity of death for the pure-death process in state n at time t

$\sigma^2(t)$ = variance of the random variable, $N(t)$

$\sigma_w^2(t)$ = variance of the experimentally measurable variable, $W(t)$

τ = dimensionless time

CHAPTER 5 - Conclusions and Recommendations for Future Work

In this dissertation, the formation of carbon adsorbents, including activated carbons (ACs) and carbon molecular sieves (CMSs), has been analyzed and modeled by resorting to stochastic processes. What follows are the significant conclusions reached as well as recommendations for future work.

Conclusions

The formation of activated carbons (ACs) from a carbonaceous substrate has been stochastically analyzed and modeled as a pure-birth process with a linear intensity function based on a single random variable. The solution of the master equation of the process yields the mean and variance of the number of pores that have been formed on the internal surfaces of the carbonaceous substrate; this number is regarded as the process' random variable. The model has been validated with the available experimental data for the formation of ACs from a carbonaceous substrate. In general, the model's mean value follows the trend of these data; moreover, the model's kinetic constant obeys the Arrhenius law. It is expected that the linear stochastic model for the formation of ACs be an insightful preliminary exploration of the process of concern.

Subsequently, two stochastic models for the formation of carbon molecular sieves (CMSs) on ACs have been derived; each of them is based on a single random variable. The first of the two models has been formulated as a pure-birth process with a non-linear intensity function. The random variable of the process is identified as the number of packets that have already deposited onto the pores' mouths of ACs, which increases temporally. Naturally, the resultant master equation is non-linear; the complexity in solving it is circumvented via a rational approximation method, the system-size expansion. The mean and variance of the amount of carbon deposited onto the pores' mouth of ACs have been computed from expressions obtained from the system-size expansion of the master equation. In general, the model is in accord with

the available experimental data for the formation of CMSs on ACs. Moreover, the non-linear master equation of the process has been simulated with the Monte Carlo method via the event-driven as well as time-driven approaches. The simulation has been carried out at the process' early stage where the number of carbon packets depositing onto the pores of ACs is exceedingly small, thereby magnifying the fluctuations of the process around its mean. The mean and variance computed from simulation are in line with their corresponding analytical results. Simulating the process' non-linear master equation with the Monte Carlo method is of special significance: In some instances, this might be the only viable avenue for reliably estimating the means and variances of highly non-linear processes. In contrast, the second of the two models has been formulated as a pure-death process; its random variable is the number of open pores on ACs, which decreases temporally as they are narrowed. The non-linear intensity function accounts for the number of pores that have already been narrowed as well as that of open pores. Because the resultant master equation is non-linear, it has also been solved by resorting to the system-size expansion, thereby resulting in expressions for the process' mean and variance. The model's mean values at various times are in good accord with the available experimental data.

Recommendations

The stochastic analysis and modeling of the kinetics of formation of ACs is far from complete. A natural sequel of the linear stochastic model presented in this dissertation would be a stochastic model with a non-linear intensity function based on single random variable. Various forms of such an intensity function could be investigated by including a second-order function or an exponential-like function. It would be desirable that the non-linear intensity function incorporates several structural parameters of the carbonaceous materials from which ACs are manufactured. An expression in light of the random pore model for fluid-solid reactions might offer an alternative for the definition of the non-linear intensity function.

The stochastic analysis and modeling of the formation of CMSs could be further extended by formulating a stochastic model that couples the pore-narrowing with the subsequent pore-blocking. Naturally, the resultant model including both pore-narrowing and pore-blocking would involve two random variables and two intensity functions. For a given stochastic model, these two intensity functions could be linear, non-linear, or their combination thereof.

References

1. Schluender EU, Liedy W, Tietz M, Wagner R, Kupka S. Desorption of a binary mixture from activated carbon and the resulting separation effect. *Chem Eng Sci.* 1988;43:2391-2397.
2. Rao MB, Sircar S. Production of motor fuel grade alcohol by concentration swing adsorption. *Separ Sci Tech.* 1992;27:1875-1887.
3. Triebe RW, Tezel FH. Adsorption of nitrogen, carbon monoxide, carbon dioxide and nitric oxide on molecular sieves. *Gas Separ Purif.* 1995;9:223-230.
4. Sircar S, Golden TC, Rao MB. Activated carbon for gas separation and storage. *Carbon.* 1996;34:1-12.
5. Moreira RFPM, Jose HJ, Rodrigues AE. Modification of pore size in activated carbon by polymer deposition and its effects on molecular sieve selectivity. *Carbon.* 2001;39:2269-2276.
6. Shirley AI, Lemcoff NO. Air separation by carbon molecular sieves. *Adsorption.* 2002;8:147-155.
7. Soares JL, Jose HJ, Moreira RFPM. Preparation of a carbon molecular sieve and application to separation of N₂, O₂ and CO₂ in a fixed bed. *Braz J Chem Eng.* 2003;20:75-80.
8. Moore SV, Trimm DL. The preparation of carbon molecular sieves by pore blocking. *Carbon.* 1977;15:177-180.

9. Salinas-Martinez De Lecea, C., Linares-Solano A, Vannice MA. Carbon black and activated carbon as supports in catalysts prepared from $\text{Fe}_3(\text{CO})_{12}$ and $\text{Mn}_2(\text{CO})_{10}$ clusters. *Carbon*. 1990;28:467-476.
10. Grunewald GC, Drago RS. Carbon molecular sieves as catalysts and catalyst supports. *J Am Chem Soc*. 1991;113:1636-1639.
11. Miura K, Hayashi J, Kawaguchi T, Hashimoto K. Shape-selective catalyst utilizing a molecular sieving carbon with sharp pore distribution. *Carbon*. 1993;31:667-674.
12. Fortuny A, Font J, Fabregat A. Wet air oxidation of phenol using active carbon as catalyst. *Appl Catal B Environ*. 1998;19:165-173.
13. Zhu ZH, Wang S, Lu GQ, Zhang D-. The role of carbon surface chemistry in N_2O conversion to N_2 over ni catalyst supported on activated carbon. *Catal Today*. 1999;53:669-681.
14. Chi-Sheng W, Zhi-An L, Feng-Ming T, Jen-Wei P. Low-temperature complete oxidation of BTX on Pt/activated carbon catalysts. *Catal Today*. 2000;63:419-426.
15. Ikenaga N, Tsuruda T, Senma K, Yamaguchi T, Sakurai Y, Suzuki T. Dehydrogenation of ethylbenzene with carbon dioxide using activated carbon-supported catalysts. *Ind Eng Chem Res*. 2000;39:1228-1234.
16. Karagoz S, Yanik J, Ucar S, Song C. Catalytic coprocessing of low-density polyethylene with VGO using metal supported on activated carbon. *Energ Fuel*. 2002;16:1301-1304.
17. Moreno-Castilla C, Perez-Cadenas AF, Maldonado-Hodar FJ, Carrasco-Marin F, Fierro, J LG. Influence of carbon-oxygen surface complexes on the surface acidity of tungsten oxide catalysts supported on activated carbons. *Carbon*. 2003;41:1157-1167.
18. Bai Z, Chen H, Li B, Li W. Catalytic decomposition of methane over activated carbon. *J Anal Appl Pyrol*. 2005;73:335-341.

19. Lazaro MJ, Galvez ME, Artal S, Palacios JM, Moliner R. Preparation of steam-activated carbons as catalyst supports. *J Anal Appl Pyrol.* 2007;78:301-315.
20. Rodríguez-Reinoso F. Activated carbon: Structure, characterization, preparation and applications. In: Marsh H, Heintz EA, Rodríguez-Reinoso F, eds. *Introduction to Carbon Technologies*. Alicante, Spain: Publicaciones de la Universidad de Alicante; 1997:35-41.
21. Xia J, Noda K, Kagawa S, Wakao N. Production of activated carbon from bagasse (waste) of sugarcane grown in Brazil. *J Chem Eng Jpn.* 1998;31:987-990.
22. Alaya MN, Girgis BS, Mourad WE. Activated carbon from some agricultural wastes under action of one-step steam pyrolysis. *J Porous Mater.* 2000;7:509-517.
23. Zhang T, Walawender WP, Fan LT, Fan M, Daugaard D, Brown RC. Preparation of activated carbon from forest and agricultural residues through CO₂ activation. *Chem Eng J.* 2004;105:53-59.
24. Azhar Uddin M, Shinozaki Y, Furusawa N, Yamada T, Yamaji Y, Sasaoka E. Preparation of activated carbon from asphalt and heavy oil fly ash and coal fly ash by pyrolysis. *J Anal Appl Pyrol.* 2007;78:337-342.
25. Botha FD, McEnaney B. Chemical activation of a South African coal using phosphoric acid. *Adsorption Science and Technology.* 1993;10:181-192.
26. Akash BA, O'Brien WS. Production of activated carbon from a bituminous coal. *Int J Energ Res.* 1996;20:913-922.
27. Dalai AK, Zaman J, Hall ES, Tollefson EL. Preparation of activated carbon from Canadian coals using a fixed-bed reactor and a spouted bed-kiln system. *Fuel.* 1996;75:227-237.
28. Martin-Gullon I, Asensio M, Font R, Marcilla A. Steam-activated carbons from a bituminous coal in a continuous multistage fluidized bed pilot plant. *Carbon.* 1996;34:1515-1520.

29. Teng H, Ho JA, Hsu YF, Hsieh CT. Preparation of activated carbons from bituminous coals with CO₂ activation. 1. effects of oxygen content in raw coals. *Ind Eng Chem Res.* 1996;35:4043-4049.
30. Toles C, Rimmer S, Hower JC. Production of activated carbons from a Washington lignite using phosphoric acid activation. *Carbon.* 1996;34:1419-1426.
31. Sun J, Hippo EJ, Marsh H, O'Brien WS, Crelling JC. Activated carbon produced from an Illinois basin coal. *Carbon.* 1997;35:341-352.
32. Hsisheng T, Lin HG. Activated carbon production from low ash subbituminous coal with CO₂ activation. *AIChE J.* 1998;44:1170-1176.
33. Tamarkina YV, Shendrik TG. Activation of coals modified by nitration. *Solid Fuel Chem.* 2002;36:1-7.
34. Yardim MF, Ekinci E, Minkova V, et al. Formation of porous structure of semicokes from pyrolysis of Turkish coals in different atmospheres. *Fuel.* 2003;82:459-463.
35. Peredery MA. Carbonaceous sorbents from fossil coals: The status of the problem and prospects of development. *Solid Fuel Chem.* 2005;39:68-81.
36. Baquero MC, Giraldo L, Moreno JC, Suarez-Garcia F, Martinez-Alonso A, Tascon JMD. Activated carbons by pyrolysis of coffee bean husks in presence of phosphoric acid. *J Anal Appl Pyrol.* 2003;70:779-784.
37. Aggarwal P, Dollimore D. Production of active carbon from corn cobs by chemical activation. *Journal of Thermal Analysis.* 1997;50:525-531.
38. Wu CC, Walawender WP, Fan LT. Chemical agents for production of activated carbons from extrusion cooked grain products. 1997:116-117.
39. Kutics K, Szolcsanyi P, Argyelan J, Kotsis L. Production of activated carbon from walnut shells. I. adsorption investigations and study of application characteristics. *Hung J Ind Chem.* 1984;12:319-327.

40. Guo J, Lua AC. Experimental and kinetic studies on pore development during CO₂ activation of oil-palm-shell char. *J Porous Mater.* 2001;8:149-157.
41. Diao Y, Walawender WP, Fan LT. Production of activated carbons from wheat using phosphoric acid activation. *Adv Environ Res.* 1999;3:333-342.
42. Diao Y, Walawender WP, Fan LT. Activated carbons prepared from phosphoric acid activation of grain sorghum. *Bioresource Technology.* 2002;81:45-52.
43. Murillo R, Navarro MV, Garcia T, et al. Production and application of activated carbons made from waste tire. *Ind Eng Chem Res.* 2005;44:7228-7233.
44. Tam MS, Antal MJ, Jr. Preparation of activated carbons from macadamia nut shell and coconut shell by air activation. *Ind Eng Chem Res.* 1999;38:4268-4276.
45. Mameri N, Aiouèche F, Belhocine D, et al. Preparation of activated carbon from olive mill solid residue. *J Chem Tech Biotechnol.* 2000;75:625-631.
46. Rodriguez-Reinoso F, Pastor AC, Marsh H, Martinez MA. Preparation of activated carbon cloths from viscous rayon. part II: Physical activation processes. *Carbon.* 2000;38:379-395.
47. Gonzalez JF, Encinar JM, Gonzalez-Garcia CM, et al. Preparation of activated carbons from used tyres by gasification with steam and carbon dioxide. *Appl Surf Sci.* 2006;252:5999-6004.
48. Rio S, Le Coq L, Faur C, Le Cloirec P. Production of porous carbonaceous adsorbent from physical activation of sewage sludge: Application to wastewater treatment. *Water Sci Tech.* 2006;53:237-244.
49. Sentorun-Shalaby C, Ucak-Astarlioglu MG, Artok L, Sarici C. Preparation and characterization of activated carbons by one-step steam pyrolysis/activation from apricot stones. *Microporous and Mesoporous Materials.* 2006;88:126-134.

50. Kailappan R, Gothandapani L, Viswanathan R. Production of activated carbon from prosopis (*Prosopis juliflora*). *Bioresource Technology*. 2000;75:241-243.
51. Okada K, Yamamoto N, Kameshima Y, Yasumori A. Porous properties of activated carbons from waste newspaper prepared by chemical and physical activation. *J Colloid Interface Sci*. 2003;262:179-193.
52. Stavropoulos GG, Zabaniotou AA. Production and characterization of activated carbons from olive-seed waste residue. *Microporous and Mesoporous Materials*. 2005;82:79-85.
53. Olivares-Marin M, Fernandez-Gonzalez C, Macias-Garcia A, Gomez-Serrano V. Preparation of activated carbon from cherry stones by chemical activation with $ZnCl_2$. *Appl Surf Sci*. 2006;252:5967-5971.
54. Guo Y, Rockstraw DA. Activated carbons prepared from rice hull by one-step phosphoric acid activation. *Microporous and Mesoporous Materials*. 2007;100:12-19.
55. Stoeckli F, Guillot A, Slasli AM, Hugi-Cleary D. The comparison of experimental and calculated pore size distributions of activated carbons. *Carbon*. 2002;40:383-388.
56. Ruthven DM. *Principles of Adsorption and Adsorption Processes*. New York: Wiley; 1984.
57. Vyas SN, Patwardhan SR, Gangadhar B. Carbon molecular sieves from bituminous coal by controlled coke deposition. *Carbon*. 1992;30:605-612.
58. Lizzio AA, Rostam-Abadi M. Production of carbon molecular sieves from Illinois coal. *Fuel Process Tech*. 1993;34:97-122.
59. Hu Z, van Sant, E. F. Carbon molecular sieves produced from walnut shell. *Carbon*. 1995;33:561-567.
60. Horikawa T, Hayashi J, Muroyama K. Preparation of molecular sieving carbon from waste resin by chemical vapor deposition. *Carbon*. 2002;40:709-714.

61. Zhang T, Walawender WP, Fan LT. Preparation of carbon molecular sieves by carbon deposition from methane. *Bioresource Technology*. 2005;96:1929-1935.
62. Verma SK, Walker PLJ. Preparation of carbon molecular sieves by propylene pyrolysis over microporous carbons. *Carbon*. 1992;30:829-836.
63. Cabrera AL, Zellner JF, Coe CG, Gaffney TR, Farris TS, Armor JN. Preparation of carbon molecular sieves, I. two-step hydrocarbon deposition with a single hydrocarbon. *Carbon*. 1993;31:969-976.
64. Prasetyo I, Do DD. Pore structure alteration of porous carbon by catalytic coke deposition. *Carbon*. 1999;37:1909-1918.
65. Freitas MMA, Figueiredo JL. Preparation of carbon molecular sieves for gas separations by modification of the pore sizes of activated carbons. *Fuel*. 2001;80:1-6.
66. David E, Talaie A, Stanciu V, Nicolae AC. Synthesis of carbon molecular sieves by benzene pyrolysis over microporous carbon materials. *J Mater Process Tech*. 2004;157-158:290-296.
67. Doob JL. *Stochastic Processes*. New York: Wiley; 1953.
68. Feller W. *An Introduction to Probability Theory and its Applications*. Vol I. Third ed. New York: Wiley; 1968.
69. Gardiner CW. *Handbook of Stochastic Methods*. Berlin: Springer; 2004.
70. Cox DR, Miller HD. *The Theory of Stochastic Processes*. New York: Wiley; 1965.
71. van Kampen, NG *Stochastic Processes in Physics and Chemistry*. Amsterdam: North-Holland; 1992.
72. Taylor HM, Karlin S. *Introduction to Stochastic Modeling*. San Diego: Academic Press; 1998.

73. Oppenheim I, Shuler KE, Weiss GH. *Stochastic Processes in Chemical Physics: The Master Equation*. Cambridge, MA: The MIT Press; 1977.
74. Gillespie DT. *Markov Processes - an Introduction for Physical Scientists*. San Diego, CA: Academic Press; 1992.
75. Sobol' IM. *A Primer for the Monte Carlo Method*. Boca Raton, FL: CRC Press; 1994.
76. Byrne JF, Marsh H. Introductory overview. In: Patrick JW, ed. *Porosity in Carbons: Characterization and Applications*. London: Edward Arnold; 1995:2-3.
77. McQuarrie DA. Kinetics of small systems. I. *J Chem Phys*. 1963;38:433-436.
78. McQuarrie DA, Jachimowski CJ, Russell ME. Kinetics of small systems. II. *J Chem Phys*. 1964;40:2914-2921.
79. Gillespie DT. A general method for numerically simulating the stochastic time evolution of coupled chemical reactions. *J Comput Phys*. 1976;22:403-434.
80. Chou ST, Fan LT, Nassar R. Modeling of complex chemical reactions in a continuous-flow reactor: A Markov chain approach. *Chem Eng Sci*. 1988;43:2807-2815.
81. Sagues F, Ramirez-Piscina L, Sancho JM. Stochastic dynamics of the chlorite-iodide reaction. *J Chem Phys*. 1990;92:4786-92.
82. Nassar R, Chou ST, Fan LT. Stochastic analysis of stepwise cellulose degradation. *Chem Eng Sci*. 1991;46:1651-1657.
83. Mai J, Casties A, von Niessen W, Kuzovkov VN. A stochastic model and a Monte Carlo simulation for the description of CO oxidation on Pt/Sn alloys. *J Chem Phys*. 1995;102:5037-44.
84. Reichert C, Starke J, Eiswirth M. Stochastic model of CO oxidation on platinum surfaces and deterministic limit. *J Chem Phys*. 2001;115:4829-38.

85. Gomez-Uribe CA, Verghese GC. Mass fluctuation kinetics: Capturing stochastic effects in systems of chemical reactions through coupled mean-variance computations. *J Chem Phys.* 2007;126:024109.
86. Petersen EE. Reaction of porous solids. *AIChE J.* 1957;3:443-448.
87. Szekely J, Evans JW. A structural model for gas-solid reactions with a moving boundary. *Chem Eng Sci.* 1970;25:1091-1107.
88. Dutta S, Wen CY, Belt RJ. Reactivity of coal and char. 1. in carbon dioxide atmosphere. *Ind Eng Chem Proc Des Dev.* 1977;16:20-30.
89. Georgakis C, Chang CW, Szekely J. A changing grain size model for gas-solid reactions. *Chem Eng Sci.* 1979;34:1072-1075.
90. Bhatia SK, Perlmutter DD. A random pore model for fluid-solid reactions: I. isothermal, kinetic control. *AIChE J.* 1980;26:379-386.
91. Gavalas GR. A random capillary model with application to char gasification at chemically controlled rates. *AIChE J.* 1980;26:577-585.
92. Bhatia SK, Perlmutter DD. Unified treatment of structural effects in fluid-solid reactions. *AIChE J.* 1983;29:281-289.
93. Kasaoka S, Sakata Y, Tong C. Kinetic evaluation of the reactivity of various coal chars for gasification with carbon dioxide in comparison with steam. *Int Chem Eng.* 1985;25:160-175.
94. Szargan P, Moebius R, Spindler H, Kraft M. Kinetics of partial gasification and pore evolution of activated carbon materials. *Chem Tech.* 1988;40:251-254.
95. Fuertes AB, Pis JJ, Perez AJ, Lorenzana JJ, Rubiera F. Kinetic study of the reaction of a metallurgical coke with CO₂. *Solid State Ionics.* 1990;38:75-80.
96. Gray PG, Do DD. Modelling of the interaction of nitrogen dioxide with activated carbon. II. kinetics of reaction with pore evolution. *Chem Eng Comm.* 1993;125:109-120.

97. Bagreev AA, Ledovskikh AV, Tarasenko YA, Strelko VV. Modeling of kinetics for formation of porous structure in active carbons. *Dopovidi Natsional'noi Akademii Nauk Ukraini*. 2000;132-137.
98. Ochoa J, Cassanello MC, Bonelli PR, Cukierman AL. CO₂ gasification of Argentinean coal chars: A kinetic characterization. *Fuel Process Tech*. 2001;74:161-176.
99. Rafsanjani HH, Jamshidi E, Rostam-Abadi M. A new mathematical solution for predicting char activation reactions. *Carbon*. 2002;40:1167-1171.
100. Murillo R, Navarro MV, Lopez JM, et al. Kinetic model comparison for waste tire char reaction with CO₂. *Ind Eng Chem Res*. 2004;43:7768-7773.
101. Navarro MV, Murillo R, Lopez JM, Garcia T, Callen MS, Mastral AM. Modeling of activated carbon production from lignite. *Energy and Fuels*. 2006;20:2627-2631.
102. Beeckman JW, Froment GF. Catalyst deactivation by active site coverage and pore blockage. *Ind Eng Chem Fund*. 1979;18:245-256.
103. Beeckman JW, Froment GF. Deactivation of catalysts by coke formation in the presence of internal diffusional limitation. *Ind Eng Chem Fund*. 1982;21:243-250.
104. Sahimi M, Tsotsis TT. A percolation model of catalyst deactivation by site coverage and pore blockage. *J Catal*. 1985;96:552-562.
105. Shah N, Ottino JM. Transport and reaction in evolving, disordered composites - II. coke deposition in a catalytic pellet. *Chem Eng Sci*. 1987;42:73-82.
106. Demicheli MC, Ponzi EN, Ferretti OA, Yeramian AA. Kinetics of carbon formation from CH₄-H₂ mixtures on nickel-alumina catalyst. *Chem Eng J Biochem Eng J*. 1991;46:129-136.
107. Reyes SC, Scriven LE. Analysis of zeolite catalyst deactivation during catalytic cracking reactions. *Ind Eng Chem Res*. 1991;30:71-82.

108. Garcia-Ochoa F, Santos A. Isomerization of 1-butene on silica-alumina: Kinetic modeling and catalyst deactivation. *AIChE J.* 1995;41:286-300.
109. Fan LT, Argoti A, Walawender WP, Chou S. Stochastic modeling and simulation of the formation of carbon molecular sieves by carbon deposition. *Ind Eng Chem Fund.* 2005;44:2343-2348.
110. Chou S, Argoti A. A simple Markovian model for the initial stage of the formation of carbon molecular sieves by carbon deposition. *J Chin Inst Chem Eng.* 2006;37:431-438.
111. Casella G, Berger RL. *Statistical Inference.* Pacific Grove, CA: Duxbury; 2002.
112. Rao PV. *Statistical Research Methods in the Life Sciences.* Pacific Grove, CA: Duxbury; 1998.
113. Fan LT, Chen HT, Aldis D. An adaptive random search procedure for large scale industrial and process systems synthesis. Karlovy Vary, Czechoslovakia: Czechoslovak Chem. Soc; 1975;I:279-291.
114. Chen HT, Fan LT. Multiple minima in a fluidized reactor-heater system. *AIChE J.* 1976;22:680-685.
115. Vignal V, Morawski AW, Konno H, Inagaki M. Quantitative assessment of pores in oxidized carbon spheres using scanning tunneling microscopy. *J Mater Res.* 1999;14:1102-12.
116. Allport HB. Activated carbon. In: *McGraw-Hill Encyclopedia of Science & Technology.* Vol 1. 9th ed. New York: McGraw-Hill; 2002:109.
117. Froment GF, Bischoff KB. *Chemical Reactor Analysis and Design.* New York: Wiley; 1990.
118. Verma SK, Walker PLJ. Preparation of carbon molecular sieves by propylene pyrolysis over nickel-impregnated activated carbons. *Carbon.* 1993;31:1203-1207.

119. Kawabuchi Y, Kawano S, Mochida I. Molecular sieving selectivity of active carbons and active carbon fibers improved by chemical vapour deposition of benzene. *Carbon*. 1996;34:711-717.
120. Kendall DG. An artificial realization of a simple "birth-and-death" process. *J Roy Stat Soc B*. 1950;12:116-119.
121. Gillespie DT. Exact stochastic simulation of coupled chemical reactions. *J Phys Chem*. 1977;81:2340-2361.
122. Shah BH, Borwanker JD, Ramkrishna D. Monte Carlo simulation of microbial population growth. *Math Biosci*. 1976;31:1-23.
123. Shah BH, Ramkrishna D, Borwanker JD. Simulation of particulate systems using the concept of the interval of quiescence. *AIChE J*. 1977;23:897-904.
124. Rajamani K, Pate WT, Kinneberg DJ. Time-driven and event-driven Monte Carlo simulations of liquid-liquid dispersions: A comparison. *Ind Eng Chem Fund*. 1986;25:746-752.
125. Rao CV, Arkin AP. Stochastic chemical kinetics and the quasi-steady-state assumption: Application to the Gillespie algorithm. *J Chem Phys*. 2003;118:4999-5010.
126. Cao Y, Gillespie DT, Petzold LR. Accelerated stochastic simulation of the stiff enzyme-substrate reaction. *J Chem Phys*. 2005;123:144917-1-144917-12.
127. Ullah M, Schmidt H, Cho K-, Wolkenhauer O. Deterministic modelling and stochastic simulation of biochemical pathways using MATLAB. *IEE Proc. Syst. Biol*. 2006;153:53-60.
128. Rod V, Misek T. Stochastic modelling of dispersion formation in agitated liquid-liquid systems. *Transactions of the Institution of Chemical Engineers*. 1982;60:48-53.
129. Steinfeld JJ, Francisco JS, Hase WL. *Chemical Kinetics and Dynamics*. Englewood Cliffs, NJ: Prentice Hall; 1989.

130. Perry RH, Green DW, Maloney JO, eds. *Perry's Chemical Engineers' Handbook*. New York: McGraw-Hill; 1997.
131. Jeffreys H, Jeffreys B. *Methods of Mathematical Physics*. 3rd ed. Cambridge: Cambridge University Press; 1999.
132. McQuarrie DA. *Mathematical Methods for Scientists and Engineers*. Sausalito, CA: University Science Books; 2003.
133. Gallager RG. *Discrete Stochastic Processes*. Boston: Kluwer Academic Publishers; 1996.
134. Fan LT, Argoti Caicedo A, Chou ST, Chen WY. Stochastic modeling of thermal death kinetics of a cell population: Revisited. *Chem Eng Educ*. 2003;37:228-235.

Appendix A - Derivation of the Master Equation of a Pure-Birth Process

Suppose that a system comprising a population of particulate or discrete entities in a given space is to be stochastically modeled as a pure-birth process. The random variable characterizing this process is denoted by $N(t)$ with realization n ; moreover, the intensity of birth is denoted by $\lambda_n(t)$. Thus, one of the following two events is considered to occur during time interval $(t, t + \Delta t)$. First, the number of entities increases by one, which is a birth event, with conditional probability $\{[\lambda_n(t)]\Delta t + o(\Delta t)\}$. Second, the number of entities changes by a number other than one with conditional probability $o(\Delta t)$, which is defined such that

$$\lim_{\Delta t \rightarrow 0} \frac{o(\Delta t)}{\Delta t} = 0 \quad (\text{A.1})$$

Naturally, the conditional probability of no change in the number of entities during this time interval is $(1 - \{[\lambda_n(t)]\Delta t + o(\Delta t)\})$.

Let the probability that exactly n entities are present at time t be denoted as $p_n(t) = \Pr[N(t) = n]$, where $n \in (0, 1, 2, \dots, n_\infty - 1, n_\infty)$; n_∞ is the maximum possible number of entities in the system. For the two adjacent time intervals, $(0, t)$ and $(t, t + \Delta t)$, the occurrence of exactly n entities being present at time $(t + \Delta t)$ can be realized in the following mutually exclusive ways; see Figure A.1.

(1) With a probability of $\{[\lambda_{n-1}(t)]\Delta t + o(\Delta t)\}p_{n-1}(t)$, the number of entities will increase by one during time interval $(t, t + \Delta t)$, provided that exactly $(n - 1)$ entities are present at time t .

(2) With a probability of $o(\Delta t)$, the number of entities will change by exactly j entities during time interval $(t, t + \Delta t)$, provided that exactly $(n - j)$ entities are present at time t , where $2 \leq j \leq n_\infty$.

(3) With a probability of $(1 - \{[\lambda_n(t)]\Delta t + o(\Delta t)\})p_n(t)$, the number of entities will remain unchanged during time interval $(t, t + \Delta t)$, provided that n entities are present at time t .

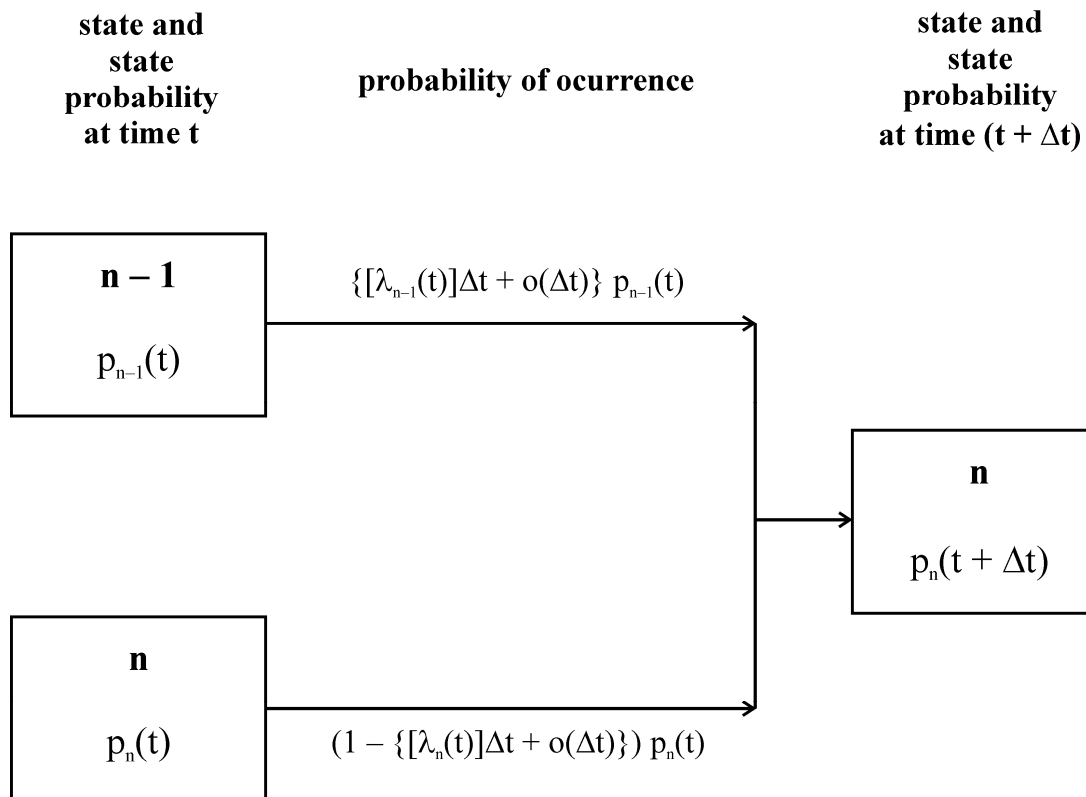


Figure A.1. Probability balance for the pure-birth process involving the mutually exclusive events in the time interval, (t, t + Δt).

Summing all these probabilities and consolidating all quantities of $o(\Delta t)$ yield

$$p_n(t + \Delta t) = \{\lambda_{n-1}(t)\Delta t\} p_{n-1}(t) + \{1 - [\lambda_n(t)\Delta t]\} p_n(t) + o(\Delta t) \quad (\text{A.2})$$

Rearranging this equation, dividing it by Δt , and taking the limit as $\Delta t \rightarrow 0$ yield the master equation of the pure-birth process as^{71, 73}

$$\frac{d}{dt} p_n(t) = \lambda_{n-1}(t) p_{n-1}(t) - \lambda_n(t) p_n(t) \quad (\text{A.3})$$

This is Eq. (2.2) in Chapter 2 with $n \in (0, 1, 2, \dots, n_L - 1, n_L)$, and also Eq. (3.1) in Chapter 3 with $n \in (0, 1, 2, \dots, n_M - 1, n_M)$.

Appendix B - Formation of Activated Carbons: Derivation of Mean and Variance of the Pure-Birth Process with Linear Intensity of Transition Based on a Single Random Variable

The master equation of the pure-birth process of interest is given by Eq. (2.2) in the text as

$$\frac{d}{dt} p_n(t) = \lambda_{n-1}(t) p_{n-1}(t) - \lambda_n(t) p_n(t), \quad n = 0, 1, 2, \dots, n_L - 1, n_L \quad (\text{B.1})$$

The mean and variance of the pure-birth process can be computed from this equation by resorting to the one-step operator, \mathbb{E} . This operator is defined by its effect on an arbitrary function, $f(n)$, as

$$\mathbb{E}f(n) = f(n+1) \quad \text{and} \quad \mathbb{E}^{-1}f(n) = f(n-1) \quad (\text{B.2})$$

In light of this definition, Eq. (B.1) becomes

$$\frac{d}{dt} p_n(t) = \mathbb{E}^{-1} \lambda_n(t) p_n(t) - \lambda_n(t) p_n(t)$$

or

$$\frac{d}{dt} p_n(t) = (\mathbb{E}^{-1} - 1) \lambda_n(t) p_n(t) \quad (\text{B.3})$$

For any arbitrary functions, $f(n)$ and $g(n)$, of integer n , the following expression holds

$$\sum_{n=0}^{n_L-1} [g(n) \mathbb{E} f(n)] = \sum_{n=1}^{n_L} [f(n) \mathbb{E}^{-1} g(n)]$$

When $g(-1) = f(n_L + 1) = 0$, this equation becomes

$$\sum_{n=0}^{n_L} [g(n) \mathbb{E} f(n)] = \sum_{n=0}^{n_L} [f(n) \mathbb{E}^{-1} g(n)] \quad (\text{B.4})$$

This property of \mathbb{E} facilitates the evaluation of the mean and variance of the pure-birth process of interest from its master equation.

Mean

The mean, $E[N(t)]$ or $m(t)$, which is the expected value (first moment) of the distribution of random variable $N(t)$ is defined as

$$E[N(t)] = \sum_n np(n; t) \quad (\text{B.5})$$

The mean or expected value, $E[N(t)]$, is the weighted sum of the realizations of random variable $N(t)$ where the weights are the corresponding probabilities to those realizations.^[111] By multiplying both sides of Eq. (B.3) by n and summing over the state space of $N(t)$, i.e., all values of n , we have

$$\sum_{n=0}^{n_L} n \frac{d}{dt} p_n(t) = \sum_{n=0}^{n_L} n(\mathbb{E}^{-1} - 1)\lambda_n(t) p_n(t)$$

By virtue of Eq. (B.4), this equation can be rewritten as

$$\sum_{n=0}^{n_L} n \frac{d}{dt} p_n(t) = \sum_{n=0}^{n_L} \lambda_n(t) p_n(t)(\mathbb{E} - 1) n$$

or

$$\sum_{n=0}^{n_L} n \frac{d}{dt} p_n(t) = \sum_{n=0}^{n_L} \lambda_n(t) p_n(t) \quad (\text{B.6})$$

Inserting Eq. (2.1) in text for $\lambda_n(t)$ into the above equation gives

$$\sum_{n=0}^{n_L} n \frac{d}{dt} p_n(t) = \sum_{n=0}^{n_L} \kappa(n_L - n) p_n(t) \quad (\text{B.7})$$

or

$$\sum_{n=0}^{n_L} n \frac{d}{dt} p_n(t) = \kappa n_L \sum_{n=0}^{n_L} p_n(t) - \kappa \sum_{n=0}^{n_L} n p_n(t) \quad (\text{B.8})$$

By definition,

$$\sum_{n=0}^{n_L} p_n(t) = 1 \quad (\text{B.9})$$

Moreover, the mean of $N(t)$, $E[N(t)]$ or $m(t)$, is given by

$$E[N(t)] = \sum_{n=0}^{n_L} n p_n(t) \quad (\text{B.10})$$

and thus,

$$\frac{d}{dt} E[N(t)] = \sum_{n=0}^{n_L} n \frac{d}{dt} p_n(t) \quad (\text{B.11})$$

By virtue of Eqs. (B.9) through (B.11), Eq. (B.8) reduces to

$$\frac{d}{dt} E[N(t)] = \kappa n_L - \kappa E[N(t)]$$

or

$$\frac{d}{dt} E[N(t)] + \kappa E[N(t)] = \kappa n_L \quad (\text{B.12})$$

From the initial conditions for the pure-birth process,

$$p_n(0) = \begin{cases} 0 & \text{if } n \neq 0 \\ 1 & \text{if } n = 0, \end{cases} \quad (\text{B.13})$$

and the definition of $E[N(t)]$, Eq. (B.10), we have

$$E[N(0)] = 0 \quad (\text{B.14})$$

Integrating Eq. (B.12) subject to this initial condition yields

$$E[N(t)] = n_L [1 - \exp(-\kappa t)] \quad (\text{B.15})$$

or

$$m(t) = n_L [1 - \exp(-\kappa t)], \quad (\text{B.16})$$

This is Eq. (2.4) in the text.

Variance

The variance, $\text{Var}[N(t)]$ or $\sigma^2(t)$, is the second moment of the distribution of random variable $N(t)$ about the mean, $E[N(t)]$; thus,

$$\text{Var}[N(t)] = \sigma^2(t) = E[\{N(t) - E[N(t)]\}^2]$$

or

$$\sigma^2(t) = \sum_n \{n - E[N(t)]\}^2 p(n; t) \quad (\text{B.17})$$

By expanding the above equation, $\sigma^2(t)$ can be related to the mean, $E[N(t)]$, as follows:

$$\sigma^2(t) = E[N^2(t)] - \{E[N(t)]\}^2 \quad (\text{B.18})$$

In this expression, $E[N^2(t)]$ is the second moment of $N(t)$, i.e.,

$$E[N^2(t)] = \sum_n n^2 p(n; t) \quad (\text{B.19})$$

By multiplying both sides of Eq. (B.3) by n^2 and summing over all values of n , we obtain

$$\sum_{n=0}^{n_L} n^2 \frac{d}{dt} p_n(t) = \sum_{n=0}^{n_L} n^2 (\mathbb{E}^{-1} - 1) \lambda_n(t) p(n; t) \quad (\text{B.20})$$

By virtue of Eq. (B.4), this equation can be transformed into

$$\sum_{n=0}^{n_L} n^2 \frac{d}{dt} p_n(t) = \sum_{n=0}^{n_L} \lambda_n(t) p_n(t) (\mathbb{E} - 1) n^2$$

or

$$\sum_{n=0}^{n_L} n^2 \frac{d}{dt} p_n(t) = \sum_{n=0}^{n_L} \lambda_n(t) p_n(t) (2n + 1)$$

Expanding and rearranging the right-hand side of this expression yield

$$\sum_{n=0}^{n_L} n^2 \frac{d}{dt} p(n; t) = 2 \sum_{n=0}^{n_L} [\lambda_n(t)] n p_n(t) + \sum_{n=0}^{n_L} [\lambda_n(t)] p_n(t) \quad (\text{B.21})$$

Inserting Eq. (2.1) in text for $\lambda_n(t)$ into the above equation gives rise to

$$\sum_{n=0}^{n_L} n^2 \frac{d}{dt} p(n; t) = 2 \sum_{n=0}^{n_L} [\kappa(n_L - n)] n p_n(t) + \sum_{n=0}^{n_L} [\kappa(n_L - n)] p_n(t) \quad (\text{B.22})$$

or

$$\sum_{n=0}^{n_L} n^2 \frac{d}{dt} p_n(t) = -2 \kappa \sum_{n=0}^{n_L} n^2 p_n(t) + \kappa (2n_L - 1) \sum_{n=0}^{n_L} n p(t) + \kappa n_L \sum_{n=0}^{n_L} p_n(t) \quad (\text{B.23})$$

By definition,

$$\sum_{n=0}^{n_L} p_n(t) = 1 \quad (\text{B.24})$$

and

$$E[N(t)] = \sum_{n=0}^{n_L} n p_n(t) \quad (\text{B.25})$$

Moreover,

$$E[N^2(t)] = \sum_{n=0}^{n_L} n^2 p_n(t) \quad (\text{B.26})$$

and thus,

$$\frac{d}{dt} E[N^2(t)] = \sum_{n=0}^{n_L} n^2 \frac{d}{dt} p_n(t) \quad (\text{B.27})$$

In light of Eqs. (B.24) through (B.27), Eq. (B.23) can be transformed into

$$\frac{d}{dt} E[N^2(t)] = -2\kappa E[N^2(t)] + \kappa(2n_L - 1)E[N(t)] + \kappa n_L$$

or

$$\frac{d}{dt} E[N^2(t)] + 2\kappa E[N^2(t)] = \kappa(2n_L - 1)E[N(t)] + \kappa n_L \quad (\text{B.28})$$

The expression for $E[N^2(t)]$, Eq. (B.26), in conjunction with the initial conditions for the birth-death process, Eq. (B.13), lead to

$$E[N^2(0)] = 0 \quad (\text{B.29})$$

Inserting Eq. (B.15) for $E[N(t)]$ into Eq. (B.28) and integrating the resulting expression subject to the initial condition given above yield

$$E[N^2(t)] = n_L^2 - 2n_L^2 \exp(-\kappa t) + n_L \exp(-\kappa t) + n_L^2 \exp(-2\kappa t) - n_L \exp(-2\kappa t) \quad (\text{B.30})$$

Consequently, this equation in conjunction with Eqs. (B.15) and (B.18) give rise to

$$\sigma^2(t) = n_L [1 - \exp(-\kappa t)] \exp(-\kappa t) \quad (\text{B.31})$$

This is Eq. (2.6) in the text.

Appendix C - Formation of Carbon Molecular Sieves: System-Size Expansion of the Master Equation of the Pure-Birth Process with a Non-Linear Intensity of Transition Based on a Single Random Variable

The master equation of the pure-birth process of interest is given by Eq. (3.1) in the text as

$$\frac{d}{dt} p_n(t) = \lambda_{n-1}(t)p_{n-1}(t) - \lambda_n(t)p_n(t), \quad n = 0, 1, 2, \dots, n_M - 1, n_M \quad (C.1)$$

In light of the one-step operator, \mathbb{E} , as defined by Eq. (B.2), this equation can be transformed into

$$\frac{d}{dt} p_n(t) = (\mathbb{E}^{-1} - 1)\lambda_n(t)p_n(t), \quad n = 0, 1, 2, \dots, n_M - 1, n_M \quad (C.2)$$

The intensity of birth, $\lambda_n(t)$, in this expression is given by Eq. (3.2) in the text as

$$\lambda_n(t) = \frac{dn}{dt} = \alpha(n_M - n)^2 \quad (C.3)$$

where α is a proportionality constant. Substituting the above expression into Eq. (C.2) yields

$$\frac{d}{dt} p_n(t) = \alpha(\mathbb{E}^{-1} - 1)[(n_M - n)^2]p_n(t) \quad (C.4)$$

It is expected that at later time t , the probability distribution of $N(t)$, $p_n(t)$ or $p(n;t)$, exhibits a sharp peak at some position of order Ω , while its width is of order $\Omega^{1/2}$; see Figure C.1. The symbol, Ω , signifies the system's size, which is n_M in this case. To formulate this formally, $N(t)$ is expressed as the sum of the macroscopic term, $\Omega\varphi(t)$, and the fluctuation term, $\Omega^{1/2}\Xi(t)$ as

$$N(t) = \Omega\varphi(t) + \Omega^{1/2}\Xi(t)$$

or

$$N(t) = n_M\varphi(t) + n_M^{1/2}\Xi(t) \quad (C.5)$$

whose realization is

$$n = n_M\varphi(t) + n_M^{1/2}\xi \quad (C.6)$$

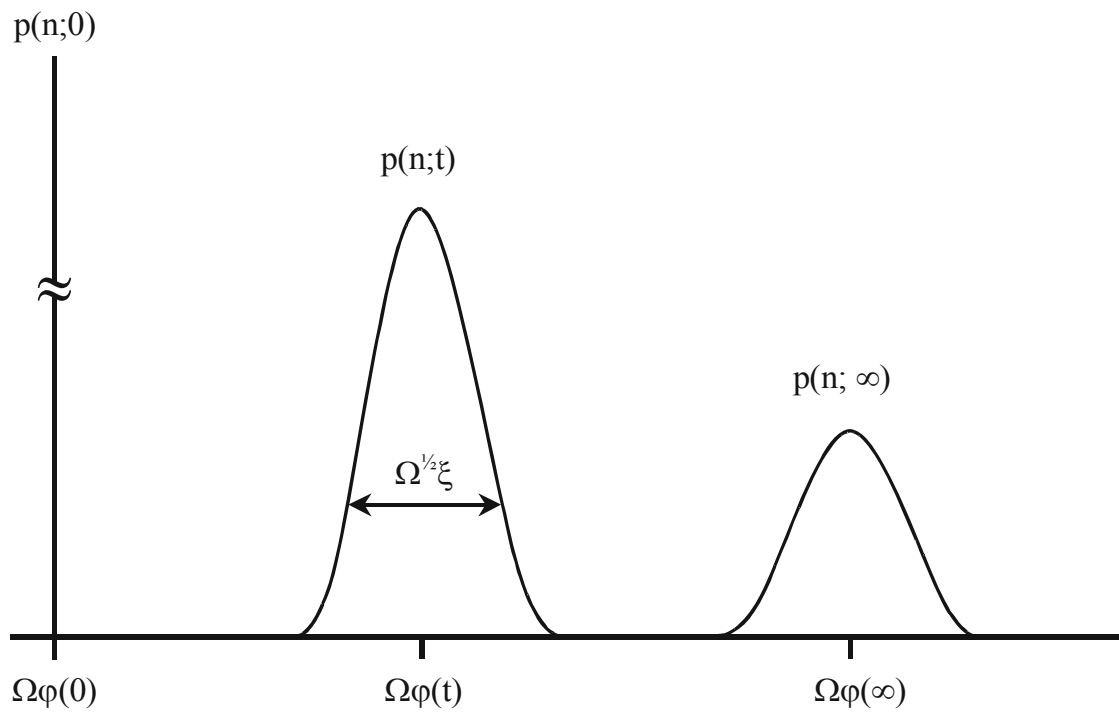


Figure C.1. Temporal evolution of the probability distribution, $p_n(t)$ or $p(n;t)$.

The function, $\varphi(t)$, in these two equations is adjusted to follow the motion of the peak in time; consequently, $p(n;t)$ is transformed into function $\pi(\xi;t)$, which depends on realization ξ of $\Xi(t)$, as

$$p(n;t) = \pi(\xi;t) \quad (C.7)$$

where $\pi(\xi;t) = \Pr[\Xi(t) = \xi]$. From Eq. (C.6), we have

$$\xi = n(n_M^{-1/2}) - n_M^{1/2}\varphi(t) \quad (C.8)$$

Given that n is fixed, the time derivative of the above expression is obtained as

$$\frac{d\xi}{dt} = -n_M^{1/2} \frac{d\varphi}{dt} \quad (C.9)$$

where $\varphi = \varphi(t)$. Differentiating Eq. (C.7) with respect to time leads to

$$\frac{d}{dt} p(n;t) = \frac{\partial}{\partial t} \pi(\xi;t)$$

or

$$\frac{d}{dt} p(n;t) = \frac{\partial \pi}{\partial t} + \frac{\partial \pi}{\partial \xi} \left(\frac{d\xi}{dt} \right) \quad (C.10)$$

where $\pi = \pi(\xi;t)$. By inserting Eq. (C.9) into this equation, we obtain

$$\frac{d}{dt} p(n;t) = \frac{\partial \pi}{\partial t} - n_M^{1/2} \left(\frac{d\varphi}{dt} \right) \frac{\partial \pi}{\partial \xi} \quad (C.11)$$

In light of the one-step operator, \mathbb{E} , we have

$$\mathbb{E}^{-1} n = n - 1$$

Substituting Eq. (C.6) for n on the right-hand side of this equation gives rise to

$$\begin{aligned} \mathbb{E}^{-1} n &= [n_M \varphi(t) + n_M^{1/2} \xi] - 1 \\ &= [n_M \varphi(t) + n_M^{1/2} \xi] - [n_M^{1/2} n_M^{-1/2}] \end{aligned}$$

or

$$\mathbb{E}^{-1} n = n_M \varphi(t) + n_M^{1/2} (\xi - n_M^{-1/2})$$

In other words, \mathbb{E}^{-1} transforms n into $(n-1)$, and therefore, ξ into $(\xi - n_M^{-1/2})$; as a result, from

Eq. (C.7),

$$\mathbb{E}^{-1} p(n;t) = \mathbb{E}^{-1} \pi(\xi;t)$$

or

$$p(n-1; t) = \pi(\xi - n_M^{-1/2}; t) \quad (\text{C.12})$$

The Taylor expansion of $\pi(\xi - n_M^{-1/2}; t)$ about ξ , is obtained as

$$\pi(\xi - n_M^{-1/2}; t) = \pi(\xi; t) + (-n_M^{-1/2}) \frac{\partial}{\partial \xi} \pi(\xi; t) + \frac{1}{2!} (-n_M^{-1/2})^2 \frac{\partial^2}{\partial \xi^2} \pi(\xi; t) + \dots$$

or

$$\pi(\xi - n_M^{-1/2}; t) = \left(1 - n_M^{-1/2} \frac{\partial}{\partial \xi} + \frac{1}{2} n_M^{-1} \frac{\partial^2}{\partial \xi^2} - \dots \right) \pi(\xi; t) \quad (\text{C.13})$$

In view of Eqs. (C.7) and (C.12), the above expression can be transformed to

$$p(n-1; t) = \left(1 - n_M^{-1/2} \frac{\partial}{\partial \xi} + \frac{1}{2} n_M^{-1} \frac{\partial^2}{\partial \xi^2} - \dots \right) p(n; t)$$

or

$$\mathbb{E}^{-1} p(n; t) = \left(1 - n_M^{-1/2} \frac{\partial}{\partial \xi} + \frac{1}{2} n_M^{-1} \frac{\partial^2}{\partial \xi^2} - \dots \right) p(n; t)$$

By comparing both sides of this expression, we have

$$\mathbb{E}^{-1} = 1 - n_M^{-1/2} \frac{\partial}{\partial \xi} + \frac{1}{2} n_M^{-1} \frac{\partial^2}{\partial \xi^2} - \dots \quad (\text{C.14})$$

Substituting this expression in conjunction with Eqs. (C.6), (C.7), and (C.11) into the master equation, Eq. (C.4), leads to

$$\begin{aligned} & \frac{\partial \pi}{\partial t} - n_M^{1/2} \left(\frac{d\varphi}{dt} \right) \frac{\partial \pi}{\partial \xi} \\ &= \alpha n_M^2 \left(-n_M^{-1/2} \frac{\partial}{\partial \xi} + \frac{1}{2} n_M^{-1} \frac{\partial^2}{\partial \xi^2} - \dots \right) [1 - (\varphi + n_M^{-1/2} \xi)]^2 \pi \end{aligned} \quad (\text{C.15})$$

Absorbing the system's size, n_M , into the time variable, t , as

$$n_M t = \gamma$$

and truncating the terms after the second-order derivative for large n_M give

$$\begin{aligned}
& \frac{\partial \pi}{\partial \gamma} - n_M^{1/2} \left(\frac{d\varphi}{d\gamma} \right) \frac{\partial \pi}{\partial \xi} \\
&= \alpha n_M \left(-n_M^{-1/2} \frac{\partial}{\partial \xi} + \frac{1}{2} n_M^{-1} \frac{\partial^2}{\partial \xi^2} \right) (1 - \varphi - n_M^{-1/2} \xi)^2 \pi
\end{aligned} \tag{C.16}$$

By expanding the right-hand side of this equation and collecting the resultant terms of orders $n_M^{1/2}$ and n_M^0 separately, we have

$$\begin{aligned}
& \frac{\partial \pi}{\partial \gamma} - n_M^{1/2} \left(\frac{d\varphi}{d\gamma} \right) \frac{\partial \pi}{\partial \xi} \\
&= n_M^0 \left[2\alpha (1 - \varphi) \frac{\partial}{\partial \xi} (\xi \pi) + \frac{1}{2} \alpha (1 - \varphi)^2 \frac{\partial^2 \pi}{\partial \xi^2} \right] \\
& \quad - n_M^{1/2} \left[\alpha (1 - \varphi)^2 \frac{\partial \pi}{\partial \xi} \right] \\
& \quad + \alpha n_M^{-1/2} \left[-\frac{\partial^2}{\partial \xi^2} (\xi \pi) - \frac{\partial}{\partial \xi} (\xi^2 \pi) + \varphi \frac{\partial^2}{\partial \xi^2} (\xi \pi) + \frac{1}{2} n_M^{-1/2} \frac{\partial^2}{\partial \xi^2} (\xi^2 \pi) \right]
\end{aligned} \tag{C.17}$$

Comparing both sides of the above expression gives rise to

$$\frac{d\varphi}{d\gamma} = \alpha (1 - \varphi)^2 \tag{C.18}$$

and

$$\frac{\partial \pi}{\partial \gamma} = 2\alpha (1 - \varphi) \frac{\partial}{\partial \xi} (\xi \pi) + \frac{1}{2} \alpha (1 - \varphi)^2 \frac{\partial^2 \pi}{\partial \xi^2} \tag{C.19}$$

Of these two equations, the former is the macroscopic equation governing the overall behavior of the process, and the latter is a linear Fokker-Plank equation governing the fluctuations of the process around the macroscopic values and whose coefficients depend on t through φ , i.e., $\varphi(t)$.

Appendix D - Formation of Carbon Molecular Sieves: Derivation of the Mean and Variance for the Pure-Birth Process with a Non-Linear Intensity of Transition Based on a Single Random Variable

For convenience, Eq. (C.5) for random variable $N(t)$ is rewritten below

$$N(t) = n_M \varphi(t) + n_M^{1/2} \Xi(t) \quad (D.1)$$

As defined earlier, the mean, $E[N(t)]$ or $m(t)$, is the expected value, or first moment, of the distribution of random variable, $N(t)$; thus, from the above equation, we obtain

$$\begin{aligned} E[N(t)] &= E[n_M \varphi(t) + n_M^{1/2} \Xi(t)] \\ &= n_M E[\varphi(t)] + n_M^{1/2} E[\Xi(t)] \end{aligned}$$

or

$$m(t) = n_M \varphi(t) + n_M^{1/2} E[\Xi(t)] \quad (D.2)$$

Similarly, the variance, $\text{Var}[N(t)]$ or $\sigma^2(t)$, which is the second moment of the distribution of $N(t)$ about the mean, $E[N(t)]$, is obtained as

$$\begin{aligned} \text{Var}[N(t)] &= \text{Var}[n_M \varphi(t) + n_M^{1/2} \Xi(t)] \\ &= n_M^2 \text{Var}[\varphi(t)] + n_M \text{Var}[\Xi(t)] \end{aligned}$$

or

$$\sigma^2(t) = n_M \text{Var}[\Xi(t)]$$

In light of Eq. (B.18), this equation can be rewritten as

$$\sigma^2(t) = n_M \left(E[\Xi^2(t)] - \{E[\Xi(t)]\}^2 \right) \quad (D.3)$$

where $E[\Xi(t)]$ and $E[\Xi^2(t)]$ are the first and second moments of the random variable, $\Xi(t)$. Clearly, the functions, $\varphi(t)$, $E[\Xi(t)]$, and $E[\Xi^2(t)]$, need be evaluated prior to obtaining the expressions for $m(t)$ and $\sigma^2(t)$; their derivation is detailed in what follows.

At the outset of the process, i.e., at $t = 0$, $N(0) = 0$; moreover, no fluctuations arise around 0, which implies that $\Xi(0) = 0$. Hence, from Eq. (D.1),

$$\varphi(0) = 0 \quad (\text{D.4})$$

The macroscopic equation governing the overall behavior of the process is given by Eq. (C.18) as

$$\frac{d\varphi}{d\gamma} = \alpha(1 - \varphi)^2$$

Because $n_M t = \gamma$, this equation can be rewritten as

$$\frac{d\varphi}{dt} = \alpha n_M (1 - \varphi)^2$$

Integration of this equation, Eq. (C.18), gives

$$\varphi(t) = 1 - \frac{1}{(\alpha n_M)t + c}$$

In view of Eq. (D.4), the constant, c , in the above expression is 1; thus,

$$\varphi(t) = \frac{(\alpha n_M)t}{(\alpha n_M)t + 1} \quad (\text{D.5})$$

As indicated in Appendix B, for any arbitrary functions f and g which take integers, the following expression holds⁷¹

$$\sum_{n=0}^{n_M-1} [g(n)\mathbb{E}f(n)] = \sum_{n=1}^{n_M} [f(n)\mathbb{E}^{-1}g(n)] \quad (\text{D.6})$$

When $g(-1) = f(n_M + 1) = 0$, this equation becomes

$$\sum_{n=0}^{n_M} [g(n)\mathbb{E}f(n)] = \sum_{n=0}^{n_M} [f(n)\mathbb{E}^{-1}g(n)] \quad (\text{D.7})$$

If functions f and g take real numbers, the central-difference approximation gives

$$\frac{\partial}{\partial x} f(x) \approx \frac{f(x + \Delta x) - f(x)}{\Delta x} \quad (\text{D.8})$$

and

$$\frac{\partial^2}{\partial x^2} f(x) \approx \frac{f(x + \Delta x) - 2f(x) + f(x - \Delta x)}{(\Delta x)^2} \quad (\text{D.9})$$

Hence,

$$\sum_x \left[g(x) \frac{\partial}{\partial x} f(x) \right] \approx \sum_x \left\{ g(x) \left[\frac{f(x + \Delta x) - f(x)}{\Delta x} \right] \right\}$$

or

$$\sum_x \left[g(x) \frac{\partial}{\partial x} f(x) \right] \approx \frac{1}{\Delta x} \left\{ \sum_x [g(x)f(x + \Delta x)] - \sum_x [g(x)f(x)] \right\} \quad (\text{D.10})$$

By extending the property of the one-step operator, Eq. (B-7), to the domain of the real numbers, the right-hand side of the above expression can be transformed to

$$\begin{aligned} & \sum_x \left[g(x) \frac{\partial}{\partial x} f(x) \right] \\ & \approx \frac{1}{\Delta x} \left\{ \sum_x [g(x)f(x + \Delta x)] - \sum_x [g(x)f(x)] \right\} \\ & = \frac{1}{\Delta x} \left\{ \sum_x [g(x)\mathbb{E}f(x)] - \sum_x [g(x)f(x)] \right\} \end{aligned}$$

or

$$\begin{aligned} & \sum_x \left[g(x) \frac{\partial}{\partial x} f(x) \right] \\ & = \frac{1}{\Delta x} \left\{ \sum_x [f(x)\mathbb{E}^{-1}g(x)] - \sum_x [g(x)f(x)] \right\} \\ & = \frac{1}{\Delta x} \left\{ \sum_x [f(x)g(x - \Delta x)] - \sum_x [f(x)g(x)] \right\} \end{aligned}$$

or

$$\begin{aligned} & \sum_x \left[g(x) \frac{\partial}{\partial x} f(x) \right] \\ & = \sum_x \left\{ f(x) \left[\frac{g(x - \Delta x) - g(x)}{\Delta x} \right] \right\} \\ & = -\sum_x \left\{ f(x) \left[\frac{g(x) - g(x - \Delta x)}{\Delta x} \right] \right\} \quad (\text{D.11}) \end{aligned}$$

In light of Eq. (D.8), this expression reduces to

$$\sum_x \left[g(x) \frac{\partial}{\partial x} f(x) \right] = -\sum_x \left[f(x) \frac{\partial}{\partial x} g(x) \right] \quad (\text{D.12})$$

Similarly,

$$\begin{aligned}
& \sum_x \left[\mathbf{g}(\mathbf{x}) \frac{\partial^2}{\partial \mathbf{x}^2} f(\mathbf{x}) \right] \\
& \approx \sum_x \left\{ \mathbf{g}(\mathbf{x}) \left[\frac{f(\mathbf{x} + \Delta \mathbf{x}) - 2f(\mathbf{x}) + f(\mathbf{x} - \Delta \mathbf{x})}{(\Delta \mathbf{x})^2} \right] \right\} \\
& \approx \frac{1}{(\Delta \mathbf{x})^2} \left\{ \sum_x [\mathbf{g}(\mathbf{x})f(\mathbf{x} + \Delta \mathbf{x})] - 2 \sum_x [\mathbf{g}(\mathbf{x})f(\mathbf{x})] + \sum_x [\mathbf{g}(\mathbf{x})f(\mathbf{x} - \Delta \mathbf{x})] \right\}
\end{aligned} \tag{D.13}$$

By virtue of Eq. (D.7), we obtain

$$\begin{aligned}
& \sum_x \left[\mathbf{g}(\mathbf{x}) \frac{\partial^2}{\partial \mathbf{x}^2} f(\mathbf{x}) \right] \\
& = \frac{1}{(\Delta \mathbf{x})^2} \left\{ \sum_x [\mathbf{g}(\mathbf{x})\mathbb{E}f(\mathbf{x})] - 2 \sum_x [\mathbf{g}(\mathbf{x})f(\mathbf{x})] + \sum_x [\mathbf{g}(\mathbf{x})\mathbb{E}^{-1}f(\mathbf{x})] \right\} \\
& = \frac{1}{(\Delta \mathbf{x})^2} \left\{ \sum_x [f(\mathbf{x})\mathbb{E}^{-1}\mathbf{g}(\mathbf{x})] - 2 \sum_x [\mathbf{g}(\mathbf{x})f(\mathbf{x})] + \sum_x [f(\mathbf{x})\mathbb{E}\mathbf{g}(\mathbf{x})] \right\}
\end{aligned}$$

or

$$\begin{aligned}
& \sum_x \left[\mathbf{g}(\mathbf{x}) \frac{\partial^2}{\partial \mathbf{x}^2} f(\mathbf{x}) \right] \\
& = \frac{1}{(\Delta \mathbf{x})^2} \left\{ \sum_x [f(\mathbf{x})\mathbf{g}(\mathbf{x} - \Delta \mathbf{x})] - 2 \sum_x [f(\mathbf{x})\mathbf{g}(\mathbf{x})] + \sum_x [f(\mathbf{x})\mathbf{g}(\mathbf{x} + \Delta \mathbf{x})] \right\} \\
& = \sum_x \left\{ f(\mathbf{x}) \left[\frac{\mathbf{g}(\mathbf{x} + \Delta \mathbf{x}) - 2\mathbf{g}(\mathbf{x}) + \mathbf{g}(\mathbf{x} - \Delta \mathbf{x})}{(\Delta \mathbf{x})^2} \right] \right\}
\end{aligned}$$

or in view of Eq. (D.9),

$$\sum_x \left[\mathbf{g}(\mathbf{x}) \frac{\partial^2}{\partial \mathbf{x}^2} f(\mathbf{x}) \right] = \sum_x \left[f(\mathbf{x}) \frac{\partial^2}{\partial \mathbf{x}^2} \mathbf{g}(\mathbf{x}) \right] \tag{D.14}$$

The linear Fokker-Plank equation governing the fluctuations of the process around the macroscopic values is given by Eq. (C.19) as

$$\frac{\partial \pi}{\partial \gamma} = 2\alpha(1-\varphi) \frac{\partial}{\partial \xi} (\xi \pi) + \frac{1}{2} \alpha (1-\varphi)^2 \frac{\partial^2 \pi}{\partial \xi^2} \tag{D.15}$$

Because $n_M t = \gamma$, this equation can be rewritten as

$$\frac{\partial \pi}{\partial t} = 2\alpha n_M (1-\varphi) \frac{\partial}{\partial \xi} (\xi \pi) + \frac{1}{2} \alpha n_M (1-\varphi)^2 \frac{\partial^2 \pi}{\partial \xi^2} \quad (\text{D.16})$$

Multiplying both sides of the above equation by ξ and summing over all values of ξ yield

$$\sum_{\xi} \xi \frac{\partial}{\partial t} \pi = [2\alpha n_M (1-\varphi)] \left[\sum_{\xi} \xi \frac{\partial}{\partial \xi} (\xi \pi) \right] + \frac{1}{2} [\alpha n_M (1-\varphi)^2] \left[\sum_{\xi} \xi \frac{\partial^2}{\partial \xi^2} \pi \right] \quad (\text{D.17})$$

By virtue of Eqs. (B-12) and (B-14), the right-hand side of this expression can be transformed to

$$\sum_{\xi} \xi \frac{\partial}{\partial t} \pi = [2\alpha n_M (1-\varphi)] \left[-\sum_{\xi} \xi \pi \frac{\partial}{\partial \xi} \xi \right] + \frac{1}{2} [\alpha n_M (1-\varphi)^2] \left[\sum_{\xi} \pi \frac{\partial^2}{\partial \xi^2} \xi \right]$$

or

$$\sum_{\xi} \xi \frac{\partial}{\partial t} \pi = -[2\alpha n_M (1-\varphi)] \left[\sum_{\xi} \xi \pi \right] \quad (\text{D.18})$$

The first moment of random variable $\Xi(t)$, i.e., $E[\Xi(t)]$, is defined as

$$E[\Xi(t)] = \sum_{\xi} \xi \pi(\xi; t)$$

or

$$E[\Xi(t)] = \sum_{\xi} \xi \pi \quad (\text{D.19})$$

and thus,

$$\frac{d}{dt} E[\Xi(t)] = \sum_{\xi} \xi \frac{\partial}{\partial t} \pi \quad (\text{D.20})$$

In light of the above two equations, Eq. (D.18) reduces to

$$\frac{d}{dt} E[\Xi(t)] = -[2\alpha n_M (1-\varphi)] E[\Xi(t)] \quad (\text{D.21})$$

Inserting Eq. (D.5) for $\varphi(t)$ into this equation and integrating the resulting expression yield

$$E[\Xi(t)] = \frac{c'}{[(\alpha n_M)t + 1]^2} \quad (\text{D.22})$$

From the initial conditions for the transformed probability distribution, $\pi(\xi; t)$,

$$\pi(\xi; 0) = \begin{cases} 1 & \text{if } \xi = 0 \\ 0 & \text{elsewhere} \end{cases} \quad (\text{D.23})$$

and the definition of $E[\Xi(t)]$, as given by Eq. (B-19), we have

$$E[\Xi(0)] = 0, \quad (D.24)$$

thereby indicating that

$$c' = 0 \quad (D.25)$$

Hence,

$$E[\Xi(t)] = 0 \quad (D.26)$$

As discerned from this equation, the mean of random variable $\Xi(t)$ signifying the fluctuations of the process around their mean values is null.

Similarly, multiplying both sides of Eq. (D.16) by ξ^2 and summing over all values of ξ yield

$$\sum_{\xi} \xi^2 \frac{\partial}{\partial t} \pi = [2\alpha n_M (1-\phi)] \left[\sum_{\xi} \xi^2 \frac{\partial}{\partial \xi} (\xi \pi) \right] + \frac{1}{2} [\alpha n_M (1-\phi)^2] \left[\sum_{\xi} \xi^2 \frac{\partial^2}{\partial \xi^2} \pi \right] \quad (D.27)$$

By virtue of Eqs. (D.12) and (D.14), the right-hand side of the above expression can be transformed to

$$\sum_{\xi} \xi^2 \frac{\partial}{\partial t} \pi = [2\alpha n_M (1-\phi)] \left[-\sum_{\xi} \xi \pi \frac{\partial}{\partial \xi} \xi^2 \right] + \frac{1}{2} [\alpha n_M (1-\phi)^2] \left[\sum_{\xi} \pi \frac{\partial^2}{\partial \xi^2} \xi^2 \right]$$

or

$$\sum_{\xi} \xi^2 \frac{\partial}{\partial t} \pi = -4[\alpha n_M (1-\phi)] \left[\sum_{\xi} \xi^2 \pi \right] + [\alpha n_M (1-\phi)^2] \left[\sum_{\xi} \pi \right] \quad (D.28)$$

For the transformed probability distribution, $\pi(\xi;t)$, the following property must hold

$$\sum_{\xi} \pi(\xi;t) = 1$$

or

$$\sum_{\xi} \pi = 1 \quad (D.29)$$

Thus, Eq. (D.28) can be rewritten as

$$\sum_{\xi} \xi^2 \frac{\partial}{\partial t} \pi = -4[\alpha n_M (1-\phi)] \left[\sum_{\xi} \xi^2 \pi \right] + [\alpha n_M (1-\phi)^2] \quad (D.30)$$

The second moment of random variable $\Xi(t)$, i.e., $E[\Xi^2(t)]$, is defined as

$$E[\Xi^2(t)] = \sum_{\xi} \xi^2 \pi(\xi;t)$$

or

$$E[\Xi^2(t)] = \sum_{\xi} \xi^2 \pi \quad (D.31)$$

and thus,

$$\frac{d}{dt} E[\Xi^2(t)] = \sum_{\xi} \xi^2 \frac{\partial}{\partial t} \pi \quad (D.32)$$

In view of the above two equations, Eq. (B-30) reduces to

$$\frac{d}{dt} E[\Xi^2(t)] = -4[\alpha n_M (1-\phi)] E[\Xi^2(t)] + [\alpha n_M (1-\phi)^2] \quad (D.33)$$

Inserting Eq. (D.5) for $\phi(t)$ into this equation and integrating the resulting expression yield

$$E[\Xi^2(t)] = \frac{1}{3[(\alpha n_M)t+1]^4} + \frac{c''}{[(\alpha n_M)t+1]^4} \quad (D.34)$$

From the aforementioned initial conditions for the transformed probability distribution, $\pi(\xi;t)$, as given by Eq. (D.23), and the expression of $E[\Xi^2(t)]$ as defined by Eq. (D.31), we have

$$E[\Xi^2(0)] = 0, \quad (D.35)$$

thereby indicating that

$$c'' = -\frac{1}{3} \quad (D.36)$$

Hence,

$$E[\Xi^2(t)] = \frac{1}{3[(\alpha n_M)t+1]} \left\{ 1 - \frac{1}{[(\alpha n_M)t+1]^3} \right\} \quad (D.37)$$

The mean, $E[N(t)]$ or $m(t)$, is obtained by substituting Eqs. (D.5) and (D.26) into (D.2) as

$$m(t) = n_M \left[\frac{(\alpha n_M)t}{(\alpha n_M)t+1} \right]$$

or

$$m(t) = n_M \left(\frac{\alpha t}{\alpha t+1} \right) \quad (D.38)$$

where $\alpha' = (\alpha n_M)$; this is Eq. (3.4) in the text. Similarly, the variance, $\text{Var}[N(t)]$ or $\sigma^2(t)$, is obtained by inserting Eqs. (D.26) and (D.37) into Eq. (D.3) as

$$\sigma^2(t) = n_M \left(\frac{1}{3[(\alpha n_M)t + 1]} \left\{ 1 - \frac{1}{[(\alpha n_M)t + 1]^3} \right\} \right)$$

or

$$\sigma^2(t) = \frac{n_M}{3(\alpha't + 1)} \left[1 - \frac{1}{(\alpha't + 1)^3} \right] \quad (\text{D.39})$$

This is Eq. (3.6) in the text.

Appendix E - Formation of Carbon Molecular Sieves: Derivation of the Probability Density Function and the Cumulative Distribution Function of Waiting Time for the Pure-Birth Process with a Non-Linear Intensity of Transition Based on a Single Random Variable

Let T_n be a random variable representing the waiting time between events for the pure-birth process of interest with the intensity of birth, $\lambda_n(t)$; a realization of T_n is denoted by v . Given that it is in state n at time t , the system is assumed to remain in this state during time interval $(t, t+v)$; at the end of which, i.e., at $(t+v)$, a transition occurs and the state of the system changes. The probability that a transition occurs during time interval $(t, t+v)$ is specified by the cumulative distribution function, cdf, of T_n with realization v . This function is denoted by $H_n(v)$ and defined as

$$H_n(v) = \Pr[T_n \leq v] \quad (\text{E.1})$$

By definition, $H_n(v)$ is within the range from 0 to 1. Moreover, the probability that no transition occurs during time interval $(t, t+v)$ given that the system is in state n at time t , $G_n(v)$, is⁷²

$$G_n(v) = \Pr[T_n > v] = 1 - H_n(v) \quad (\text{E.2})$$

For the succeeding small time interval $[(t+v), (t+v) + \Delta v]$,^{74, 122}

$$H_n(\Delta v) = [\lambda_n(t+v)]\Delta v + o(\Delta v) \quad (\text{E.3})$$

where $o(\Delta v)$ is defined such that

$$\lim_{\Delta v \rightarrow 0} \frac{o(\Delta v)}{\Delta v} = 0,$$

Note that the intensity of birth, $\lambda_n(t)$, in Eq. (E.3) is evaluated at the time at which a transition occurs, i.e., at $(t+v)$. On the basis of Eq. (E.2), we obtain

$$G_n(\Delta v) = \{1 - [\lambda_n(t+v)]\Delta v\} + o(\Delta v) \quad (\text{E.4})$$

The Markovian property implies that disjoint time intervals are independent of one another; therefore,⁷²

$$G_n(v + \Delta v) = G_n(v)G_n(\Delta v) \quad (E.5)$$

Inserting Eq. (E.4) into the above equation results in

$$G_n(v + \Delta v) = G_n(v) \{1 - [\lambda_n(t + v)]\Delta v\} + o(\Delta v) \quad (E.6)$$

Expanding and rearranging this expression yield

$$G_n(v + \Delta v) - G_n(v) = -[\lambda_n(t + v)]G_n(v)\Delta v + o(\Delta v) \quad (E.7)$$

Dividing both sides of this equation by Δv and taking the limit as $\Delta v \rightarrow 0$ give rise to

$$\frac{d}{dv} G_n(v) = -[\lambda_n(t + v)]G_n(v) \quad (E.8)$$

By integrating this ordinary differential equation subject to the initial condition,^{72, 74, 122}

$$G_n(0) = 1,$$

we have

$$G_n(v) = \exp \left\{ - \int_0^v [\lambda_n(t + v')] dv' \right\} \quad (E.9)$$

Equation (D.2) in conjunction with the above equation leads to

$$H_n(v) = 1 - \exp \left\{ - \int_0^v [\lambda_n(t + v')] dv' \right\} \quad (E.10)$$

Differentiating both sides of this equation with respect to v gives

$$\frac{d}{dv} H_n(v) = [\lambda_n(t + v)] \exp \left\{ - \int_0^v [\lambda_n(t + v')] dv' \right\} \quad (E.11)$$

The probability density function, pdf, of T_n given that the system is in state n at time t , $h_n(v)$, is defined as

$$h_n(v) = \frac{d}{dv} H_n(v) \quad (E.12)$$

Naturally,

$$H_n(v) = \int_0^v h_n(v') dv' \quad (E.13)$$

In light of Eq. (E.12), Eq. (E.11) can be rewritten as

$$h_n(v) = [\lambda_n(t+v)] \exp \left\{ - \int_0^v [\lambda_n(t+v')] dv' \right\} \quad (\text{E.14})$$

The above equation in conjunction with Eq. (E.10) reveal that the pdf of T_n is exponential.^{74, 122} Clearly, the parameter of this pdf depends on the form of the intensity of birth, $\lambda_n(t)$. Inserting Eq. (3.2) in the text for $\lambda_n(t)$ into Eq. (E.10) yields

$$H_n(v) = 1 - \exp \left\{ - \int_0^v [\alpha(n_M - n)^2] dv' \right\} \quad (\text{E.15})$$

Upon integration of this expression, we obtain

$$H_n(v) = 1 - \exp \left\{ - [\alpha(n_M - n)^2] v \right\} \quad (\text{E.16})$$

In light of Eq. (E.12),

$$h_n(v) = [\alpha(n_M - n)^2] \exp \left\{ - [\alpha(n_M - n)^2] v \right\} \quad (\text{E.17})$$

These two equations indicate that the pdf of random variable T_n is exponential with parameter $\alpha(n_M - n)^2$, i.e., the intensity of birth, $\lambda_n(t)$, of the pure-birth process of concern, which is dependent only on realization n but independent of time t .

Appendix F - Formation of Carbon Molecular Sieves: Estimation of Waiting Time for the Pure-Birth Process with a Non-Linear Intensity of Transition Based on a Single Random Variable

As indicated in the preceding appendix, the random variable, T_n , with realization v represents the waiting time between successive events for a birth-death process. Equation (E.1) repeated below defines $H_n(v)$, i.e., the cdf of T_n , as

$$H_n(v) = \Pr[T_n \leq v] \tag{F.1}$$

This cdf signifies the probability that the system undergoes a transition during time interval $(t, t + v)$ given that it is in state n at time t .

Let U be a random variable defined as

$$U = H_n(T_n) \tag{F.2}$$

Thus, u , which is a realization of U , is

$$u = H_n(v) \tag{F.3}$$

By definition, any realization u is within the range from 0 to 1. Naturally, the cdf of U with realization u , i.e., $F_U(u)$, is given by

$$F_U(u) = \Pr[U \leq u] \tag{F.4}$$

Substituting Eqs. (E.2) and (E.3) into this equation yields

$$F_U(u) = \Pr[H_n(T_n) \leq H_n(v)] \tag{F.5}$$

The inverse function of any given function, $y = f(x)$, is defined as $x = f^{-1}(y)$, or $x = f^{-1}[f(x)]$, provided that $f(x)$ is continuous and strictly increasing.^[131, 132] In other words, the inverse function, $x = f^{-1}(y)$, reverses what the original function, $y = f(x)$, performs over any value x of its domain, thereby returning x . Note that the inverse function of $f(x)$ is not its reciprocal or multiplicative inverse, which is given by $[1/f(x)]$ or $[f(x)]^{-1}$. Herein, $y = f(x)$ stands for $U = H_n(T_n)$ on the basis of Eq. (F.2); thus, its inverse function is given by

$$T_n = H_n^{-1}(U)$$

Inserting Eq. (F.2) into the above equation yields

$$T_n = H_n^{-1}[H_n(T_n)] \quad (\text{F.6})$$

and therefore,

$$v = H_n^{-1}[H_n(v)] \quad (\text{F.7})$$

Given that the functions, $H_n(T_n)$ and $H_n(v)$, are continuous and strictly increasing, they can be substituted by $H_n^{-1}[H_n(T_n)]$ and $H_n^{-1}[H_n(v)]$, respectively, in the inequality within the bracket on the right-hand side of Eq. (F.5) without altering the inequality^[111]; hence,

$$F_U(u) = \Pr \{ H_n^{-1}[H_n(T_n)] \leq H_n^{-1}[H_n(v)] \} \quad (\text{F.8})$$

In light of Eqs. (F.6) and (F.7), this equation reduces to

$$F_U(u) = \Pr[T_n \leq v] \quad (\text{F.9})$$

Note that the right-hand side of this expression is $H_n(v)$ as defined by Eq. (F.1); thus,

$$F_U(u) = H_n(v) \quad (\text{F.10})$$

Because of Eq. (F.3),

$$F_U(u) = u \quad (\text{F.11})$$

This is the expression for the cdf of U with realization u ; by definition, its pdf is

$$f_U(u) = \frac{d}{du} F_U(u)$$

Substituting Eq. (F.11) into the right-hand side of this equation gives

$$f_U(u) = \frac{d}{du} (u)$$

or

$$f_U(u) = 1 \quad (\text{F.12})$$

This equation in conjunction with Eq. (F.11) imply that U is the uniform random variable on interval $(0, 1)$.^[111] As a result, a realization of T_n , i.e., v , can be estimated by sampling a realization of U , i.e., u , on interval $(0, 1)$, and solving Eq. (F.3) for v as^[74]

$$v = H_n^{-1}(u) \quad (\text{F.13})$$

Figure F.1 illustrates this scheme to estimate waiting time v . For the pure-birth process of interest, Eq. (F.3) is

$$u = 1 - \exp\{-[\alpha(n_M - n)^2]v\} \quad (\text{F.14})$$

Clearly, the right-hand side of this expression is $H_n(v)$ as given by Eq. (E.16). By solving the above equation for v , we obtain

$$v = \frac{-1}{[\alpha(n_M - n)^2]} \ln(1 - u) \quad (\text{F.15})$$

This is Eq. (3.20) in the text. Note that v is dependent on realization n but independent of time t .

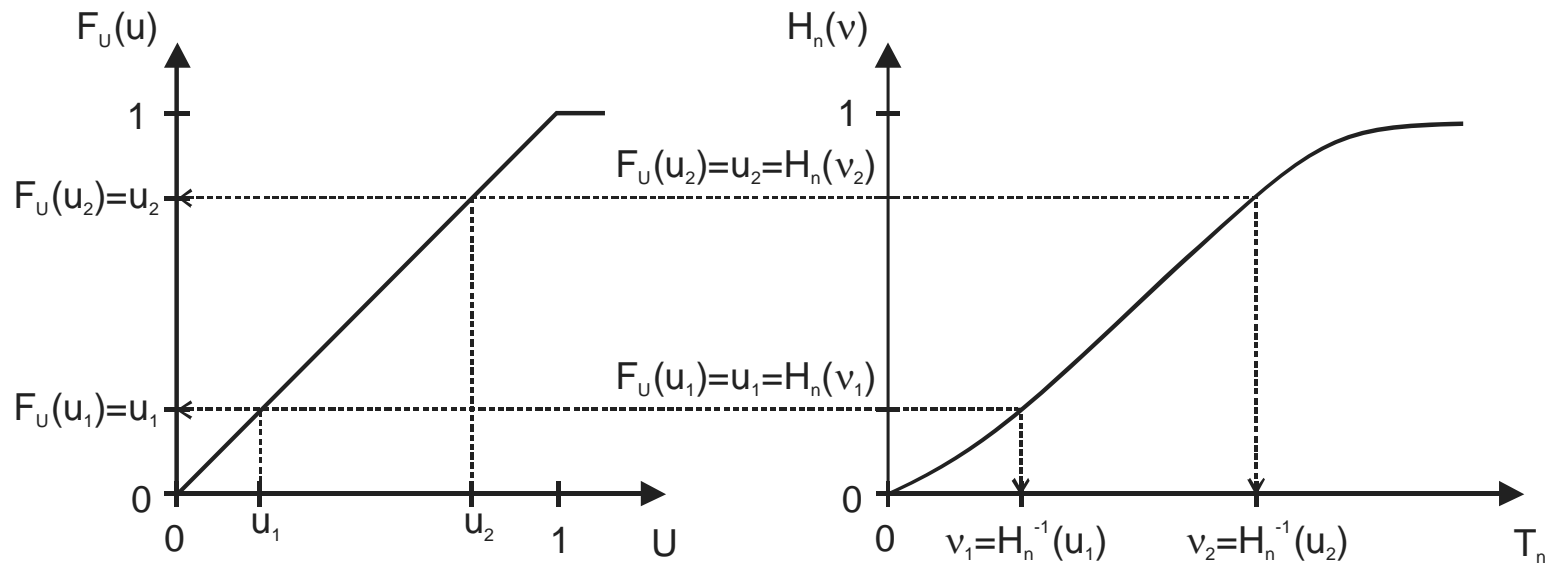


Figure F.1. Schematic for estimating realization v of the random variable, T_n , representing the waiting time on the basis of realization u of the uniform random variable, U , on interval $(0,1)$.

Appendix G - Formation of Carbon Molecular Sieves: Computer Codes for Performing Monte Carlo Simulation of the Pure-Birth Process with a Non-Linear Intensity of Transition Based on a Single Random Variable via the Event-Driven and Time-Driven Approaches

Two computer codes have been written in Microsoft Visual Basic for simulating the pure-birth process of interest through the Monte Carlo method via the event-driven and time-driven approaches on two separate spreadsheets of Microsoft Excel for Windows. The resultant codes for the event-driven approach as well as for the time-driven approach are listed in Tables G.1 and G.2, respectively.

Table G.1. Computer Code in Microsoft Visual Basic for Performing Monte Carlo Simulation of the Pure-Birth Process via the Event-Driven Approach.

```
Sub EventDriven()
```

```
'MONTE CARLO SIMULATION VIA EVENT-DRIVEN APPROACH
```

```
'CMS FORMATION AS A PURE-BIRTH PROCESS WITH A NON-LINEAR
```

```
'INTENSITY FUNCTION BASED ON A SINGLE RANDOM VARIABLE
```

```
Randomize
```

```
Dim OutputData As Integer
```

```
OutputData = 19
```

```
Range("B" + CStr(OutputData)).Select
```

```
Range(Selection, Selection.End(xlToRight).End(xlDown)).ClearContents
```

```
Range("B" + CStr(OutputData)).Select
```

```
'Constants
```

```
alfa = Range("c3").Value
```

```
nM = Range("c4").Value
```

```
n0 = Range("c5").Value
```

```
t0 = Range("c6").Value
```

```
tf = Range("c7").Value
```

```
dtheta = Range("c8").Value
```

```
Zf = Range("c9").Value
```


Do While (theta < t)

' Column of data-recording time

Range("B" + CStr(OutputData)).Value = theta

' Column of realizations of N(t)

Range("C" + CStr(OutputData)).Value = n

' Column of sum of realizations

Range("D" + CStr(OutputData)).Value = Range("D" + CStr(OutputData)).Value +
Range("C" + CStr(OutputData)).Value

' Column of means

Range("E" + CStr(OutputData)).Value = Range("D" + CStr(OutputData)).Value / Zf

' Column of sum of squares of realizations

Range("F" + CStr(OutputData)).Value = (Range("F" + CStr(OutputData)).Value) +
(Range("C" + CStr(OutputData)).Value) ^ 2

' Column of variances

Range("G" + CStr(OutputData)).Value = (1 / (Zf - 1)) * (Range("F" +
CStr(OutputData)).Value - (1 / Zf) * (Range("D" + CStr(OutputData)).Value) ^ 2)

' Column of means plus standard deviations

Range("H" + CStr(OutputData)).Value = Range("E" + CStr(OutputData)).Value +
Sqr(Range("G" + CStr(OutputData)).Value)

' Column of means minus standard deviations

```
Range("I" + CStr(OutputData)).Value = Range("E" + CStr(OutputData)).Value -  
Sqr(Range("G" + CStr(OutputData)).Value)
```

```
OutputData = OutputData + 1
```

```
If theta <= tf Then
```

```
    theta = theta + dtheta
```

```
Else
```

```
    Exit Do
```

```
End If
```

```
Loop
```

```
n = (n + 1)
```

```
Loop
```

```
Next Z
```

```
End Sub
```

Table G.2. Computer Code in Microsoft Visual Basic for Performing Monte Carlo Simulation of the Pure-Birth Process via the Time-Driven Approach.

Sub TimeDriven()

'MONTE CARLO SIMULATION VIA TIME-DRIVEN APPROACH

'CMS FORMATION AS A PURE-BIRTH PROCESS WITH A NON-LINEAR

'INTENSITY FUNCTION BASED ON A SINGLE RANDOM VARIABLE

Randomize

Dim OutputData As Integer

OutputData = 18

Range("B" + CStr(OutputData)).Select

Range(Selection, Selection.End(xlToRight).End(xlDown)).ClearContents

Range("B" + CStr(OutputData)).Select

OutputData = 18

Range("B" + CStr(OutputData)).Select

' Constants

alpha = Range("c3").Value

nM = Range("c4").Value

n0 = Range("c5").Value

t0 = Range("c6").Value

tf = Range("c7").Value

```
dt = Range("c8").Value
Zf = Range("c9").Value
```

```
For Z = 1 To Zf
```

```
    OutputData = 18
```

```
    'Range("B" + CStr(OutputData)).Select
```

```
    t = t0                ' Initial value of clock time
```

```
    n = n0                ' Initial value of random variable N(t)
```

```
    Do Until t >= tf
```

```
        ' Column of time
```

```
        Range("B" + CStr(OutputData)).Value = t
```

```
        ' Column of realizations of random variable N(t)
```

```
        Range("C" + CStr(OutputData)).Value = n
```

```
        ' Column of sum of realizations
```

```
        Range("D" + CStr(OutputData)).Value = Range("D" + CStr(OutputData)).Value +
Range("C" + CStr(OutputData)).Value
```

```
        ' Column of means
```

```
        Range("E" + CStr(OutputData)).Value = Range("D" + CStr(OutputData)).Value / Zf
```

```
        ' Column of sum of squares of realizations
```

```
        Range("F" + CStr(OutputData)).Value = (Range("F" + CStr(OutputData)).Value) +
(Range("C" + CStr(OutputData)).Value) ^ 2
```

```

' Column of variances
Range("G" + CStr(OutputData)).Value = (1 / (Zf - 1)) * (Range("F" +
CStr(OutputData)).Value - (1 / Zf) * (Range("D" + CStr(OutputData)).Value) ^ 2)

' Column of means plus standard deviations
Range("H" + CStr(OutputData)).Value = Range("E" + CStr(OutputData)).Value +
Sqr(Range("G" + CStr(OutputData)).Value)

' Column of means minus standard deviations
Range("I" + CStr(OutputData)).Value = Range("E" + CStr(OutputData)).Value -
Sqr(Range("G" + CStr(OutputData)).Value)

OutputData = OutputData + 1

t = t + dt

u = Rnd(1) ' Uniform random number

lambdadt = alpha * (nM - n) ^ 2 * dt ' Probability of occurrence for the birth event

```

If $u \leq \text{lambdadt}$ Then

$n = n + 1$

Else

$n = n$

End If

Loop

Next Z

End Sub

Appendix H - Formation of Carbon Molecular Sieves: Simulation of Experimental Data for the Pure-Birth Process with a Non-Linear Intensity of Transition Based on a Single Random Variable

At the outset, or early stage, of the pore-narrowing, the number of carbon packets depositing onto the pores' mouths is minute. Consequently, the random variable, $N(t)$, with realization n can be assumed to obey a Poisson probability distribution given by^{110, 132, 133}

$$\Pr[N(t) = n] = \frac{(\beta t)^n}{n!} \exp[-(\beta t)] \quad (\text{H.1})$$

where the positive parameter, (βt) , corresponds to the distribution's mean, $m_p(t)$; thus,

$$m_p(t) = \beta t \quad (\text{H.2})$$

Naturally, this is the equation of a straight line whose slope is β ; hence,

$$\beta = \frac{[m_p(t_f) - m_p(t_0)]}{(t_f - t_0)} \quad (\text{H.3})$$

where t_0 and t_f are the initial and final times of an experiment performed at certain temperature.

An estimate of β , which is denoted by $\hat{\beta}$, can be computed in view of Eq. (H.3) as

$$\hat{\beta} = \frac{(n_f - n_0)}{(t_f - t_0)} \quad (\text{H.4})$$

where n_0 and n_f are the realizations of $N(t)$ at t_0 and t_f , respectively. In terms of $\hat{\beta}$, Eq. (H.2) can be rewritten as

$$m_p(t) \cong \hat{\beta} t \quad (\text{H.5})$$

At any time t , the random variable, $W(t)$, representing the amount of carbon already deposited on ACs is given by Eq. (3.13) in the text as

$$W(t) = \omega N(t)$$

where ω is the weight of a single packet of carbon; naturally, a realization of $W(t)$ is

$$w = (\omega n) \quad (\text{H.6})$$

Moreover, the mean weight of carbon deposited per unit weight of ACs, $m_w(t)$, is expressed by Eq. (3.14) in the text as

$$m_w(t) = W_M \left(\frac{\alpha' t}{\alpha' t + 1} \right) \quad (\text{H.7})$$

Solving this equation for t gives

$$t = \left(\frac{1}{\alpha'} \right) \frac{\left[\frac{m_w(t)}{W_M} \right]}{\left\{ 1 - \left[\frac{m_w(t)}{W_M} \right] \right\}} \quad (\text{H.8})$$

At the outset of the pore-narrowing, $m_w(t) \ll W_M$, and thus, this expression reduces to

$$t = \left(\frac{1}{\alpha'} \right) \left[\frac{m_w(t)}{W_M} \right]$$

By assuming that $m_w(t) \cong w$, this equation can be rewritten as

$$t = \left(\frac{1}{\alpha'} \right) \left[\frac{w}{W_M} \right] \quad (\text{H.9})$$

For illustration, $n_0 = 0$ and $n_f = 100$; thus, from Eq. (H.6), we have

$$w_0 = 0 \quad (\text{H.10})$$

and

$$w_f = (100 \omega) \quad (\text{H.11})$$

respectively. The values of t_0 and t_f corresponding to w_0 and w_f are obtained from the above two equations in conjunction of Eq. (H.9) as

$$t_0 = 0 \quad (\text{H.12})$$

and

$$t_f = \left(\frac{1}{\alpha'} \right) \left[\frac{100 \omega}{W_M} \right] \quad (\text{H.13})$$

By assuming that the experiment is performed at 973 K; the values of W_M and α' have been recovered from the experimental data⁶⁵ as 0.385 mg C and 0.022 min⁻¹, respectively, in Chapter 3. Moreover, the weight of a single packet is estimated to be $0.63 \cdot 10^{-13}$ mg C; thus, t_f is

computed from the above equation as $7.44 \cdot 10^{-10}$ min. Clearly, this value of t_f verifies that the simulated experiment is being performed at the very outset of the pore-narrowing.

Inserting the values of n_0 , n_f , t_0 , and t_f into Eq. (H.4) gives $\hat{\beta}$ as $1.36 \cdot 10^{11}$ packets \cdot min $^{-1}$. With this value of $\hat{\beta}$, a realization of $N(t)$, i.e., n , at any time t can be simulated by sampling a random number, or deviate, from a Poisson distribution whose mean is given by Eq. (H.5). A set of j Poisson deviates constitutes a set of simulated experimental data at the temperature of interest. Given in Table H.1 is the computer code written in R for generating these deviates.

Table H.1. Computer Code in R for Generating Simulated Experimental Data as Poisson Deviates for the Pure-Birth Process.

```
function(j, betahat, t0, tf){  
  
  # This function generates j Poisson deviates  
  # on time interval (t0, tf). The proportionality  
  # constant is denoted by betahat.  
  
  timestep<-(tf-t0)/j  
  
  times<-seq(t0, tf, by=timestep)  
  
  means<-betahat*times  
  
  devs<-rpois(j+1,means)  
  
  solution<-cbind(times, devs)  
  
  plot(times,devs)  
  
  solution  
  
}
```

Appendix I - Derivation of the Master Equation of a Pure-Death Process

Suppose that a system comprising a population of particulate or discrete entities in a given space is to be stochastically modeled as a pure-death process. The random variable characterizing this process is denoted by $N(t)$ with realization n ; moreover, the intensity of death is denoted by $\mu_n(t)$. Thus, one of the following two events is considered to occur during time interval $(t, t + \Delta t)$. First, the number of entities decreases by one, which is a death event, with conditional probability $\{[\mu_n(t)]\Delta t + o(\Delta t)\}$. Second, the number of entities changes by a number other than one with conditional probability $o(\Delta t)$, which is defined such that

$$\lim_{\Delta t \rightarrow 0} \frac{o(\Delta t)}{\Delta t} = 0 \quad (\text{I.1})$$

Naturally, the conditional probability of no change in the number of entities during this time interval is $(1 - \{[\mu_n(t)]\Delta t + o(\Delta t)\})$.

Let the probability that exactly n entities are present at time t be denoted as $p_n(t) = \Pr[N(t) = n]$, where $n \in (n_0, n_0 - 1, \dots, 2, 1, 0)$; n_0 is the initial number of entities in the system. For the two adjacent time intervals, $(0, t)$ and $(t, t + \Delta t)$, the occurrence of exactly n entities being present at time $(t + \Delta t)$ can be realized in the following mutually exclusive ways; see Figure I.1.

(1) With a probability of $\{[\mu_{n+1}(t)]\Delta t + o(\Delta t)\}p_{n+1}(t)$, the number of entities will decrease by one during time interval $(t, t + \Delta t)$, provided that exactly $(n + 1)$ entities are present at time t .

(2) With a probability of $o(\Delta t)$, the number of entities will change by exactly j entities during time interval $(t, t + \Delta t)$, provided that exactly $(n - j)$ entities are present at time t , where $2 \leq j \leq n_0$.

(3) With a probability of $(1 - \{[\mu_n(t)]\Delta t + o(\Delta t)\})p_n(t)$, the number of entities will remain unchanged during time interval $(t, t + \Delta t)$, provided that n entities are present at time t .

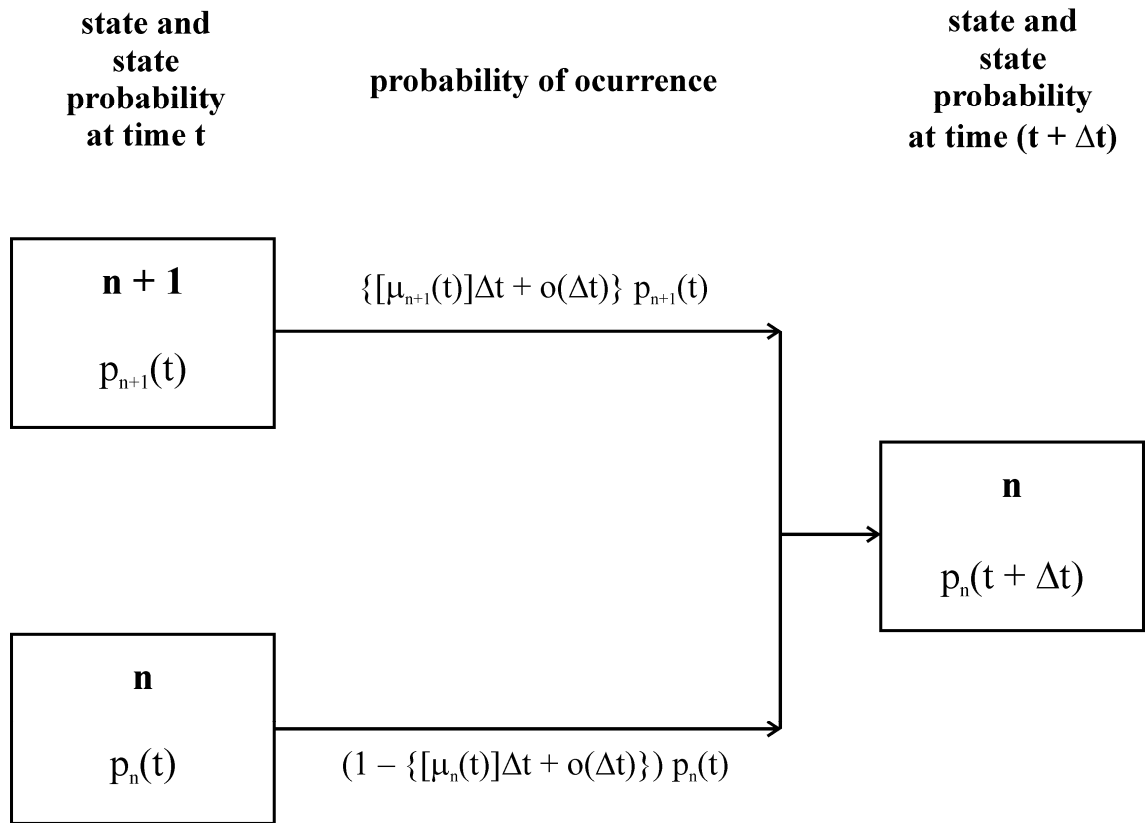


Figure I.1. Probability balance for the pure-death process involving the mutually exclusive events in the time interval, $(t, t + \Delta t)$.

Summing all these probabilities and consolidating all quantities of $o(\Delta t)$ yield

$$p_n(t + \Delta t) = \{\mu_{n+1}(t)\Delta t\} p_{n+1}(t) + \{1 - [\mu_n(t)]\Delta t\} p_n(t) + o(\Delta t) \quad (I.2)$$

Rearranging this equation, dividing it by Δt , and taking the limit as $\Delta t \rightarrow 0$ yield the master equation of the pure-death process as;^{73, 134}

$$\frac{d}{dt} p_n(t) = \mu_{n+1}(t) p_{n+1}(t) - \mu_n(t) p_n(t) \quad (I.3)$$

This in Eq. (4.1) in the text.

Appendix J - Formation of Carbon Molecular Sieves: System-Size Expansion of the Master Equation for the Pure-Death Process with a Non-Linear Intensity of Transition Based on a Single Random Variable

As derived in the preceding appendix, the master equation of the pure-death process, Eq. (I.3), is given by

$$\frac{d}{dt}p_n(t) = \mu_{n+1}(t)p_{n+1}(t) - \mu_n(t)p_n(t), \quad n = n_0, n_0 - 1, \dots, 2, 1, 0 \quad (\text{J.1})$$

In light of the one-step operator, \mathbb{E} , this equation is reduced to

$$\frac{d}{dt}p_n(t) = (\mathbb{E} - 1)\mu_n(t)p_n(t), \quad n = n_0, n_0 - 1, \dots, 2, 1, 0 \quad (\text{J.2})$$

The intensity of death, $\mu_n(t)$, in this expression is given by Eq. (4.2) in the text as

$$\mu_n(t) = -\frac{dn}{dt} = kn + k'n(n_0 - n)$$

where k and k' are proportionality constants. By expanding and rearranging the right-hand side of this expression, we obtain

$$\mu_n(t) = -\frac{dn}{dt} = (k + k'n_0)n - k'n^2 \quad (\text{J.3})$$

Substituting the above equation into Eq. (J.2) yields

$$\frac{d}{dt}p_n(t) = (\mathbb{E} - 1)[(k + k'n_0)n - k'n^2]p_n(t) \quad (\text{J.4})$$

As elaborated in Appendix C, the random variable, $N(t)$, is expressed as the sum of the macroscopic term, $\Omega\varphi(t)$, and the fluctuation term, $\Omega^{1/2}\Xi(t)$ as

$$N(t) = \Omega\varphi(t) + \Omega^{1/2}\Xi(t)$$

For the pure-death process of interest, the system's size, Ω , in this expression is identified as n_0 ; thus,

$$N(t) = n_0\varphi(t) + n_0^{1/2}\Xi(t) \quad (\text{J.5})$$

whose realization given by

$$n = n_0\varphi(t) + n_0^{1/2}\xi \quad (\text{J.6})$$

Accordingly, $p_n(t)$ or $p(n;t)$ is transformed into function $\pi(\xi;t)$ as

$$p(n;t) = \pi(\xi;t) \quad (\text{J.7})$$

Differentiating this expression with respect to t gives rise to

$$\frac{d}{dt}p(n;t) = \frac{\partial\pi}{\partial t} - n_0^{1/2} \left(\frac{d\varphi}{dt} \right) \frac{\partial\pi}{\partial\xi} \quad (\text{J.8})$$

where $\pi = \pi(\xi;t)$. In light of the one-step operator, \mathbb{E} , we obtain

$$\mathbb{E}n = n + 1$$

Substituting Eq. (J.6) for n on the right-hand side of this equation yields

$$\begin{aligned} \mathbb{E}n &= [n_0\varphi(t) + n_0^{1/2}\xi] + 1 \\ &= [n_0\varphi(t) + n_0^{1/2}\xi] + [n_0^{1/2}n_0^{-1/2}] \end{aligned}$$

or

$$\mathbb{E}n = n_0\varphi(t) + n_0^{1/2}(\xi + n_0^{-1/2})$$

In other words, \mathbb{E} transforms n into $(n + 1)$, and therefore, ξ into $(\xi + n_0^{-1/2})$; as a result, from Eq.

(J.7),

$$\mathbb{E}p(n;t) = \mathbb{E}\pi(\xi;t)$$

or

$$p(n+1;t) = \pi(\xi + n_0^{-1/2}; t) \quad (\text{J.9})$$

The Taylor expansion of $\pi(\xi + n_0^{-1/2}; t)$ about ξ , is obtained as

$$\pi(\xi + n_0^{-1/2}; t) = \pi(\xi; t) + n_0^{-1/2} \frac{\partial}{\partial\xi} \pi(\xi; t) + \frac{1}{2!} (n_0^{-1/2})^2 \frac{\partial^2}{\partial\xi^2} \pi(\xi; t) + \dots$$

or

$$\pi(\xi + n_0^{-1/2}; t) = \left(1 + n_0^{-1/2} \frac{\partial}{\partial\xi} + \frac{1}{2} n_0^{-1} \frac{\partial^2}{\partial\xi^2} + \dots \right) \pi(\xi; t) \quad (\text{J.10})$$

In view of Eqs. (J.7) and (J.9), the above expression can be transformed to

$$p(n+1; t) = \left(1 + n_0^{-1/2} \frac{\partial}{\partial \xi} + \frac{1}{2} n_0^{-1} \frac{\partial^2}{\partial \xi^2} + \dots \right) p(n; t)$$

or

$$\mathbb{E}p(n; t) = \left(1 + n_0^{-1/2} \frac{\partial}{\partial \xi} + \frac{1}{2} n_0^{-1} \frac{\partial^2}{\partial \xi^2} + \dots \right) p(n; t)$$

By comparing both sides of this expression, we have

$$\mathbb{E} = 1 + n_0^{-1/2} \frac{\partial}{\partial \xi} + \frac{1}{2} n_0^{-1} \frac{\partial^2}{\partial \xi^2} + \dots \quad (\text{J.11})$$

Substituting this equation in conjunction with Eqs. (J.6), (J.7), and (J.8) into the master equation, Eq. (J.4), leads to

$$\begin{aligned} & \frac{\partial \pi}{\partial t} - n_0^{1/2} \left(\frac{d\varphi}{dt} \right) \frac{\partial \pi}{\partial \xi} \\ &= n_0 \left(n_0^{-1/2} \frac{\partial}{\partial \xi} + \frac{1}{2} n_0^{-1} \frac{\partial^2}{\partial \xi^2} + \dots \right) [(k + k'n_0)(\varphi + n_0^{-1/2}\xi) - k'n_0(\varphi + n_0^{-1/2}\xi)^2] \pi \end{aligned} \quad (\text{J.12})$$

Absorbing the system's size, n_0 , into the time variable, t , as

$$n_0 t = \gamma$$

and truncating the terms after the second-order derivative for large n_0 give

$$\begin{aligned} & \frac{\partial \pi}{\partial \gamma} - n_0^{1/2} \left(\frac{d\varphi}{d\gamma} \right) \frac{\partial \pi}{\partial \xi} \\ &= \left(n_0^{-1/2} \frac{\partial}{\partial \xi} + \frac{1}{2} n_0^{-1} \frac{\partial^2}{\partial \xi^2} \right) [(k + k'n_0)(\varphi + n_0^{-1/2}\xi) - k'n_0(\varphi + n_0^{-1/2}\xi)^2] \pi \end{aligned} \quad (\text{J.13})$$

Expanding the right-hand side of this equation and collecting the resultant terms of orders $n_0^{1/2}$ and n_0^0 separately give

$$\begin{aligned} & \frac{\partial \pi}{\partial \gamma} - n_0^{1/2} \left(\frac{d\varphi}{d\gamma} \right) \frac{\partial \pi}{\partial \xi} \\ &= n_0^0 \left\{ \left[-(2\varphi - 1)k' + \frac{k}{n_0} \right] \frac{\partial}{\partial \xi} (\xi\pi) + \frac{1}{2} \left[-k'\varphi(\varphi - 1) + \frac{k}{n_0}\varphi \right] \frac{\partial^2 \pi}{\partial \xi^2} \right\} \\ & \quad - n_0^{1/2} \left\{ \left[k'\varphi(\varphi - 1) - \frac{k}{n_0}\varphi \right] \frac{\partial \pi}{\partial \xi} \right\} \end{aligned}$$

$$+n_0^{-1/2} \left[\left(\frac{1}{2} k n_0^{-1} + \frac{1}{2} k' - k' \varphi \right) \frac{\partial^2}{\partial \xi^2} (\xi \pi) - k' \frac{\partial}{\partial \xi} (\xi^2 \pi) - \frac{1}{2} k' n_0^{-1/2} \frac{\partial^2}{\partial \xi^2} (\xi^2 \pi) \right] \quad (\text{J.14})$$

Comparing both sides of the above expression gives rise to

$$\frac{d\varphi}{d\gamma} = k' \varphi (\varphi - 1) - \frac{k}{n_0} \varphi \quad (\text{J.15})$$

and

$$\frac{\partial \pi}{\partial \gamma} = \left[-(2\varphi - 1)k' + \frac{k}{n_0} \right] \frac{\partial}{\partial \xi} (\xi \pi) + \frac{1}{2} \left[-k' \varphi (\varphi - 1) + \frac{k}{n_0} \varphi \right] \frac{\partial^2 \pi}{\partial \xi^2} \quad (\text{J.16})$$

Of these two equations, the former is the macroscopic equation governing the overall behavior of the process, and the latter is a linear Fokker-Plank equation governing the fluctuations of the process around the macroscopic values and whose coefficients depend on t through $\varphi(t)$.

Appendix K - Formation of Carbon Molecular Sieves: Derivation of the Mean and Variance of the Pure-Death Process with a Non-Linear Intensity of Transition Based on a Single Random Variable

For convenience, Eq. (A-6) for the random variable, $N(t)$, is rewritten below

$$N(t) = n_0\varphi(t) + n_0^{1/2}\Xi(t) \quad (\text{K.1})$$

From this equation, the mean of $N(t)$, i.e., $E[N(t)]$ or $m(t)$, is obtained as

$$\begin{aligned} E[N(t)] &= E[n_0\varphi(t) + n_0^{1/2}\Xi(t)] \\ &= n_0E[\varphi(t)] + n_0^{1/2}E[\Xi(t)] \end{aligned}$$

or

$$m(t) = n_0\varphi(t) + n_0^{1/2}E[\Xi(t)] \quad (\text{K.2})$$

Similarly, the variance, $\text{Var}[N(t)]$ or $\sigma^2(t)$, is

$$\begin{aligned} \text{Var}[N(t)] &= \text{Var}[n_0\varphi(t) + n_0^{1/2}\Xi(t)] \\ &= n_0^2\text{Var}[\varphi(t)] + n_0\text{Var}[\Xi(t)] \end{aligned}$$

or

$$\sigma^2(t) = n_0\text{Var}[\Xi(t)] \quad (\text{K.3})$$

As indicated by Eq. (B.18), for any arbitrary random variable $N(t)$, $\sigma^2(t)$ can be related to $E[N(t)]$ as

$$\sigma^2(t) = E[N^2(t)] - \{E[N(t)]\}^2 \quad (\text{K.4})$$

In view of this expression, Eq. (K.3) can be rewritten as

$$\sigma^2(t) = n_0 \left(E[\Xi^2(t)] - \{E[\Xi(t)]\}^2 \right) \quad (\text{K.5})$$

Because $N(0) = n_0$ and $\Xi(0) = 0$, we have, from Eq. (K.1)

$$\varphi(0) = 1 \quad (\text{K.6})$$

The macroscopic equation governing the overall behavior of the system is given by Eq. (J.15) as

$$\frac{d\varphi}{d\gamma} = k'\varphi(\varphi - 1) - \frac{k}{n_0}\varphi$$

Because $n_0 t = \gamma$, this equation can be rewritten as

$$\frac{d\varphi}{dt} = k' n_0 \varphi (\varphi - 1) - k \varphi \quad (\text{K.7})$$

Upon integration, this expression yields

$$\varphi(t) = \frac{(k + k' n_0)}{c \exp[(k + k' n_0)t] + k' n_0}$$

In view of Eq. (K.6), the constant, c , in the above expression is k ; thus,

$$\varphi(t) = \frac{(k + k' n_0)}{k \exp[(k + k' n_0)t] + k' n_0} \quad (\text{K.8})$$

For convenience, Eqs. (D.12) and (D.14) are rewritten below

$$\sum_x \left[g(x) \frac{\partial}{\partial x} f(x) \right] = - \sum_x \left[f(x) \frac{\partial}{\partial x} g(x) \right] \quad (\text{K.9})$$

and

$$\sum_x \left[g(x) \frac{\partial^2}{\partial x^2} f(x) \right] = \sum_x \left[f(x) \frac{\partial^2}{\partial x^2} g(x) \right] \quad (\text{K.10})$$

The linear Fokker-Plank equation governing the fluctuations of the process around the macroscopic values is given by Eq. (J.16) as

$$\frac{\partial}{\partial \gamma} \pi = \left[-(2\varphi - 1)k' + \frac{k}{n_0} \right] \frac{\partial}{\partial \xi} (\xi \pi) + \frac{1}{2} \left[-k' \varphi (\varphi - 1) + \frac{k}{n_0} \varphi \right] \frac{\partial^2}{\partial \xi^2} \pi \quad (\text{K.11})$$

Because $n_0 t = \gamma$, this equation can be transformed into

$$\frac{\partial}{\partial t} \pi = [-(2\varphi - 1)k' n_0 + k] \frac{\partial}{\partial \xi} (\xi \pi) + \frac{1}{2} [-k' n_0 \varphi (\varphi - 1) + k \varphi] \frac{\partial^2}{\partial \xi^2} \pi \quad (\text{K.12})$$

Multiplying both sides of the above equation by ξ and summing over all values of ξ yield

$$\sum_{\xi} \xi \frac{\partial}{\partial t} \pi = [-(2\varphi - 1)k' n_0 + k] \left[\sum_{\xi} \xi \frac{\partial}{\partial \xi} (\xi \pi) \right] + \frac{1}{2} [-k' n_0 \varphi (\varphi - 1) + k \varphi] \left[\sum_{\xi} \xi \frac{\partial^2}{\partial \xi^2} \pi \right] \quad (\text{K.13})$$

By virtue of Eqs. (K.9) and (K.10), the right-hand side of this expression can be transformed to

$$\sum_{\xi} \xi \frac{\partial}{\partial t} \pi = [-(2\varphi - 1)k' n_0 + k] \left[- \sum_{\xi} \xi \pi \frac{\partial}{\partial \xi} \xi \right] + \frac{1}{2} [-k' n_0 \varphi (\varphi - 1) + k \varphi] \left[\sum_{\xi} \pi \frac{\partial^2}{\partial \xi^2} \xi \right]$$

or

$$\sum_{\xi} \xi \frac{\partial}{\partial t} \pi = -[-(2\varphi - 1)k'n_0 + k] \left[\sum_{\xi} \xi \pi \right] \quad (\text{K.14})$$

The first moment of random variable $\Xi(t)$, i.e., $E[\Xi(t)]$, is defined as

$$E[\Xi(t)] = \sum_{\xi} \xi \pi(\xi; t)$$

or

$$E[\Xi(t)] = \sum_{\xi} \xi \pi \quad (\text{K.15})$$

and thus,

$$\frac{d}{dt} E[\Xi(t)] = \sum_{\xi} \xi \frac{\partial}{\partial t} \pi \quad (\text{K.16})$$

In light of the above two equations, Eq. (K.14) reduces to

$$\frac{d}{dt} E[\Xi(t)] = -[-(2\varphi - 1)k'n_0 + k] E[\Xi(t)] \quad (\text{K.17})$$

Inserting Eq. (K.8) for $\varphi(t)$ into this equation and integrating the resulting expression yield

$$E[\Xi(t)] = \frac{c' \exp[(k + k'n_0)t]}{\{k \exp[(k + k'n_0)t] + k'n_0\}^2} \quad (\text{K.18})$$

From the initial conditions for the transformed probability distribution, $\pi(\xi; t)$,

$$\pi(\xi; 0) = \begin{cases} 1 & \text{if } \xi = 0 \\ 0 & \text{elsewhere} \end{cases} \quad (\text{K.19})$$

and the definition of $E[\Xi(t)]$, as given by Eq. (K.15), we have

$$E[\Xi(0)] = 0 \quad (\text{K.20})$$

thereby indicating that

$$c' = 0 \quad (\text{K.21})$$

Hence,

$$E[\Xi(t)] = 0 \quad (\text{K.22})$$

Similarly, multiplying both sides of Eq. (K.12) by ξ^2 and summing over all values of ξ yield

$$\sum_{\xi} \xi^2 \frac{\partial}{\partial t} \pi = [-(2\varphi-1)k'n_0 + k] \left[\sum_{\xi} \xi^2 \frac{\partial(\xi\pi)}{\partial \xi} \right] + \frac{1}{2} [-k'n_0\varphi(\varphi-1) + k\varphi] \left[\sum_{\xi} \xi^2 \frac{\partial^2}{\partial \xi^2} \pi \right] \quad (\text{K.23})$$

By virtue of Eqs. (K.9) and (K.10), the right-hand side of the above expression can be transformed to

$$\sum_{\xi} \xi^2 \frac{\partial}{\partial t} \pi = [-(2\varphi-1)k'n_0 + k] \left[-\sum_{\xi} \xi \pi \frac{\partial}{\partial \xi} \xi^2 \right] + \frac{1}{2} [-k'n_0\varphi(\varphi-1) + k\varphi] \left[\sum_{\xi} \pi \frac{\partial^2}{\partial \xi^2} \xi^2 \right]$$

or

$$\sum_{\xi} \xi^2 \frac{\partial}{\partial t} \pi = -2[-(2\varphi-1)k'n_0 + k] \left[\sum_{\xi} \xi^2 \pi \right] + [-k'n_0\varphi(\varphi-1) + k\varphi] \left[\sum_{\xi} \pi \right] \quad (\text{K.24})$$

For the transformed probability distribution, $\pi(\xi;t)$, the following property must hold

$$\sum_{\xi} \pi(\xi;t) = 1$$

or

$$\sum_{\xi} \pi = 1 \quad (\text{K.25})$$

Thus, Eq. (K.24) can be rewritten as

$$\sum_{\xi} \xi^2 \frac{\partial}{\partial t} \pi = -2[-(2\varphi-1)k'n_0 + k] \left[\sum_{\xi} \xi^2 \pi \right] + [-k'n_0\varphi(\varphi-1) + k\varphi] \quad (\text{K.26})$$

The second moment of random variable $\Xi(t)$, i.e., $E[\Xi^2(t)]$, is defined as

$$E[\Xi^2(t)] = \sum_{\xi} \xi^2 \pi(\xi;t)$$

or

$$E[\Xi^2(t)] = \sum_{\xi} \xi^2 \pi \quad (\text{K.27})$$

and thus,

$$\frac{d}{dt} E[\Xi^2(t)] = \sum_{\xi} \xi^2 \frac{\partial}{\partial t} \pi \quad (\text{K.28})$$

In view of the above two equations, Eq. (K.26) reduces to

$$\frac{d}{dt} E[\Xi^2(t)] = -2[-(2\varphi-1)k'n_0 + k] E[\Xi^2(t)] - k'n_0\varphi(\varphi-1) + k\varphi \quad (\text{K.29})$$

Inserting Eq. (K.8) for $\varphi(t)$ into this equation and integrating the resulting expression give rise to

$$\begin{aligned}
& E[\Xi^2(t)] \\
&= k(k+k'n_0) \frac{\exp[(k+k'n_0)t]}{\{k \exp[(k+k'n_0)t] + k'n_0\}^4} \\
&\quad \cdot \{k^2 \exp[2(k+k'n_0)t] - (k'n_0)^2 + 2k^2k'n_0t \exp[(k+k'n_0)t] \\
&\quad + 2k(k'n_0)^2t \exp[(k+k'n_0)t]\} \\
&\quad + \frac{c'' \exp[2(k+k'n_0)t]}{\{k \exp[(k+k'n_0)t] + k'n_0\}^4} \tag{K.30}
\end{aligned}$$

From the aforementioned initial conditions for the transformed probability distribution, $\pi(\xi;t)$, as given by Eq. (K.19), and the expression of $E[\Xi^2(t)]$ as defined by Eq. (K.27), we have

$$E[\Xi^2(0)] = 0, \tag{K.31}$$

thereby indicating that

$$c'' = k(k+k'n_0)[(k'n_0)^2 - k^2] \tag{K.32}$$

Hence,

$$\begin{aligned}
& E[\Xi^2(t)] \\
&= k(k+k'n_0) \frac{\exp[(k+k'n_0)t]}{\{k \exp[(k+k'n_0)t] + k'n_0\}^4} \\
&\quad \cdot \{k^2 \exp[2(k+k'n_0)t] - (k'n_0)^2 + (k+k'n_0)[k'n_0 + k(2k'n_0t-1)] \exp[(k+k'n_0)t]\} \\
& \tag{K.33}
\end{aligned}$$

The mean, $E[N(t)]$ or $m(t)$ is obtained by substituting Eqs. (K.8) and (K.22) into Eq. (K.2) as

$$m(t) = n_0 \left\{ \frac{(k+k'n_0)}{k \exp[(k+k'n_0)t] + k'n_0} \right\} \tag{K.34}$$

By defining $\alpha = (k+k'n_0)$ and $\beta = k(k+k'n_0)^{-1}$, this expression becomes

$$m(t) = n_0 \left\{ \frac{1}{1 + \beta[\exp(\alpha t) - 1]} \right\} \tag{K.35}$$

This is Eq. (4.4) in the text. Similarly, the variance, $\text{Var}[N(t)]$ or $\sigma^2(t)$, is obtained by inserting Eqs. (K.22) and (K.33) into Eq. (K.5) as

$$\begin{aligned} & \sigma^2(t) \\ &= n_0 \frac{k(k+k'n_0)\exp[(k+k'n_0)t]}{\{k\exp[(k+k'n_0)t]+k'n_0\}^4} \\ & \cdot \left\{ k^2 \exp[2(k+k'n_0)t] - (k'n_0)^2 + (k+k'n_0)[k'n_0 + k(2k'n_0t-1)]\exp[(k+k'n_0)t] \right\} \end{aligned} \tag{K.36}$$

In terms of α and β , this expression can be transformed into

$$\begin{aligned} \sigma^2(t) &= n_0 \frac{\beta \exp(\alpha t)}{\{1 + \beta[\exp(\alpha t) - 1]\}^4} \\ & \cdot \left(2\beta - 1 + \exp(\alpha t) \left\{ 1 - 2\beta[1 + (\beta - 1)(\alpha t)] + 2\beta^2 \sinh(\alpha t) \right\} \right) \end{aligned} \tag{K.37}$$

This is Eq. (4.6) in the text.